# OVERWASH INDUCED BY STORM CONDITIONS

A Dissertation

by

YOUNG HYUN PARK

Submitted to the Office of Graduate Studies of
Texas A&M University
in partial fulfillment of the requirements for the degree of

DOCTOR OF PHILOSOPHY

December 2006

Major Subject: Ocean Engineering

# OVERWASH INDUCED BY STORM CONDITIONS

A Dissertation

by

YOUNG HYUN PARK

Submitted to the Office of Graduate Studies of
Texas A&M University
in partial fulfillment of the requirements for the degree of

DOCTOR OF PHILOSOPHY

Approved by:

Chair of Committee, Billy L. Edge
Committee Members, Robert E. Randall
Patrick J. Lynett
Douglas J. Sherman
Head of Department, David V. Rosowsky

December 2006

Major Subject: Ocean Engineering

## ABSTRACT

Overwash Induced by Storm Conditions.

(December 2006)

Young Hyun Park, B.S., Dankook University;

M.S., Seoul National University

Chair of Advisory Committee: Dr. Billy L. Edge

Erosion problems are not only in the Texas area, but exist also along the coastline all over the world. Even though many researchers have studied coastal processes related with beach erosion and deposition over the decades, these processes are too complex to understand completely and field measurements are difficult to obtain during landfall of storms which cause fatal damages.

Overwash is strongly suspected to cause extreme erosion as seen from long-term field measurements in the upper Texas coast. Overwash and washover are the source of cross-shore erosion and deposition of beach material along the coast, respectively. Waves superimposed on increased storm surges overtop and generate serious erosion of the berm. However, the data for these processes do not completely describe the shoreline erosion problems. Providing better descriptions requires field measurements and laboratory experiments with careful calibration.

This study was conducted in two major sections. First was a field measurement and second was a laboratory experiment.

This study used the RTK-DGPS to measure the change in the beach profile over multi year period. The GPS system is one of the ways to have the best resolution.

The laboratory experiment was done in a 2D wave tank on mid-scale based on similitude law at Texas A&M University. The experiment was necessary to obtain better empirical formulas.

The erosion rate of the sand was measured at different wave conditions and slopes of the berm or upper beach face in regular and irregular waves respectively. The erosion rate is much bigger at higher wave height, longer wave period and steeper beach face. The erosion rate is increased proportional to speed of bore and it is decreased with time.

The empirical formulas were the first approach to simulate the impact of overwash. The laboratory results represented good agreement with the field data and might be applicable to predict the shoreline recession by overwash induced by storms. Further improvements can be expected by adding these empirical formulas to a numerical model to predict sediment transport in the swash zone.

# ACKNOWLEDGMENTS

I would like to give special thanks to my advisor Dr. Billy L. Edge, for inspiration and guidance during my study at Texas A&M University. He always has amazing enthusiasm and energy in his life, even though he is 29 years older than me. I learned how to live as a professor by working beside him; and he gave me the unforgettable memory of a beautiful sun set in the Caribbean.

I would, also, like to thank Dr. Robert E. Randall, Dr. Patrick J. Lynett and Dr. Douglas J. Sherman for serving on my committee and for providing valuable insight. Their priceless knowledge from their studies and experiences makes my dissertation perfect.

I want to thank my grandmother and parents for their love and support. They have been waiting for my degree for a very long time but they always gave me strength to bear through this period.

I have been in Texas A&M University for six years since coming to the U.S. and the time was both bitter and sweet. I almost decided to give up this study several times but God always shows me his love. I have a chance to enjoy in a new life now but I shall never forget my life at Texas A&M.

For where your treasure is, there your heart will be also (Matthew 6:21).

I can do everything through him who gives me strength (Philippians 4:13).

# TABLE OF CONTENTS

Page

CHAPTER Page

CHAPTER Page

# LIST OF FIGURES

FIGURE Page

FIGURE Page

FIGURE Page

FIGURE Page

FIGURE Page

FIGURE Page

FIGURE Page

FIGURE Page

FIGURE Page

## LIST OF TABLES

TABLE Page

# CHAPTER I

# INTRODUCTION

## 1.1. Objectives and Scope

Berms act on the beach to reflect and dissipate wave energy which is very important in stability of coastline. Storms accompanied by large waves and sea level rise cause overtopping of the berm. During large storm surges, a large amount of sand on the berm is transported seaward or landward. Dean and Dalrymple (2002) define overwash as the transportation process of sand landward and washover is the deposition process in their book. Overwash generated by storms is a very important factor for the stability of a berm on the beach over the short period. The crest of the berm is lowered by the repeated wave actions and the berm becomes easy to overtop and becomes submerged.

Although many field measurements have been conducted for decades, there have been fewer laboratory experiments and numerical models because of difficulty to understand the correlated factors and mechanics of sediment transport.

In this study, field measurements and a laboratory experiment were conducted. Empirical formulas were developed using a linear regression from laboratory experiments and its results were verified by comparing to experimental results. The developed empirical formula was applied to estimate the volume of sand by overwash.

---

This dissertation follows the style and format of the Journal of Ocean Engineering.

For field measurements, the area near Texas state highway 87 which was damaged by Hurricane Jerry and closed since1989 was selected, because this area was notorious for retreat of beach by overwash for several decades.

The field measurements were conducted in 2004 and 2005 and there were two landfalls of storms in the study area during the period. Eight landfalls of storms have been made in upper Texas coast since 2000 (Table 1.1). These data were compared with the historical field data which had been collected by TAMU since 1999. The impacts of tropical depression Ivan and hurricane Rita were measured and analyzed for comparison between the laboratory experiment and the developed numerical model.

The laboratory experiment was conducted for two different wave heights, four different wave periods and two different beach slopes by regular and irregular waves respectively in a 2D wave tank. The measured speeds of bores and beach profiles were used to develop empirical formulas for sediment transport rate by overwash.

**Table 1.1. Upper Texas coast tropical storms since 2000 (NOAA, 2006a).**

| Name | Class/ Landfall | Date | Data (Kts/mbs) |
|---|---|---|---|
| **RITA** | **Hurricane-Cat.3 /Port Arthur** | **9/24/05** | **Pk. Wind – 120 mph Pressure – 937 mb** |
| **KATRINA** | **Hurricane-Cat.3 /Southeast Louisiana** | **8/29/05** | **Pk. Wind – 125 mph Pressure – 920 mb** |
| **IVAN** | **Tropical Storm /Port Arthur** | **9/23/04** | **Pk. Wind – 35 kt Pressure – 1003 mb** |
| BILL | Tropical Storm /Southeast Louisiana | 6/30/03 | Pk. Wind – 52 kt Pressure – 997 mb |
| CLAUDETTE | Hurricane-Cat.1 /Port O'Connor | 7/15/03 | Pk. Wind – 78 kt Pressure – 981 mb |
| GRACE | Tropical Storm /Between Port O'Connor and Freeport | 8/31/03 | Pk. Wind – 35 kt Pressure – 1007 mb |
| FAY | Tropical Storm /Palacios | 9/06/02 | Pk. Wind – 50 kt Pressure – 998 mb |
| LILI | Hurricane-Cat.2 /South Central Louisiana | 10/03/02 | Pk. Wind – 80 kt Pressure – 963 mb |

## 1.2. Description of Study Area

The study area is located in the northeast coast of Texas near the state border between Texas and Louisiana State (Fig. 1.1). The Texas Department of Transportation planned to rebuild and reopen Highway 87 which is now a beach road between Galveston Island and the border of Louisiana. Some recovery efforts such as sand fences and Geotube groins were observed during the field measurements. The sand fences were destroyed by the attack of storms. The area has been damaged repeatedly by storms in the Gulf of Mexico and the damage was shown in Fig. 1.2. Researchers showed that overwash mainly caused the retreat of beach in the study area in Morton (1975) and Lee (2003). There was no berm along this area of the coast and this accelerated the erosion by overwash. Typically the berm would be expected to resist erosion and shoreline recession. Some beach natural protections will be discussed in Chapter II.

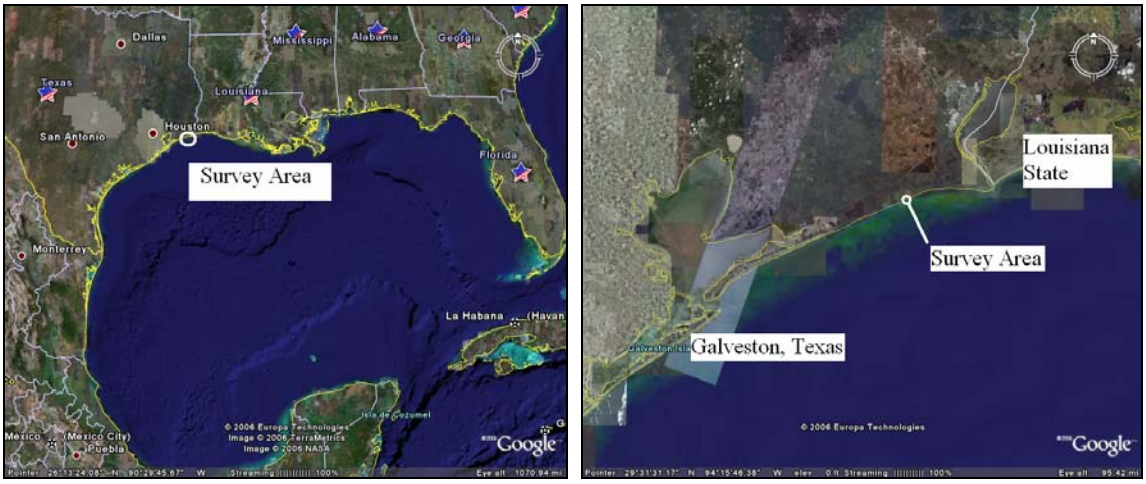


**Fig. 1.1. Survey area along the Texas coast (inside circle).**


**Fig. 1.2. The study area was damaged by tropical storm Ivan in 2004.**

# CHAPTER II

# CHARACTERISTICS OF OVERWASH

## 2.1. Coastal Management

The coastal area has been changed and will continue to be changed by many natural and human generated causes. The role of coastal engineers is to provide protection from these coastal hazards. Though most of the greatest morphological changes and the most destruction have accompanied tropical storms and hurricanes, a full understanding is not available due to the difficulties in field measurements and laboratory experiments.

Changes along the Texas coast are generated by long-term changes such as sea-level rise and decreasing of sand supply and short-term changes such as impacts of tropical storms and hurricanes along the upper Texas coast. Morton (1975) said the major factors causing the coastline changes along the Texas coast, especially between Sabine Pass and Bolivar Roads were relative sea-level rise, compactional subsidence and a deficit of sediment supply. He also mentioned that changes of vegetation line were primarily related to storms. Leatherman (1983) made a conclusion based on historical morphological studies that most Atlantic barriers were stable landforms that moved temporally by inlet modifications and entire barriers in the Gulf of Mexico migrated frequently as a result of overwash by storms. The existence of dune is important in beach management because it can slow the erosion rate by acting as a source of sand supply and a barrier against overwash during storms.

## 2.2. Tropical Storm and Hurricane Climatology and Parameters

One of the major short term causes of damages to the coastal zone is tropical storms and hurricanes. The heat and moisture from warm sea surface are used for a source of energy in developing tropical storms and hurricanes. The lower pressure is frequently associated with the higher wind speed in the center of the storms. The generated tropical depression is intensified and becomes tropical storm or hurricane by above processes. The maximum sustained wind speed and the central pressure are parameters to describe the characteristics of tropical storms and hurricanes.

The storm climatology is an important factor to forecast the intensity and amount of overwash. Historical trends say the number and intensity of tropical storms and hurricanes are being increased by atmospheric changes such as rising of sea surface temperature and low wind shear. The year of 2005 was the busiest one with 26 named tropical storms (mean is 10) including 13 hurricanes (mean is 6) and 7 of them were major hurricanes (mean is 2-3) that were higher than Category 3 on the Saffir-Simpson Hurricane Scale in Table 2.1. Many scientists (Titus, 1990; Knutson and Tuleya, 2004) believe that the greenhouse effect is a major cause to increase the number and intensity of tropical storms and hurricanes.

The definition of storm and hurricane by NOAA is as follows,

- Tropical Depression – An organized system of clouds and thunderstorms with a defined circulation and maximum sustained wind of 38 mph (33 knots) or less.
- Tropical Storms – An organized system of strong thunderstorms with a defined circulation and maximum sustained wind of 39 to 73 mph (34 - 63knots).
- Hurricane – An intense tropical weather system with a well defined circulation and

maximum sustained winds of 74 mph (64 knots) or higher.

Morton (2002) said each hurricane had each own characteristic from analysis of historical hurricanes data and March 1962 northeaster, Hurricanes Carla, Camille and Hugo were notorious for high surge and Hurricane Celia and Andrew were noted for high winds and Hurricane Beulah, Agnes and Floyd were recorded as extreme rainfall and flooding.

**Table 2.1. The Saffir-Simpson hurricane scale and characteristics (NOAA, 2006b).**

| Category | Wind Speed (km/h) | Storm Surge (m) | Damages | Hurricanes at Landfall |
|---|---|---|---|---|
| **1** | 119 – 153 | 1.2 – 1.5 | Some coastal road flooding and minor pier damage | - Hurricane Lili (2002)<br>- Hurricane Gaston (2004) |
| **2** | 154 – 177 | 1.8 – 2.4 | Coastal and low-lying escape routes flood 2-4 hours before arrival of the hurricane center | - Hurricane Isabel (2003)<br>- Hurricane Frances (2004) |
| **3** | 178 – 209 | 2.7 – 3.7 | Low-lying escape routes are cut by rising water 3-5 hours before arrival of the center of hurricane | - Hurricane Rita (2004)<br>- Hurricane Ivan (2004) |
| **4** | 211 – 250 | 4.0 – 5.5 | Low-lying escape routes are cut by rising water 3-5 hours before arrival of the center of hurricane | - Hurricane Katrina (2005)<br>- Hurricane Dennis (2005) |
| **5** | ≥ 251 | ≥ 5.5 | Low-lying escape routes are cut by rising water 3-5 hours before arrival of the center of hurricane | - Hurricane Gilbert (1988)<br>- Hurricane Andrew (1992) |

## 2.3. Overwash Processes

Dean and Dalrymple (2002) define that overwash is transportation process of sand landward and washover is deposition process in their book.

Overwash can be generated by high winds, waves, tides, swell or storms. Beaches and berms are eroded and breached by elevated storm surge and high waves during storms or northeasters and the eroded sand creates morphological shapes as shown in Fig. 2.1. Among the shapes, berm erosion, channel incision and washout show the processes of erosion and perched fans, washover terrace and sheetwash lineations represent the processes of deposition. Sallenger (2000) proposed simple storm-related scales to forecast overwash or flooding possibilities using relationships between runup height and berm elevation shown in Fig. 2.2 and Fig. 2.3. When high runup height ($R_{HIGH}$) is higher than high berm elevation ($D_{HIGH}$), overwash will be generated on the condition that low runup height ($R_{LOW}$) is lower than high berm elevation ($D_{LOW}$). Inundation will be occurred on the condition that low runup height is higher than high berm elevation based on his relationship.

The speed of bore at the top of the berm depends on the wave height, wave period, storm surge and slope of beach. The basic mechanisms have been developed but the accurate formulation is still studied by engineers, because interrelationships of factors make difficult analysis. Sand erosion and deposition generated by overwash are shown in Fig. 2.4 and Fig. 2.5.

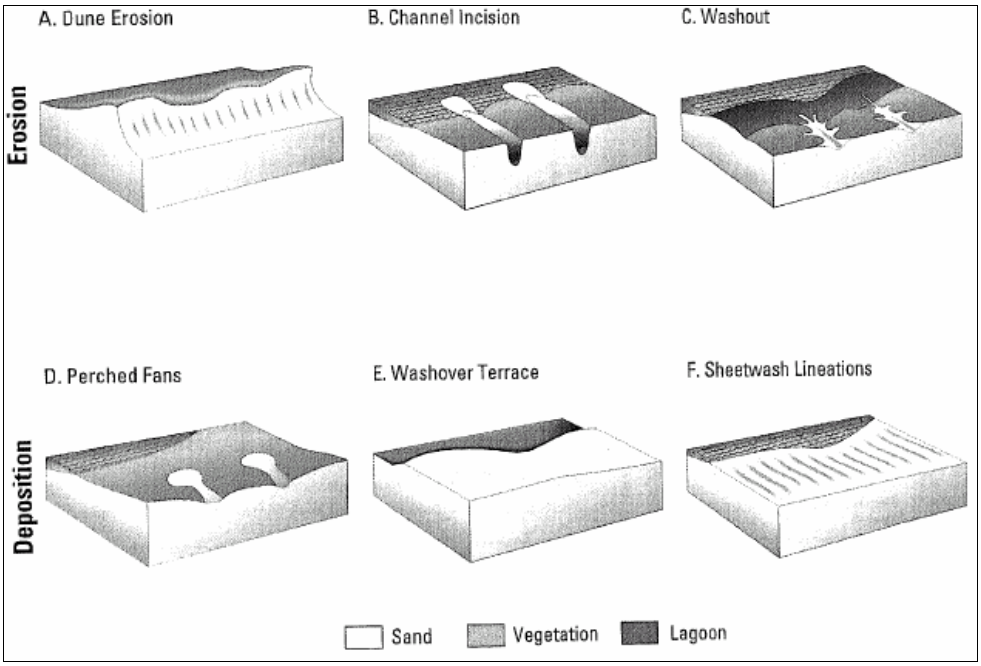


**Fig. 2.1. Types of erosional and depositional features produced by extreme storms. (Morton and Sallenger, 2003).**

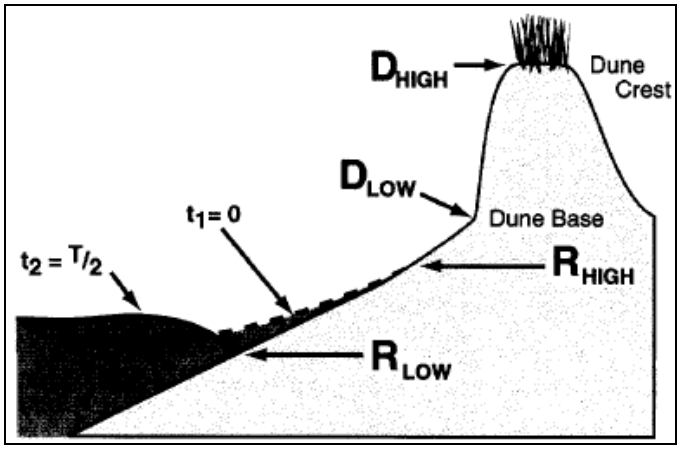


**Fig. 2.2. Definition sketch describing variables used in scaling the impact of storms on barrier islands (Sallenger, 2000). High runup height ($R_{HIGH}$), low runup height ($R_{LOW}$), high berm elevation ($D_{HIGH}$) and low berm elevation ($D_{LOW}$).**

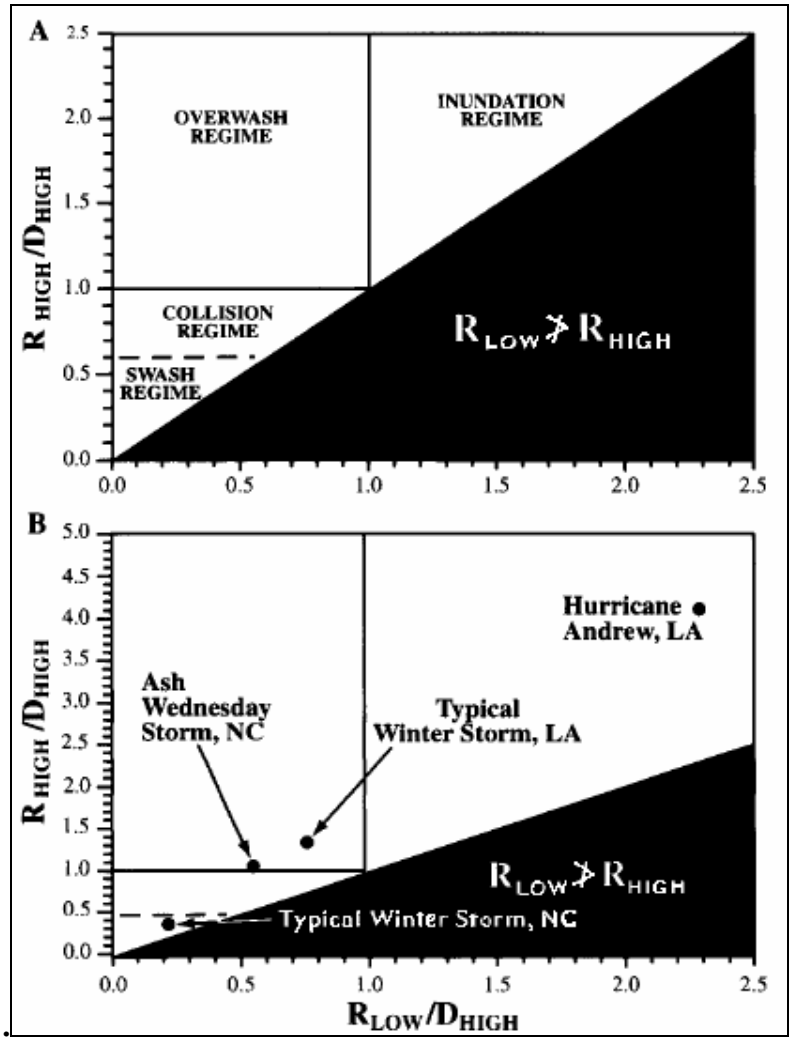


**Fig. 2.3. A. Delineation of four different regimes important to categorizing storm impacts on barrier islands. B. Characteristics of storms are plotted using available information (Sallenger, 2000).**


**Fig. 2.4. Pre/post storm aerial photography. Overwash across barrier island by hurricane Ivan, Gulf of Mexico, AL (USGS, 2004).**

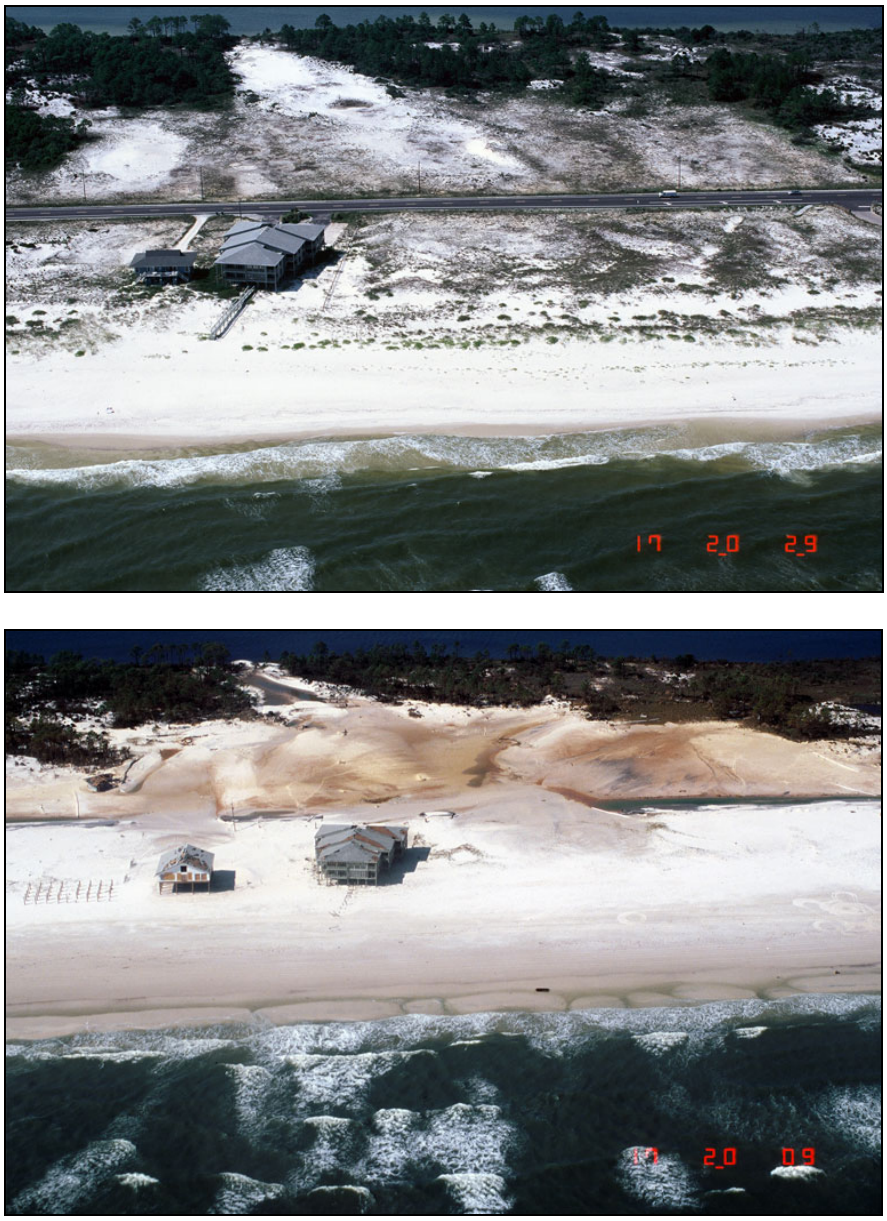

**Fig. 2.5. Pre/post storm aerial photography. Overwash fans by hurricane Ivan, Gulf of Mexico, FL (USGS, 2004).**

## 2.4. Impacts of Geological and Environmental Conditions

### 2.4.1. Coastal Dunes

Coastal dunes are formed by wind action and important for geological and ecological purposes. Barrier dune can act as a seawall against storm surge of high waves by reflecting the incident wave energy during storms conditions. Leatherman (1979) mentioned about roles of dune and acceleration of the erosion rate during landfall of storms. He said that three important roles during storm conditions were sand reservoirs, energy dissipation and barrier against storms. The reflected waves by dune are superimposed on the incident waves make a new wave system. The sum of velocity components of incident and reflected wave dune increased the energy level in swash and surf zone and then accelerated the rate of beach erosion.

The erosion by overwash begins when the summation of sea level and wave height is equal to the height of dune. Morton (2002) found that the distance of washover penetration was three times greater where dune was lost. Steeper slope allowed larger waves to reach closer to shore and resulted in greater erosion (Smith and Leatherman, 2000).

### 2.4.2. Storms and Storm Surge

Storms and storm surges affect the beach erosion and deposition directly. Morton (1975) calculated that 5.6 $m^3/m$ of sand were eroded by Tropical Storm Delia in 1973 from field measurements. Extreme hurricane can move the shoreline more than 30 m landward

per day.

Storm surge is sea level rise primarily by wind force accompanied with storms and secondary by a low pressure weather system. The generated storm surges are getting dangerous, when they are superimposed on the tides and waves. The greatest recorded storm surge was done by Hurricane Katrina and it was 9 meters high at Bay St. Louis, Mississippi, US. The storm surges are closely related to the bathymetry of ocean. If the continental shelf is short from the coast and drops steeply such as Florida, a lower surge is generated. The Gulf of Mexico has a shallow and very mild slope shelf, so higher storm surges are mostly produced in this area. Leatherman (1976) said storm surge was one of the most important factors to determine the magnitude of overwash basis of field measurement

### 2.4.3. Sea Level Rise

Sea level changes can be categorized into long-term and short-term changes. Astronomical tides are an example of short-term changes and change by effect of global warming is an example of long-term changes in sea level change. Scientists found that the effect of global warming is primary reason to cause sea level rise (Titus, 1990).

Leatherman (1984) estimated the sea level rise with four different scenarios around Galveston Island in Table 2.2. Feagin et al. (2005) calculated that the relative sea level rise was 0.33 cm/yr in Galveston Island from the difference between the record of tide gage and land subsidence. The FEMA (Federal Emergency Management Agency) estimated that sea level rise along the US coast will be 30 cm over 100 years and the trend of sea level

rise is still increasing with fluctuation.

Sea level rise causes the erosion by flooding and it accelerates the erosion by superimposing on storm surges and high waves. The barrier island is eroded from ocean side by sea level rise and the eroded sand is transported and deposited on bay side of the island. In most of cases, the erosion in ocean side is more critical than inundation, because a beach acts as a buffer against wave attacks.

**Table 2.2. Accelerated sea level rise scenarios for Galveston (Leatherman, 1984).**

| Scenario | Sea Level Rise (cm) | | |
|---|---|---|---|
| | 1980 Yr. | 2025 Yr. | 2075 Yr. |
| Baseline | 0 | 13.7 | 30.0 |
| Low | 0 | 30.7 | 92.4 |
| Medium | 0 | 48.4 | 164.5 |
| High | 0 | 66.2 | 236.9 |

### 2.4.4. Wind

The wave and current generated by extreme speed of wind increase the ability of erosion and transportation. They influence the morphology of deposition and distance of overwash fan. Storm surges strongly depend on magnitude and duration of wind. The fully

developed wind waves are generated with conditions of duration and fetch limit and the height and period of wind waves are shown in Table 2.3.

**Table 2.3. The expected wave height from wind speed and fetch length by Beaufort wind scale.**

| Wind | | | Required | | Significant Wave | |
|---|---|---|---|---|---|---|
| Speed (m/s) | Beaufort No. | Condition | Duration (Hr) | Fetch (km) | Height (m) | Period (sec) |
| 5 | 4 | Mod. Breeze | 20 | 150 | 1 | 4 |
| 15 | 7 | Mod. Breeze | 30 | 500 | 2 | 9 |
| 30 | 11 | Storm | 35 | 1100 | 15 | 14 |
| 35 | 12 | Hurricane | 35 | 1200 | 16 | 16 |

Northeaster is a term for storm whose leading winds head for landward from the northeast. It is generated by mixing of cold fronts from Canada or Arctic and warm front from Gulf of Mexico. Northeaster contains heavy, cold coastal rains in the warmer months, and winter blizzards and it mostly damages the northeastern coast in US. Kriebel et al. (1997) developed Northeaster Risk Index and they found that this index is good predictor of shoreline recession. It said ratings of 1 to 2 produce significant beach erosion but not dangerous to structures at the beach and class 3 or higher are dangerous storm. Equation

(2.1) and its parameters were developed based on the March 1962 “Ash Wednesday” storm whose wind speed reached 97 km/h and it was calibrated as a Class 5 storm in their index.

$$I = HS\left(\frac{t_d}{12}\right)^{0.3} \tag{2.1}$$

where $I$ is Northeaster Risk Index, $H$ is wave height (feet), $S$ is surge elevation (feet) and $t_d$ is storm duration.

### 2.4.5. Vegetation

Morton (2002) categorized the influence of vegetation as (1) reducing wind speed, washover current and storm surge by increasing surface friction, (2) increasing accumulation of sediment and (3) role of sediment binder against erosion. Sand is transported by wind and trapped by vegetation. The gigantic sand dune built by eolian transport is shown in Fig. 2.6 and the highest dune reaches about 10 meter from its base. It shows that vegetation area has higher dune than the area without it

Salt water intrusion accompanied with inundation causes damage to vegetation and this damage accelerates the erosion. The color of vegetation where intrusion happens is changed by salt water and it can be good evidence of overwash and measurements of washover penetration. Morton (1997) said that the vegetation line can be used for indicator of beach line instead of high water line for long term changes, because it is not affected by short term changes except extreme events such as storms.

**Fig. 2.6. The gigantic sand dune by eolian transport in South Padre Island, Texas.**

### 2.4.6. Other Factors

The man-made coastal structures were built to protect from coastal hazards but some of them produce unexpected side effect of erosion and deposition with interaction of waves and currents. Sheet erosion is produced by heavy rain. Surface runoff occurs when precipitation is higher than infiltration rate of soil. Turbulence generated by surface runoff can increase erosion rate more than impact of rain drop at the beach.

# CHAPTER III

# FIELD SURVEY WITH GPS

## 3.1. Introduction

### 3.1.1. Objectives and Scope

Field measurements were conducted to find the characteristics of morphological changes along the northeastern Texas coasts. The survey area has suffered extreme beach erosion by primarily overwash every year. The erosion occurred by wave activities occurring during large storms in the Gulf of Mexico and overwash by storms.

The survey area was selected from the historical survey data of Texas A&M University and the most important measurements were conducted to analyze overwash by storms before and after landfall of storms. The obtained data were used for comparison and development of the laboratory experiment and the numerical model.

### 3.1.2. Literature Review

Sonu (1970) found beach recovery processes within a week after passing of hurricane from his field measurement. Dolan (1972) found that the dune confines the swash zone, so that incident wave energy is dissipated in the narrow zone. It increases the intensity of turbulence and becomes susceptible to beach erosion. U.S. Army Corps of Engineers

(1973) presented a rule of thumbs of 1 per 1 (1 ft of retreat = 1 cubic yard of sand; 1.0 m of retreat = 2.53 $m^3$ of sand). Fisher et al. (1974) showed the understanding of overwash mechanism combined with eolian processes. The speed of overwash bore was measured using video technique by Holland et at. (1991). They modified conventional equation from dam breaking by Le Méhauté (1976) and proposed modified equation as $C = 2.6\sqrt{gh}$ to define the speed of the overwash bore.

Our field observations as well as investigations by Nelson and Bray (1970) indicated that between High Island and Sabine Pass where the study area is located the beach sand is only a thin veneer over the Holocene marsh and Pleistocene Beaumont Clays.

## 3.2. Study Area

The survey area was located along the northeastern Texas coast. The Texas State Highway 87 that comes from Galveston Island to the border of upper Texas has been destroyed for several decades by shoreline erosion with waves. The Coastal and Ocean Engineering Division in the Zachry Department of Civil Engineering at Texas A&M University has been monitoring these shoreline changes to study causes and solutions since 1999. High quality surveys were necessary to investigate erosion phenomenon, so RTK-DGPS (Real Time Kinematic–Differential Global Positioning System) was adapted to survey in study area for extreme accuracy within several centimeters. Morton (1975), Morton (1997), Wamsley (2000) and Lee (2003) had been investigating in the area for many years and they concluded that overwash caused by tropical storms might be a major factor to cause severe damages. Three overwash events were hindcasted in the study area January to October in 2004 and two overwash events were hindcasted by Hurricane Katrina and Rita in 2005.

### 3.2.1. Characteristics of Study Area

There are several major and minor factors to make shoreline changes. These changes depend on wind, rainfall, human activities, storms intensity and frequency, sea level rise, tides, wave actions, sand budget etc. Morton (1975) found some correlations between beach characteristics and shoreline changes in the area by analysis of other engineers' field observation results. He concluded that the vegetation line is important to understand long-

term shoreline movement, while the high-water line is more affected by short-term water level changes. He mentioned overwash and washover processes between High Island and Sabine Pass where the survey area was located and that frequent upland inundation and long-term erosion have destroyed Texas State Highway 87 on many occasions. Most of the overwash events occurred on the barrier island located in front of mainland but this study focused on overwash in the mainland. Littoral drift was moving from east to southwest along the coastline.

### 3.2.2. Selection of Study Area

This area between Galveston Island and Sabine Pass was investigated by Morton (1997) for several decades and was surveyed by Texas A&M University since 1999. The goal of this study was finding of the relationships between wave actions and overwash in storm conditions from quality field measurement results, so the selection of target area where overwash is likely to happen is very important. From their results, the most eroded area could be easily found from Fig. 3.1, Fig. 3.2, Fig. 3.3 and Table 3.1 where it showed the possibility of overwash. The erosion rate increased from Transect 17 and starts decreasing at Transect 35 and here the beach formed erosional scarp and washover terrace alternately along this area as shown in Fig. 3.2. Because overwash is expected to happen more frequently on the lowest dune elevations along the coast, the area from L126 to L128 in Fig. 3.3 could be considered to have the potential of overwash in the future. The study area was finally decided after location of some overwash evidences from several field investigations. The soil profile beneath the dune had several layers and it indicated that

overwash processes were repeated for a long time.

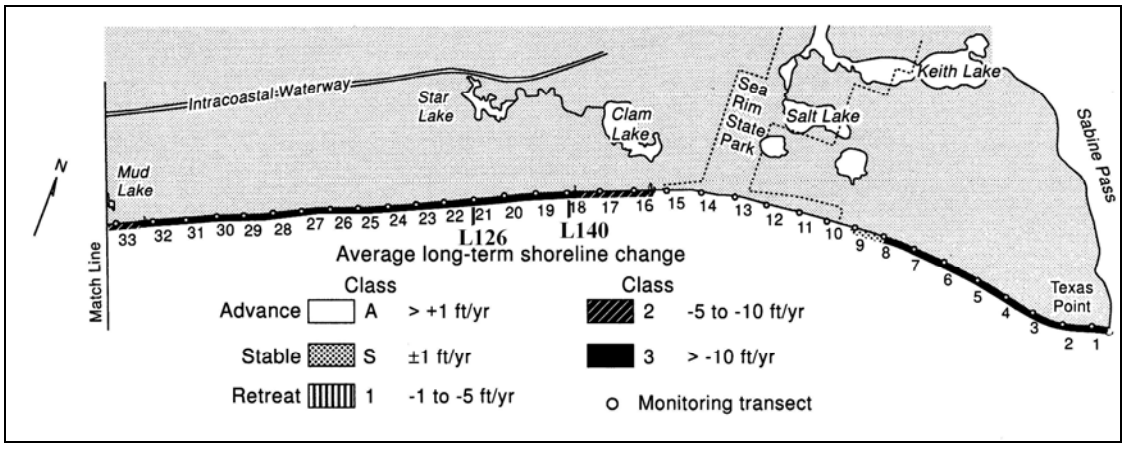


**Fig. 3.1. Average long-term shoreline change from 1974 to 1996 (from Morton, 1997).**

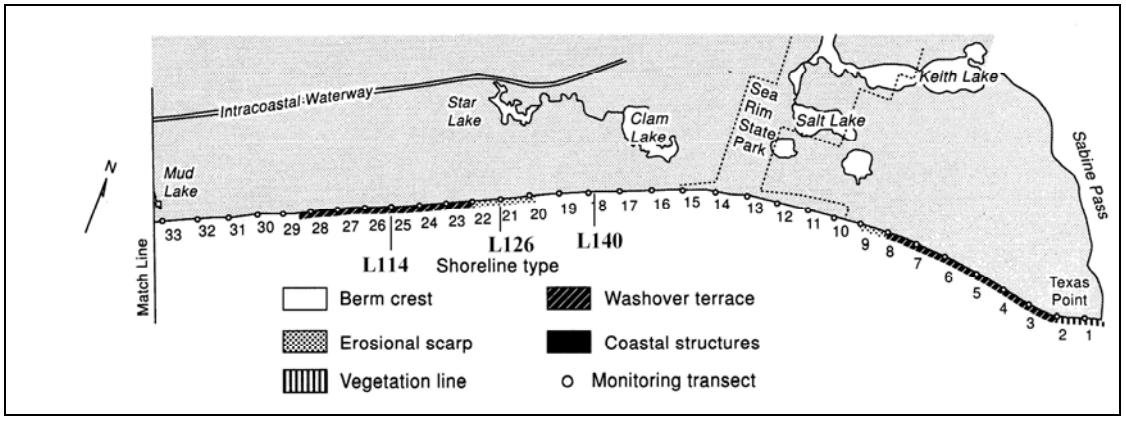


**Fig. 3.2. Shoreline types in survey area (from Morton, 1997).**

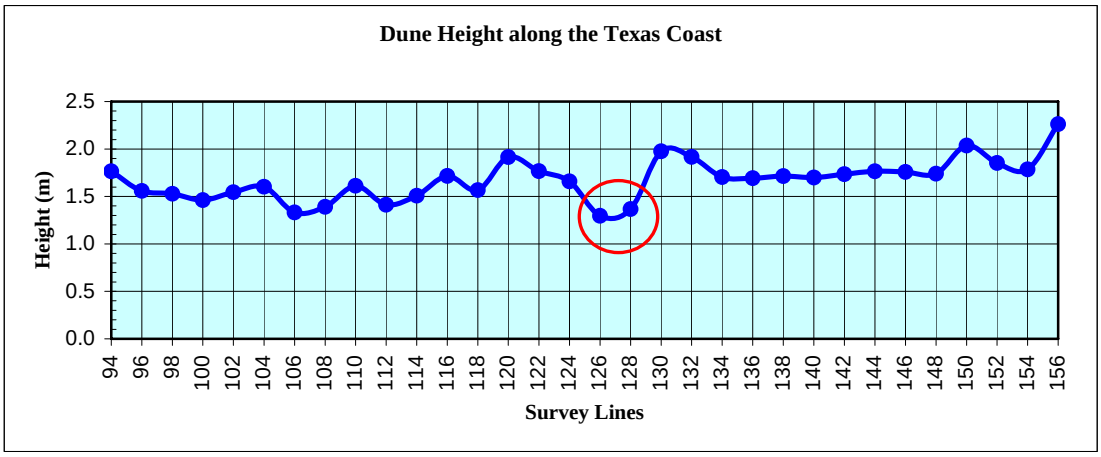


**Fig. 3.3. The peak dune height above mean sea level along the Texas coast from the Texas A&M University field survey in 2002. The study area is located between line 126 and 128 in the circle.**

**Table 3.1. Shoreline change at each transect, 1974-1996 (Morton, 1997). The survey area was located at Transect 21.**

| Transect | Net Change (m) | Average rate (m/yr) | Transect | Net Change (m) | Average rate (m/yr) |
|---|---|---|---|---|---|
| **5** | -213.4 | -9.8 | **34** | -55.8 | -2.6 |
| **6** | -194.8 | -9.0 | **35** | -60.0 | -2.8 |
| **7** | -142.0 | -6.6 | **36** | -25.3 | -1.2 |
| **8** | -1.5 | -0.1 | **37** | -5.5 | -0.2 |
| **9** | 22.3 | 1.0 | **38** | -1.5 | -0.1 |
| **10** | 76.5 | 3.5 | **39** | -11.9 | -0.5 |
| **11** | 79.6 | 3.7 | **40** | -12.8 | -0.6 |
| **12** | 14.6 | 0.7 | **41** | -8.5 | -0.4 |
| **13** | 25.0 | 1.2 | **42** | -2.4 | -0.1 |
| **14** | 28.7 | 1.3 | **43** | -33.5 | -1.6 |
| **15** | 13.4 | 0.6 | **44** | -30.2 | -1.4 |
| **16** | -35.4 | -1.6 | **45** | -37.2 | -1.7 |
| **17** | -61.3 | -2.8 | **46** | -42.1 | -1.9 |
| **18** | -80.8 | -3.7 | **47** | -27.4 | -1.3 |
| **19** | -78.3 | -3.6 | **48** | -33.2 | -1.5 |
| **20** | -75.6 | -3.5 | **49** | -32.0 | -1.5 |
| **21** | **-80.2** | **-3.7** | **50** | -15.2 | -0.7 |
| **22** | -93.9 | -4.3 | **51** | -39.9 | -1.8 |
| **23** | -114.6 | -5.3 | **52** | -23.5 | -1.1 |
| **24** | -103.3 | -4.8 | **53** | -42.7 | -2.0 |
| **25** | -89.6 | -4.1 | **54** | -50.9 | -2.3 |
| **26** | -95.4 | -4.4 | **55** | -32.9 | -1.5 |
| **27** | -102.7 | -4.7 | **56** | -17.4 | -0.8 |
| **28** | -87.8 | -4.1 | **57** | -35.4 | -1.6 |
| **29** | -77.1 | -3.5 | **58** | -4.9 | -0.2 |
| **30** | -75.3 | -3.5 | **59** | 8.5 | 0.4 |
| **31** | -73.2 | -3.4 | **60** | 14.9 | 0.7 |
| **32** | -74.7 | -3.4 | **61** | 43.3 | 2.0 |
| **33** | -64.3 | -3.0 | **62** | 115.5 | 5.3 |

A sand fence was built just in front of top of dune about 10 miles from Sabine Pass to High Island along the coast in spring, 2004, but it was destroyed by overwash after construction. Though Leatherman (1977) mentioned washover fan could serve as temporary reservoirs for redistribution of sediment by wind, the eolian effect has not been verified yet in the area. However, dominant southeast winds affected littoral drift that moved from east to southwest along the upper Texas coast. Nelson and Bray (1970) found that the beach in the area from Sabine Pass to High Island was covered by thin sand layer over the Holocene marsh and Pleistocene Beaumont clays. If this area is dominated by clay, the erosion rate will be accelerated due to deficit of sand source. From Galveston to Sabine Pass, wave height varied as much as 0.3 m alongshore in average condition. Sediment was also getting finer and changed from coarse silt to very fine silt in the same direction (Morton 1997). The averaged sand sizes which were measured from the survey results by Texas A&M University are shown in Lee (2003) and $D_{50}$ was 0.171 mm around Line 126.

## 3.3. Hurricane and Tropical Storm Impact

### 3.3.1. Hurricane Ivan

This storm had a double impact on the study site. It was developed on August 31, 2004 from the west coast of Africa and disappeared quickly after landfall at upper Texas Coast as shown in Fig. 3.4. Its first landfall was made as a 194 km/h (120 mph) hurricane (category 3 on the Saffir-Simpson scale) in Alabama on September 16, 2004 and final landfall was made as a tropical storm at Sabine Pass at 14:00 (UTC) September 24, 2004. It produced the maximum wind speed of 278 km/h (170 mph, Category 5 hurricane) and the wind speed of 74 km/h (35 mph, tropical storm) at landfall. The storm surge started rising from 0.315 m below mean sea level (MSL) 14 hours before landfall and became a peak height (0.580 m) 7 hours prior to landfall. However, sea level was decayed to 0.356 m at landfall due to the change of tide. There was overwash but it could not make severe damages. A flood was observed in Fig. 3.5 and Fig. 3.6 and a minor overwash fan was observed in Fig. 3.7. Dune breaches were produced before landfall Fig. 3.8.

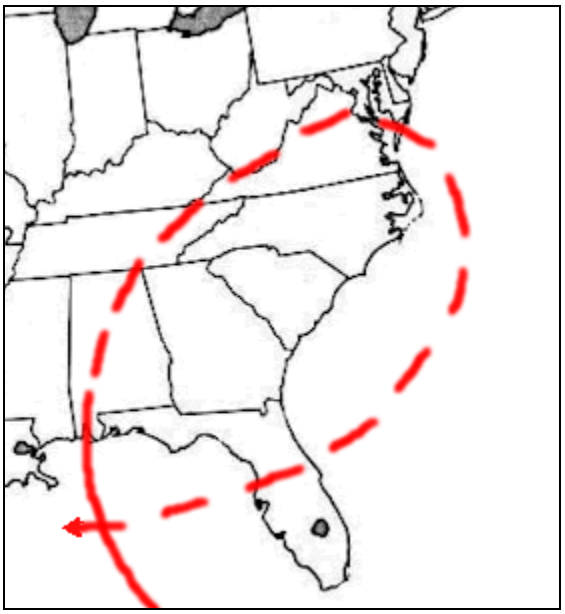

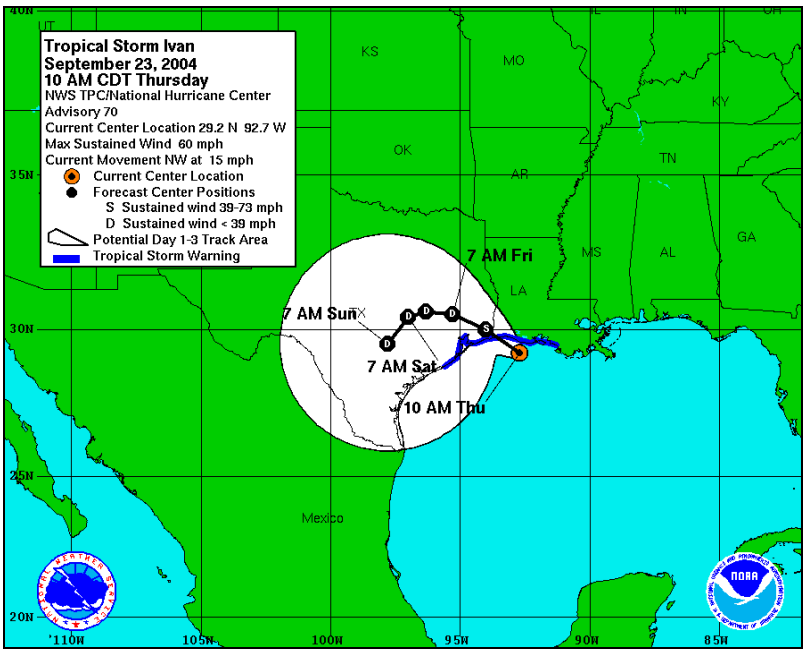


**Fig. 3.4. The track of the hurricane Ivan from Florida to Texas for two weeks. The weaken Ivan made landfall at Sabine Pass on September 23, 2004 (NOAA, 2004a).**

**Fig. 3.5. Water surface elevation was rising in the survey area on September 23, 2004, the day before landfall of tropical storm Ivan.**

**Fig. 3.6. The area behind the berm was flooded by ocean water prior to the landfall of tropical storm Ivan in the survey area on September 23, 2004.**

**Fig. 3.7. The survey area was overtopped by tropical storm Ivan in the survey area on September 23, 2004.**

**Fig. 3.8. Berm destruction by overwash prior to the landfall of tropical storm Ivan in the survey area on September 23, 2004.**

### 3.3.2. Tropical Storm Matthew

Tropical storm Matthew initially formed on October 8, 2004 from Tampico, Mexico and made landfall at Cocodrie, Louisiana on October 10, 2004. It produced the maximum wind speed of 74 km/h (46 mph) near eastern Texas and the wind speed of 65 km/h (40 mph) at landfall. Overwash was expected by the calculation of runup in this study but it did not have any impact on the study site. The track of tropical storm Matthew was shown in Fig. 3.9.

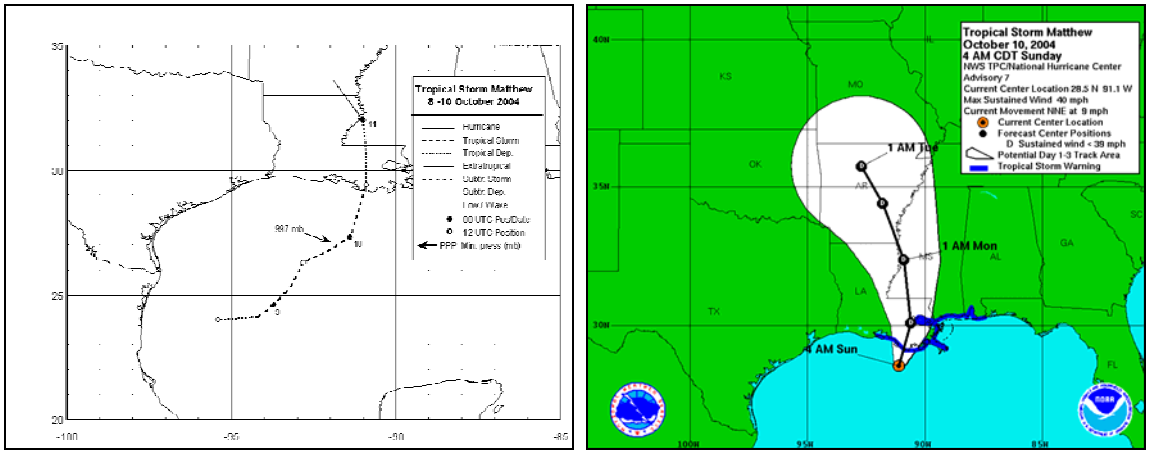


**Fig. 3.9. The track of tropical storm Matthew, 2004 (NOAA, 2004b).**

### 3.3.3. Hurricane Katrina

Hurricane Katrina initially formed on August 23, 2005 from the Bahamas. She made first landfall as a Category 1 hurricane at Miami, Florida on August 25, 2005 and second landfall near Buras-Triumph, Louisiana on August 29, 2005. It produced the maximum wind speed of 282 km/h (175 mph, Category 5 hurricane) in the Gulf of Mexico and the wind speed of 201 km/h (125 mph, Category 3 hurricane) at second landfall.

Most of New Orleans was flooded by beaching of the levee system with rising of storm surge and wave attacks. Hurricane Katrina made the most expensive natural disaster in U.S. history. Hurricane Katrina made a landfall in Louisiana but a massive overwash fan and inundation by swell were observed at landfall in the study site (Fig. 3.10). The track of hurricane Katrina was shown in Fig. 3.11.

**Fig. 3.10. Overwash fan generated by the swell of hurricane Katrina, 2005.**

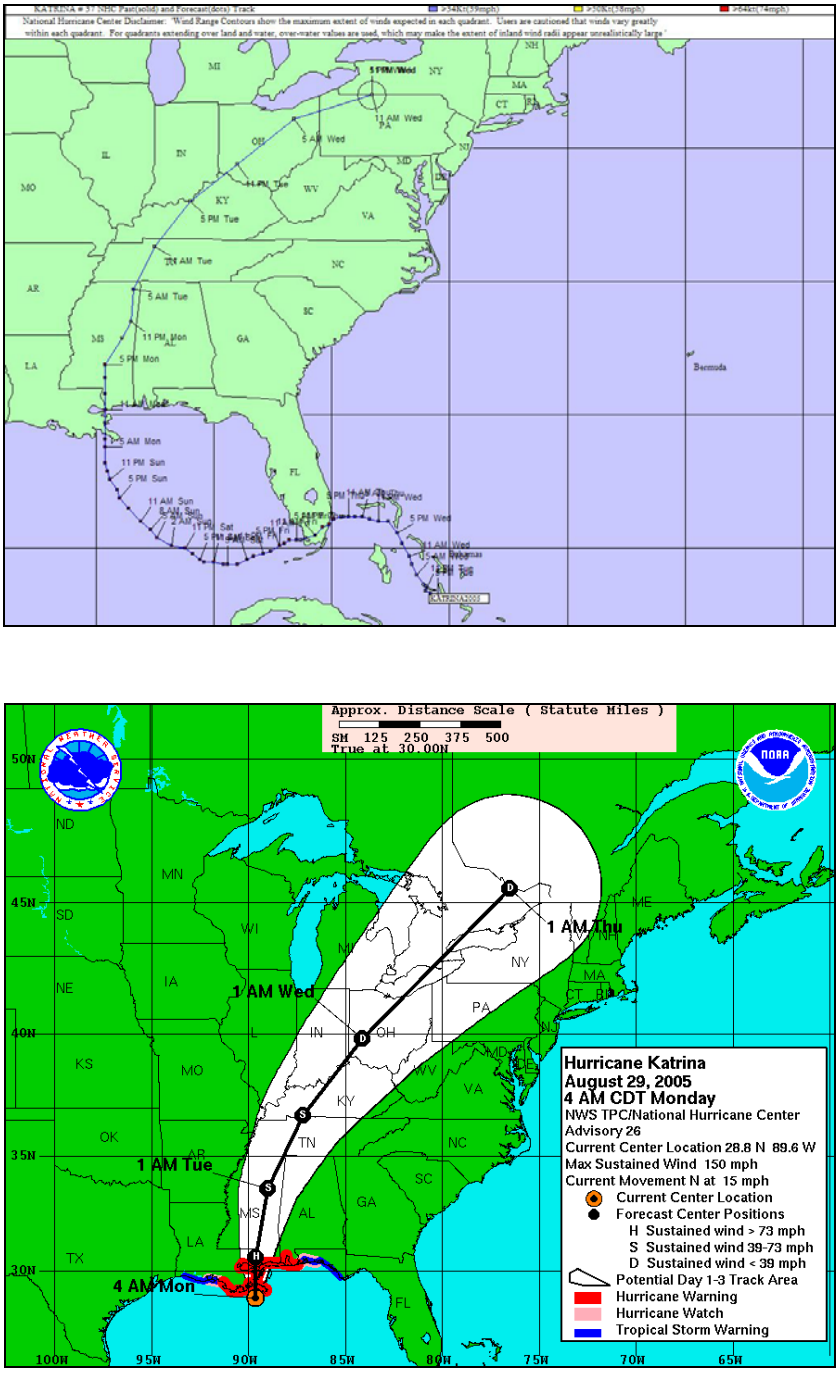


**Fig. 3.11. The track of hurricane Katrina, 2005 (NOAA, 2005).**

### 3.3.4. Hurricane Rita

Hurricane Rita initially formed on September 18, 2005 from the Turks and Caicos. She made landfall as a Category 3 hurricane at the Texas-Louisiana border on September 24, 2005. The track of hurricane Rita was shown in Fig. 3.12. It produced the maximum wind speed of 282 km/h (175 mph, Category 5 hurricane) in the Gulf of Mexico and the wind speed of 193 km/h (120 mph, Category 3 hurricane) at landfall. Local storm surge reached 4.6-6.1 m (15 to 20 feet) in southwestern Louisiana State. The one of peak storms surge was 2.8 m (9.24 feet) at Port Arthur, Texas.

The beach face was eroded completely and the clay bottom was exposed (Fig. 3.13). The eroded sand was transported by overwash and a massive deposition was made across the road. The field measurements were conducted by us on September 21, 2005 and September 29, 2005.

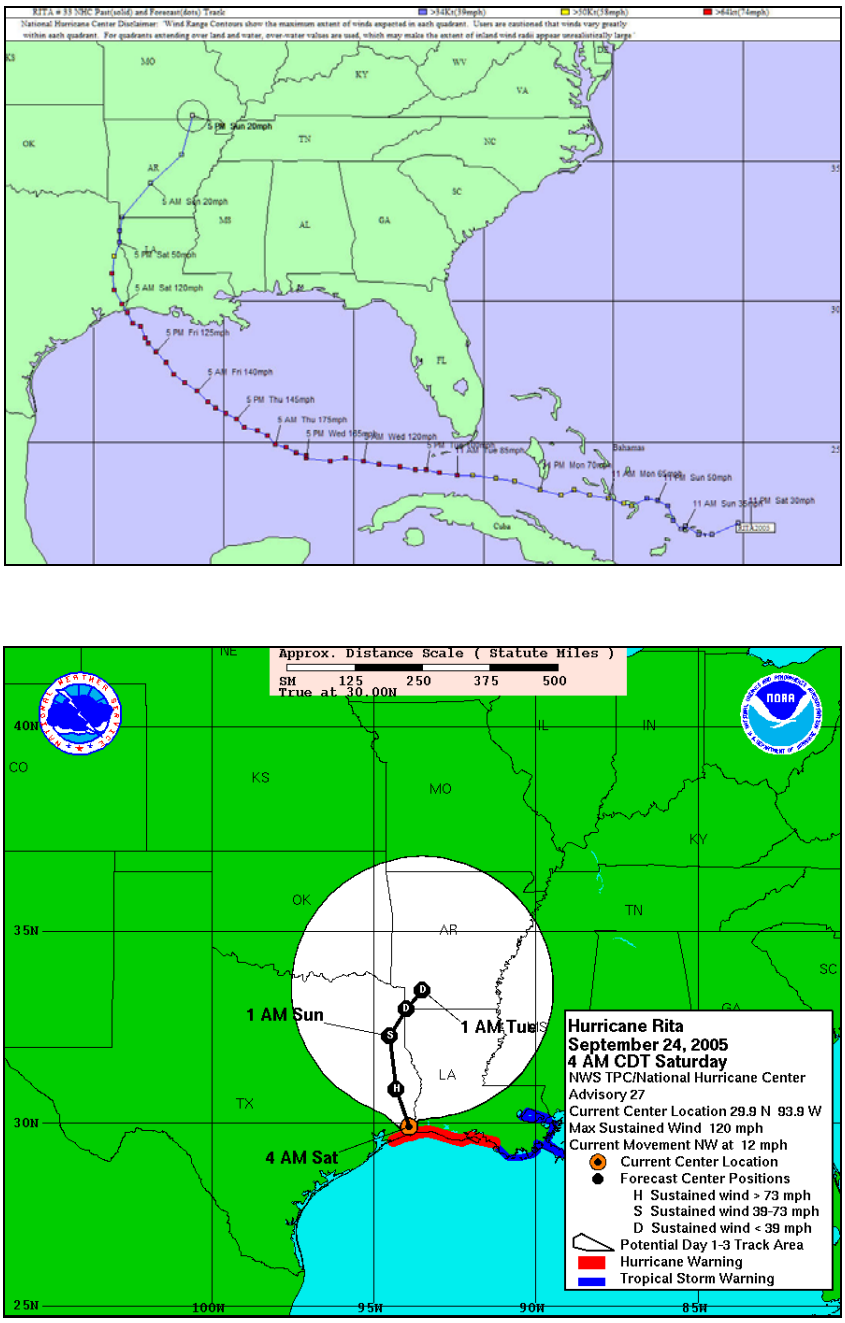


**Fig. 3.12. The track of hurricane Rita, 2005 (NOAA, 2006c).**


**Fig. 3.13. Before and after landfall of hurricane Rita, 2005. These photos were taken on September 21, 2005 and September 29, 2005.**

## 3.4. Field Survey Methods

There are several options available for surveying the shoreline. These options were reviewed to determine the best methodology for the particular objectives of this research.

### 3.4.1. GPS (Global Positioning System)

Over the centuries, men have sought the methods to figure out the exact location where they were. The GPS was developed and funded in the 1970's and has been supervised by U.S. Department of Defense for military purpose, even though millions of people have been using this system for their civilian one. The position information is obtained and calculated from the specially coded signals from 24 satellites orbiting the earth. Four satellites are sufficient to compute the four dimensions of X, Y, Z and Time at a point on the earth using triangulation. It rarely depends on weather condition but the satellite signal is degraded to limit accuracy for non-U.S. military and government users. However, the latest GPS equipment can conduct measurements within a centimeter by using the new RTK and DGPS techniques.

### 3.4.2. LIDAR (LIght Detection And Ranging)

LIDAR can be simply considered as a laser radar but they have some differences especially in wave length. LIDAR is a method using electromagnetic wave as a source for transmitting and receiving from the objects. The range of this electromagnetic wave is in

the ultraviolet, visible and infrared region at a high frequency. This radiated wave is transmitted to the object and receivers collect the reflected wave from it and get information of intensity and time delay between transmitted and reflected wave.

Recently, many researchers are applying LIDAR to remote scanning of huge area in given short period by companying with airborne system. This idea is very useful to survey pre and post changes by storms or natural activities in a certain area. However, it is difficult to measure in turbid or deep water. These short waves cannot penetrate the water and most of them can be absorbed in the water easily. As shown in Fig. 3.14 the LIDAR is mounted in the bottom of an airborne with GPS and measure the distance between the bottom of an airborne and targets on the ground. .

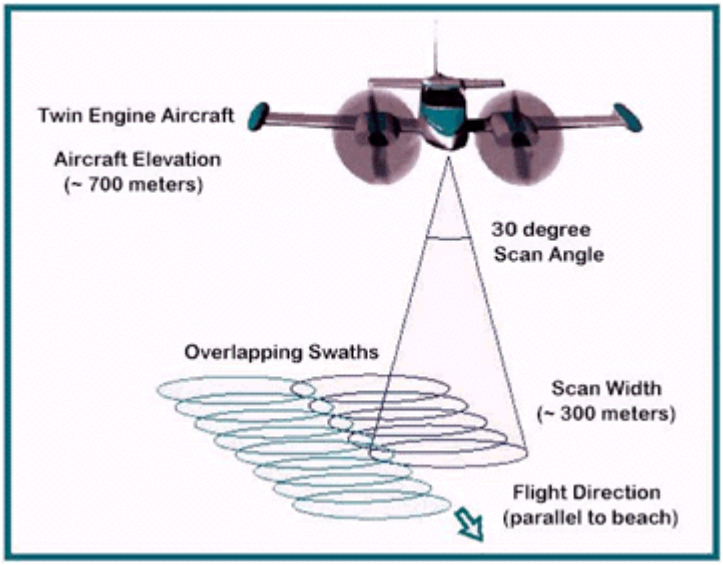


**Fig. 3.14. LIDAR with airborne system (NOAA, 1999).**

### 3.4.3. Oblique Aerial Video and Photography

Aerial photography was developed just after World War I to find structures and draw maps. These images obtained from the camera and video mounted on aircraft need to be corrected due to distortion caused by tilt of camera on aircraft. Photography also makes possible to get special information for special purposes using different wave lengths such as ultraviolet and infrared. The works and roles of this aerial photography are changing due to GIS (Geographic Information System), GPS (Global Positioning System) and digital mapping system in a rapid advancing technology. The greatest weakness of this aerial photography is lack of exact position information. Typically ground truth is obtained in combination with terrestrial surveys.

### 3.4.4. Conventional Method with Optical Equipment

Optical Equipments have been used in beach survey, geographical survey and construction for long time. This method can generate the most accurate result within a certain range but the error can be accumulated according to the survey distance. The quality of this survey depends on user's experiences, atmospheric conditions and survey equipments. Although this provides or can provide the most accurate data, it is the most labor intensive and time consuming method.

## 3.5. GPS Survey

### 3.5.1. RTK–GPS (Real Time Kinematic GPS)

RTK–GPS is a new technique to increase accuracy of measurement up to within a few centimeters. It is a much better method than conventional GPS that contains ± 50-100 m error from the actual GPS receiver position. It is a process to get correction signals from base receiver at a known location and send them to moving rover receivers for computing X, Y and Z position more accurately. RTK-GPS acts as a compensation for atmospheric signal delay and other errors in conventional GPS and gives users ultra high precise position information.

### 3.5.2. DGPS (Differential GPS)

DGPS is developed to correct bias errors at a remote location with measured bias errors at a known base or station. DGPS uses with two receivers at least to reduce the effects of satellite signal errors. GPS uses the timing signals that yield some errors for computing the position from 4 different satellites. If these two receivers are fairly close together (less than 100 km), they are considered to have virtually the same errors from the satellites. At that time, a reference receiver that is located in a known location computes corrections for each satellite signal. The calculated correction is provided to the remote or moving rover receivers with correction information. The common errors are virtually eliminated by these processes and the rover receivers have the accurate position. DGPS has

a meter accuracy in moving rover receivers and better accuracy in stationary receivers.

### 3.5.3. Trimble RTK-DGPS

The equipments used in this survey included the Trimble Total Station 4700, Trimble 5800 Limited GPS system and TRIMMARK II in Fig. 3.15. They have a horizontal and vertical accuracy of 2 cm + (1 ppm × baseline length) respectively (Trimble, 1999), it is up to ± 2.07 cm in this survey.


**Fig. 3.15. Trimble RTK-DGPS equipment in the survey.**

## 3.6. Survey Procedures

### 3.6.1. Hydrodynamic Data

Measuring waves, surge and tidal elevation was beyond the scope of this study so existing buoy information was used from NDBC 42035. The location of Station 42035 buoy (National Data Buoy Center) was 29° 14' 47" N, 94° 24' 30" W, 13.7 m deep and 27 km away from the coastline. The offshore waves that go through the offshore buoy reach the survey area about 25 minutes later. The significant wave heights and periods obtained from the Station 42035 buoy were used for calculation of maximum runup height on the beach. The Station Texas Point was located in 29° 40.7' N, 93° 50.2' W to measure tide elevation and the data from tide gage represented storm surge. The location of the buoy and tide gage were shown in Fig. 3.16. The potential of overwash was estimated from the summation of these maximum runup height and storm surge. The detailed procedures were described in next section.

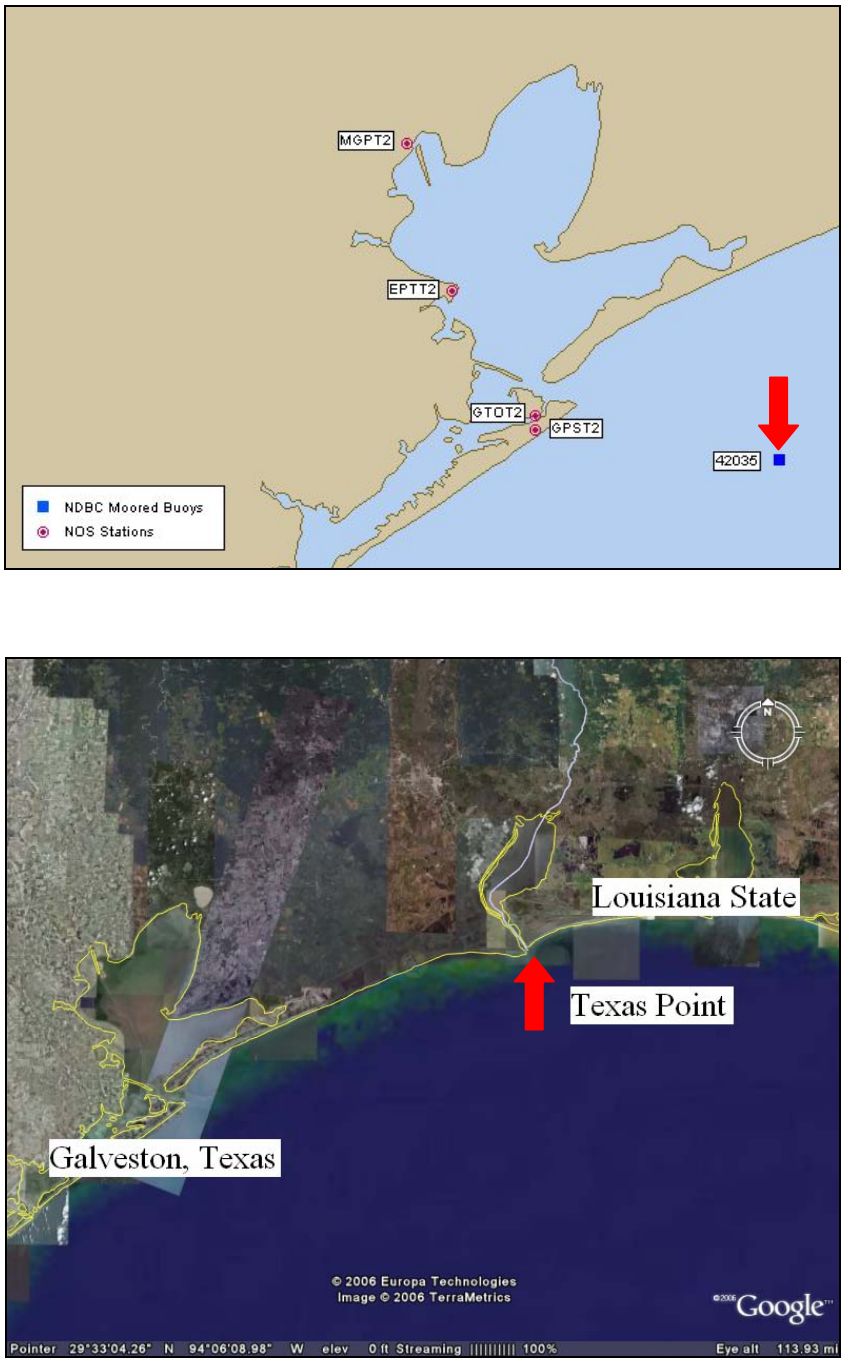


**Fig. 3.16. The National Data Buoy Center Station 42035 buoy and Station Texas Point for observation in Gulf of Mexico (NOAA, 2006d and TCOON, 2006).**

### 3.6.2. Beach Profile

The survey area contained 264 (24 × 11) measurement points and reached 115 m in the cross-shore and 400 m in the longshore direction (Table 3.2 and Fig. 3.17). Distances between points were 5 m and 40 m in cross-shore and the longshore direction respectively. The point started near the surf zone and ended approximately 40 m behind the top of berm in cross-shore direction. The reference monument, TAMU11 was chosen for the RTK-DGPS survey. Cross-shore lines T1 and T11 were in the same location as Texas A&M University survey line 126 and line 128 to share the historical survey results.

**Table 3.2. The coordinates of reference points in Texas A&M University survey. The elevation is relative to mean sea level.**

| Name | North | West | Elevation (m) |
|---|---|---|---|
| TAMU11 | 29° 38' 58.39206" N | 94° 7' 41.54936" W | 1.231 |
| T1-Start | 29° 38' 52.81474" N | 94° 7' 57.88673" W | |
| T1-End | 29° 38' 49.34858" N | 94° 7' 56.29417" W | |
| T11-Start | 29° 38' 57.92192" N | 94° 7' 44.12136" W | |
| T11-End | 29° 38' 54.46677" N | 94° 7' 42.49861" W | |

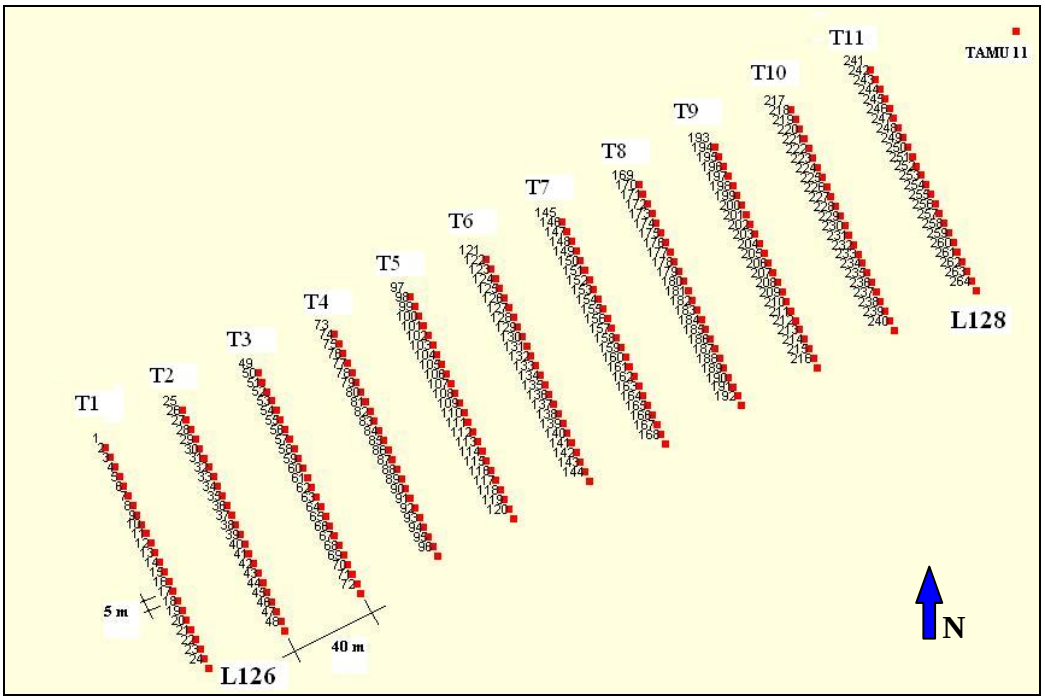


**Fig. 3.17. The measured points and monument in the survey area. Distances between points are 5 m in the cross-shore and 40 m in the longshore.**

### 3.7. Potential of Overwash

The main factor to determine potential of overwash is elevation of shoreward edge on the beach face. Overwash could be expected, when the summation of maximum runup heights, tides and storm surges was higher than the height of the berm. Total runup consisted of two primary components such as the setup and runup in swash zone and an oscillation in the swash zone having a long period (Komar 1998). The maximum runup was calculated from summation of these three components. Based on the experimental data of runup, Battjes (1974) proposed a correlation between the maximum vertical runup, offshore wave height and the Iribarren number.

$$\frac{R_{\max}}{H_s} = C\xi_o \tag{3.1}$$

$$\xi_o = \frac{S}{\sqrt{H_s / L_o}} \tag{3.2}$$

where $\xi_o$ is the Iribarren number, a dimensionless number relating to beach slope and wave conditions, $C$ is a dimensionless coefficient to be decided from experiment, $H_s$ is significant wave height in deep water, $L_o$ is wave length in deep water and $S$ is beach slope. Holman and Sallenger (1985) and Holman (1986) proposed that $C$ is approximately 0.9 on natural beach for 2 % exceedence of maximum runup, $R_{2\%}$ using results obtained from the intermediate slope beach in Duck, North Carolina.

$$R_{2\%,\max} = 0.9\frac{S}{\sqrt{H_s / L_o}} H_s \tag{3.3}$$

This equation is applicable to wave height in deep water ranged from 1.4 to 4.6 m, spectral peak period ranged from 7 to 17 sec and beach slope ranged from 0.005 to 0.047 (Ruggiero et al. 2001). This criterion was compared to the study area with a maximum

wave height in deep water about 3.0 m, spectral peak period ranges from 3 to 10 sec and averaged beach slope was 0.035 over the year 2004. It satisfied the standard suggested by Ruggiero et al. (2001) and could be used to hindcast the runup in the survey area. The averaged slope of beach face in observation area was 0.040 in September, 2004 (just before landfall of tropical storm Ivan) and became gradually a dissipative beach with time since 1999.

The 2 % exeedence of maximum runup at each offshore wave height and period based on equation (3.3) is shown in Table 3.3. If the height of berm was over 1 m, overwash started at the red cell without considering elevation of tide. Because overwash was determined from the summation of maximum runup and measured tide, tide had to be added to the calculation for overwash in a real situation.

The survey beach was categorized as the intermediate beach based on Wright and Short (1983)'s classification as follows,

- $\tan\beta \approx 0.01$ : Dissipative beach, Spilling breaker.
- $\tan\beta \approx 0.01 - 0.1$ : Intermediate beach, Plunging breaker.
- $\tan\beta \approx 0.1 - 0.2$ : Reflective beach, Plunging to surging breakers.

The morphology of the dissipative beach dissipates the wave energy generated by wind. The waves break offshore and become the spilling breakers prior to shore while losing energy continuously. The dissipative beach has a mild slope at beach and the spilling breaker. The intermediate beach has complex bar-trough systems from various water circulation patterns. It has the plunging breaker. The waves in the reflective beach break close to shore with little loss of wave energy. The reflective beach has a steep slope and the wave breaker ranges from plunging to surging breakers.

**Table 3.3. Wave runup height based on given wave height and period for slope of 0.04 (unit: meter).**

| Period \ Height | 1 | 1.5 | 2 | 2.5 | 3 | 3.5 | 4 | 4.5 | 5 |
|---|---|---|---|---|---|---|---|---|---|
| **1** | 0.04 | 0.06 | 0.06 | 0.07 | 0.08 | 0.08 | 0.09 | 0.10 | 0.10 |
| **2** | 0.09 | 0.11 | 0.13 | 0.14 | 0.16 | 0.17 | 0.18 | 0.19 | 0.20 |
| **3** | 0.13 | 0.17 | 0.19 | 0.21 | 0.23 | 0.25 | 0.27 | 0.29 | 0.30 |
| **4** | 0.18 | 0.22 | 0.25 | 0.28 | 0.31 | 0.34 | 0.36 | 0.38 | 0.40 |
| **5** | 0.22 | 0.28 | 0.32 | 0.36 | 0.39 | 0.42 | 0.45 | 0.48 | 0.50 |
| **6** | 0.27 | 0.33 | 0.38 | 0.43 | 0.47 | 0.50 | 0.54 | 0.57 | 0.60 |
| **7** | 0.31 | 0.39 | 0.45 | 0.50 | 0.55 | 0.59 | 0.63 | 0.67 | 0.70 |
| **8** | 0.36 | 0.44 | 0.51 | 0.57 | 0.62 | 0.67 | 0.72 | 0.76 | 0.80 |
| **9** | 0.40 | 0.50 | 0.57 | 0.64 | 0.70 | 0.76 | 0.81 | 0.86 | 0.91 |
| **10** | 0.45 | 0.55 | 0.64 | 0.71 | 0.78 | 0.84 | 0.90 | 0.95 | 1.01 |
| **11** | 0.49 | 0.61 | 0.70 | 0.78 | 0.86 | 0.93 | 0.99 | 1.05 | 1.11 |
| **12** | 0.54 | 0.66 | 0.76 | 0.85 | 0.93 | 1.01 | 1.08 | 1.15 | 1.21 |
| **13** | 0.58 | 0.72 | 0.83 | 0.92 | 1.01 | 1.09 | 1.17 | 1.24 | 1.31 |
| **14** | 0.63 | 0.77 | 0.89 | 1.00 | 1.09 | 1.18 | 1.26 | 1.34 | 1.41 |
| **15** | 0.67 | 0.83 | 0.95 | 1.07 | 1.17 | 1.26 | 1.35 | 1.43 | 1.51 |

### 3.8. Survey Results – Hydrodynamic

The calculation of maximum runup height based on equation (3.3), tide elevations and storm surges were used for hindcast of overwash in the survey area. Maximum water level based on the summation of maximum runup heights, tides and storm surges were calculated at each landfall of storm in Table 3.4. It showed there were five overwash events since January 2004. The wave data (Fig. 3.18 and Fig. 3.19) from the offshore buoy showed the similar high wave conditions to occur overwash events but on those cases the storm surge was not sufficient to generate overwash in this period. Any overwash was not observed in April and August 2004 (Fig. 3.20 and Fig. 3.21). The conditions on September 15, 2004 (Fig. 3.22) had a relatively longer wave than other overwash events. It meant this study area was affected by swell which had a long period from Hurricane Ivan (category 3), when it made landfall in Alabama with a strong wind (195 km/h) on September 16, 2004. Overwash by swell was also found in analysis of hurricane Katrina which made a landfall in Louisiana. Overwash was expected by tropical storm Matthew (Fig. 3.23) but erosion was not observed in Table 3.6. Though hurricane Katrina made a landfall in Louisiana, overwash by a long period swell was expected in Fig. 3.24 and observed in Fig. 3.10. Massive erosion by overwash was produced for 26 hours at landfall of hurricane Rita (category 3) and its wave height and period were shown in Fig. 3.25.

**Table 3.4. Maximum water level at Sabine Pass, Texas (wave data from NOAA).**

| Date | $H_s$ | $T_s$ | Surge | $R_{2\%,\max}$ | Maximum water level | Storm |
|---|---|---|---|---|---|---|
| **September 15, 2004** | 2.4 m | 9.4 s | 0.53 m | 0.65 m | 1.18 m | Hurricane Ivan (Alabama) |
| **September 22, 2004** | 2.1 m | 4.9 s | 0.78 m | 0.32 m | 1.10 m | Tropical storm Ivan (Texas) |
| **October 8, 2004** | 1.8 m | 5.3 s | 0.76 m | 0.32 m | 1.08 m | Tropical storm Matthew (Louisiana) |
| **August 29, 2005** | 2.6 m | 7.0 s | 0.46 m | 0.50 m | 0.96 m | Hurricane Katrina (Louisiana) |
| **September 24, 2005** | 4.5 m | 6.2 s | 0.95 m | 0.59 m | 1.54 m | Hurricane Rita (Texas) |

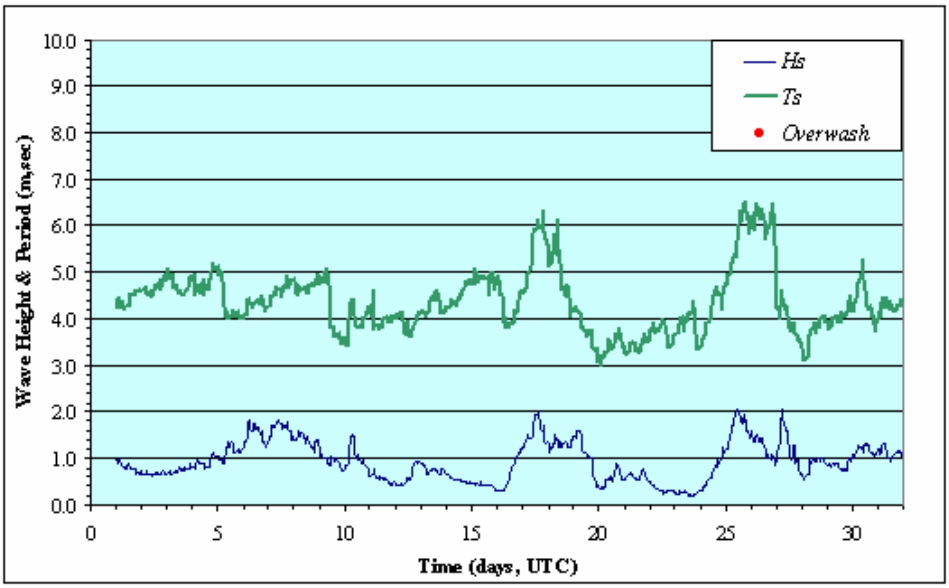


**Fig. 3.18. Observed significant wave height and period from offshore buoy in January, 2004.**

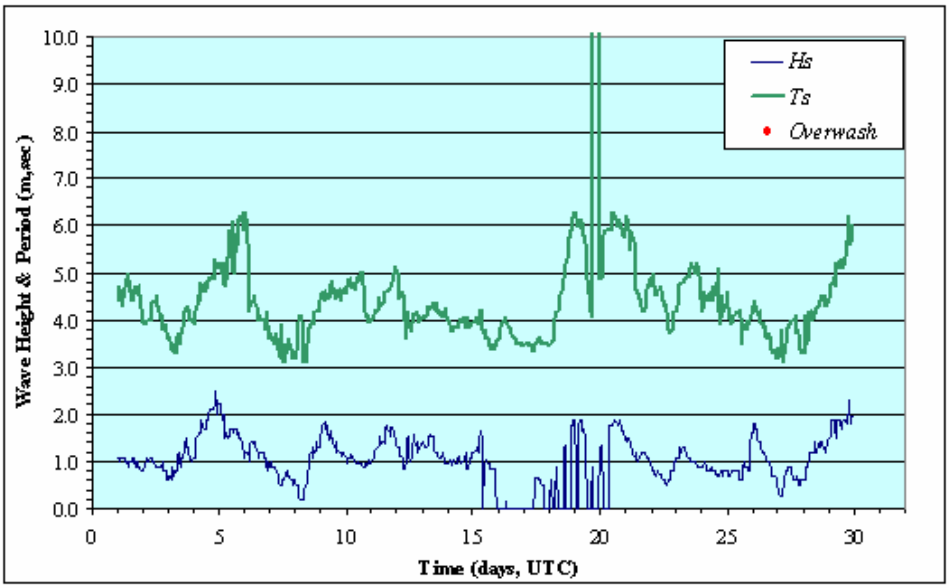


**Fig. 3.19. Observed significant wave height and period from offshore buoy in February, 2004.**

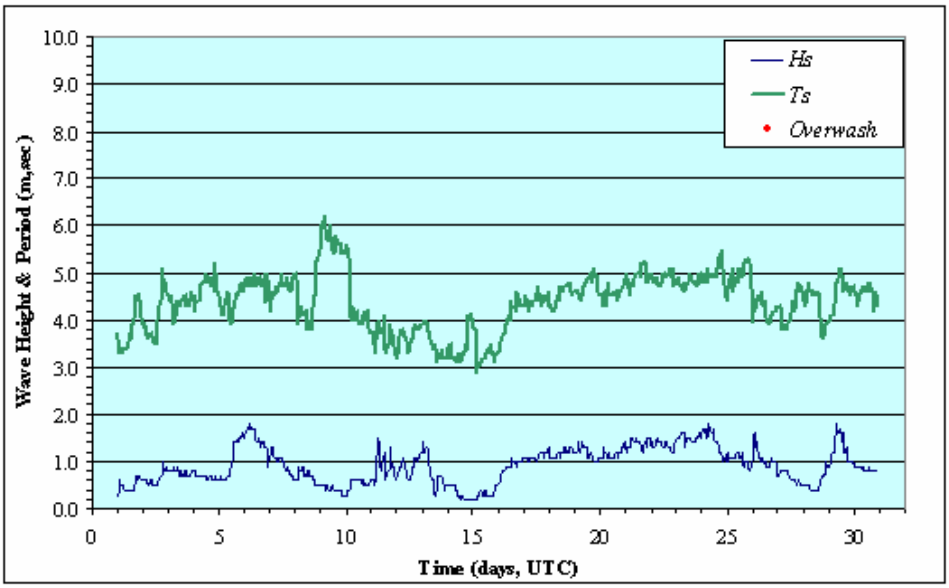


**Fig. 3.20. Observed significant wave height and period from offshore buoy in April, 2004.**

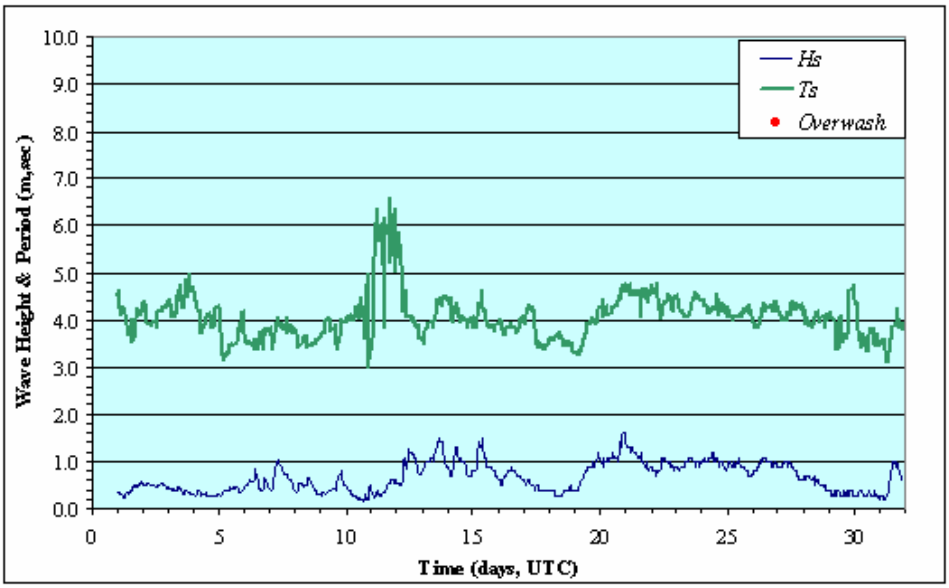


**Fig. 3.21. Observed significant wave height and period from offshore buoy in August, 2004.**

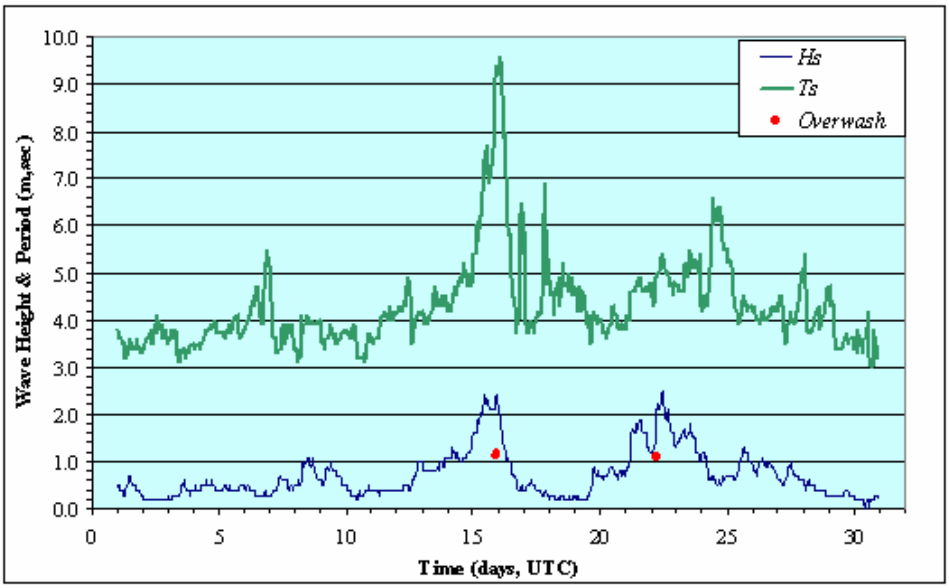


**Fig. 3.22. Observed significant wave height and period from offshore buoy in September, 2004 (hurricane Ivan).**

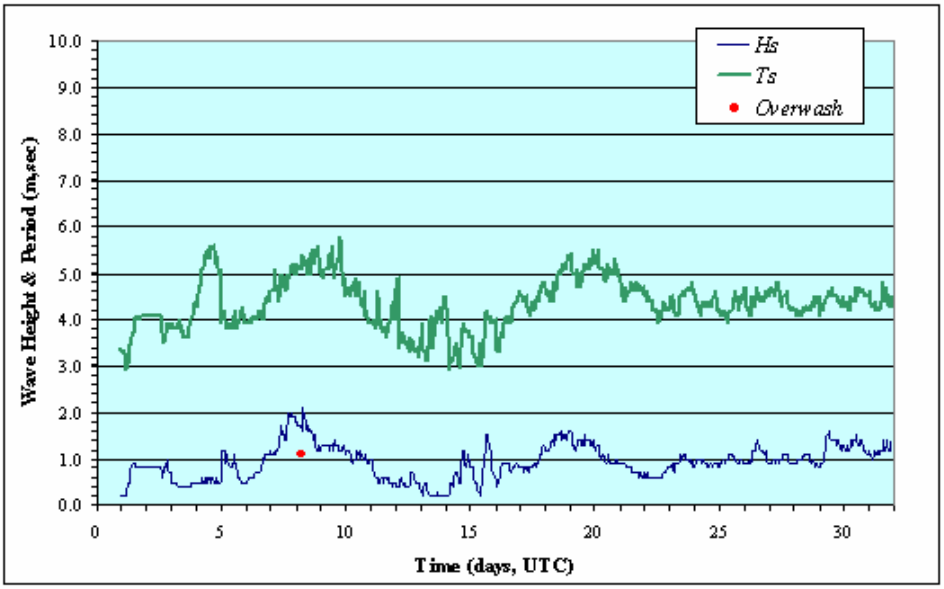


**Fig. 3.23. Observed significant wave height and period from offshore buoy in October, 2004 (tropical storm Matthew).**

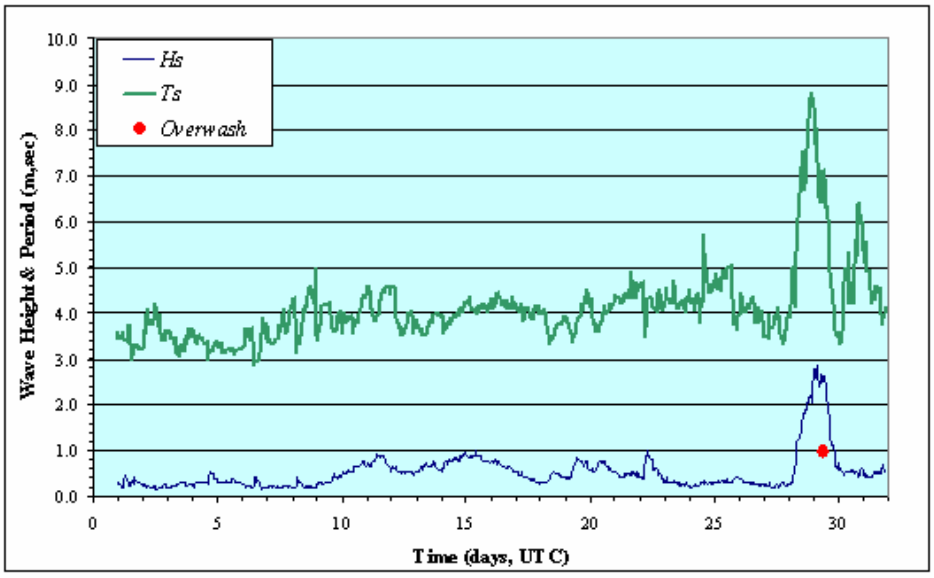


**Fig. 3.24. Observed significant wave height and period from offshore buoy in August, 2005. Hurricane Katrina made a landfall on the morning of August 29, 2005.**

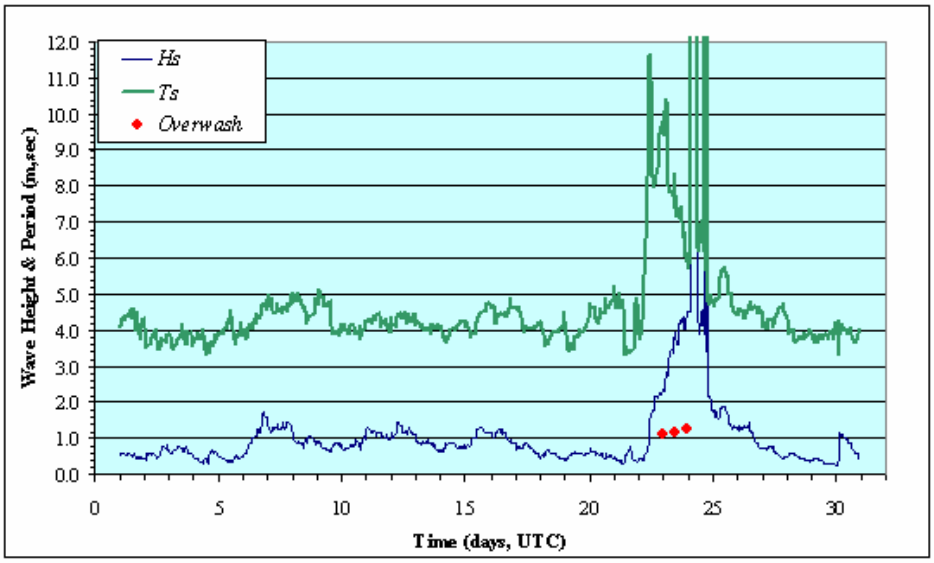


**Fig. 3.25. Observed significant wave height and period from offshore buoy in September, 2005. Hurricane Rita made a landfall on September 24, 2005.**

## 3.9. Survey Results – Beach Profile

### 3.9.1. Beach Profiles in 2D View

Beach measurements using RTK-DGPS were conducted for 8 times in Table 3.5. The survey date was selected according to abnormal event obtained from tide gage and tropical storms. No overwash was observed in Fig. 3.26, Fig. 3.27 and Fig. 3.28. The intensive berm erosion was measured by survey between August and September, 2004 (Fig. 3.29 and Fig. 3.30) and post-storm deposition was revealed in survey between September and October, 2004 (Fig. 3.31).

The extreme erosion also happened between September 21, 2005 and September 29, 2005 (Fig. 3.32 and Fig. 3.33) by landfall of hurricane Rita. The elevation data at each survey were used to calculate beach changes.

**Table 3.5. Date of field measurements and overwash events.**

| | Date of surveys | Overwash events |
|---|---|---|
| 1 | January 13, 2004 | No overwash |
| 2 | February 16, 2004 | No overwash |
| 3 | April 2, 2004 | No overwash |
| 4 | August 18, 2004 | No overwash |
| 5 | September 22, 2004 | Overwash by Ivan<br>August 15 and August 22, 2004 |
| 6 | October 3, 2004 | Overwash by Matthew<br>October 8, 2004 |
| 7 | September 21, 2005 | Overwash by hurricane Rita<br>September 23 – 24, 2005 |
| 8 | September 29, 2005 | |

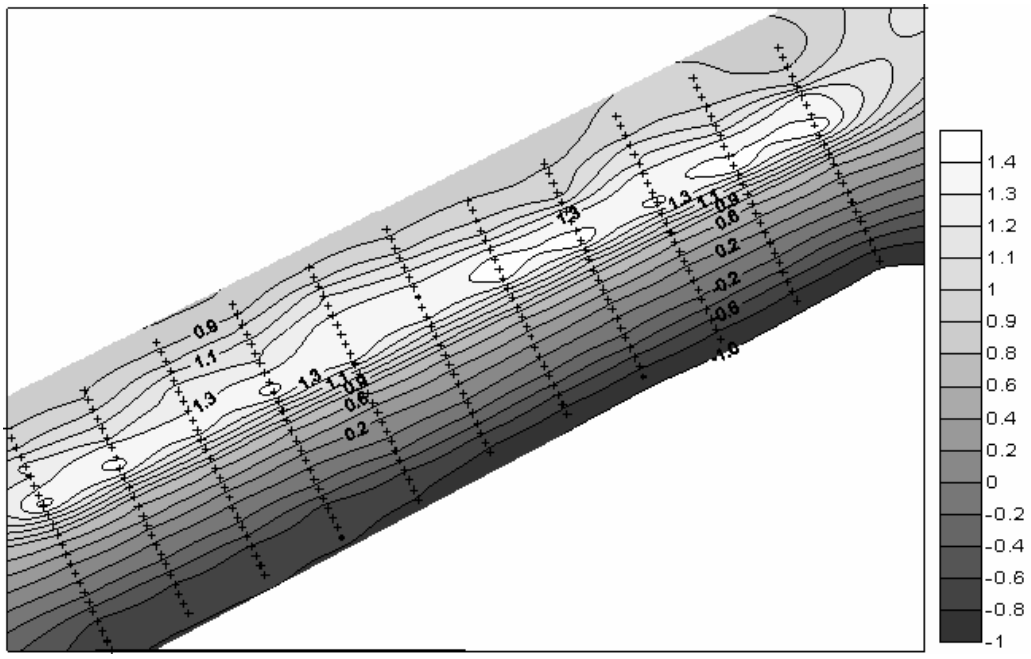


**Fig. 3.26. Contour of survey result on January 13, 2004 (Unit: meter).**

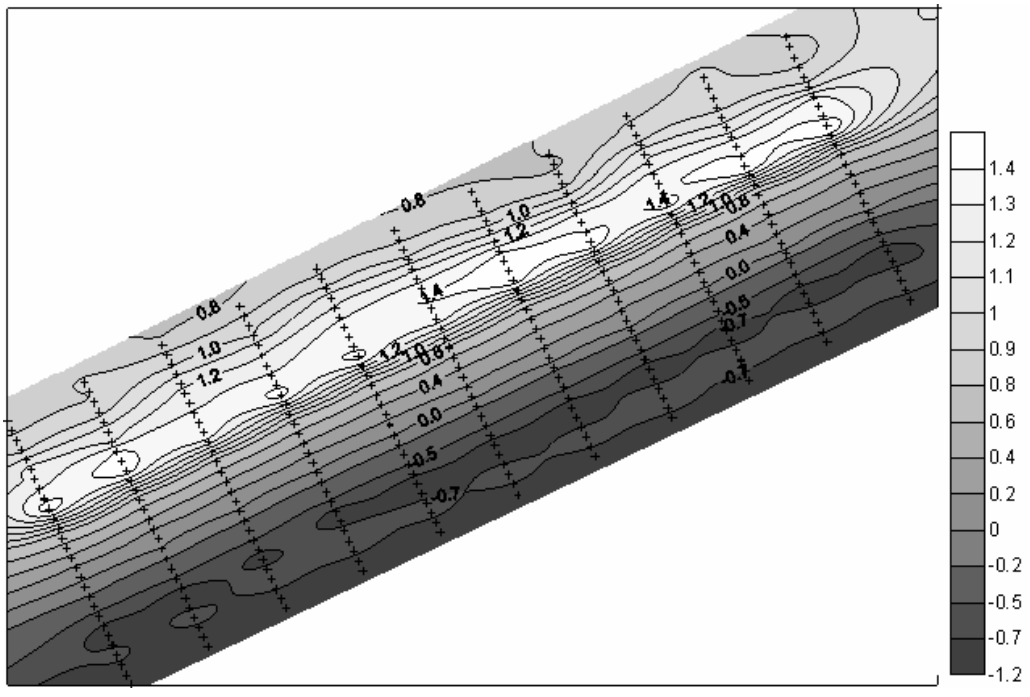


**Fig. 3.27. Contour of survey result on February 16, 2004 (Unit: meter).**

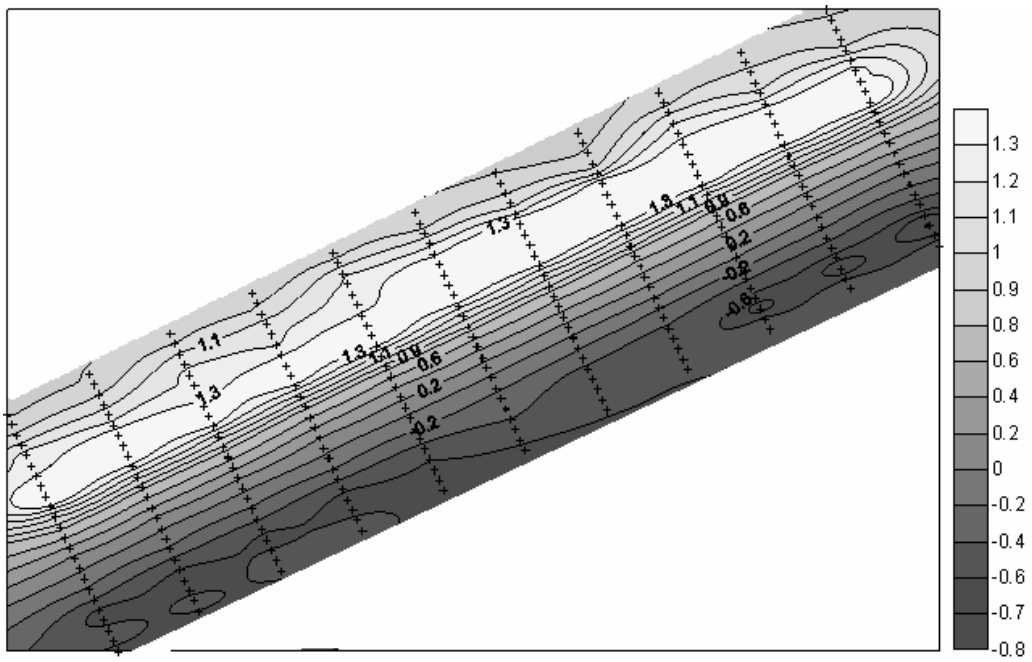


**Fig. 3.28. Contour of survey result on April 02, 2004 (Unit: meter).**

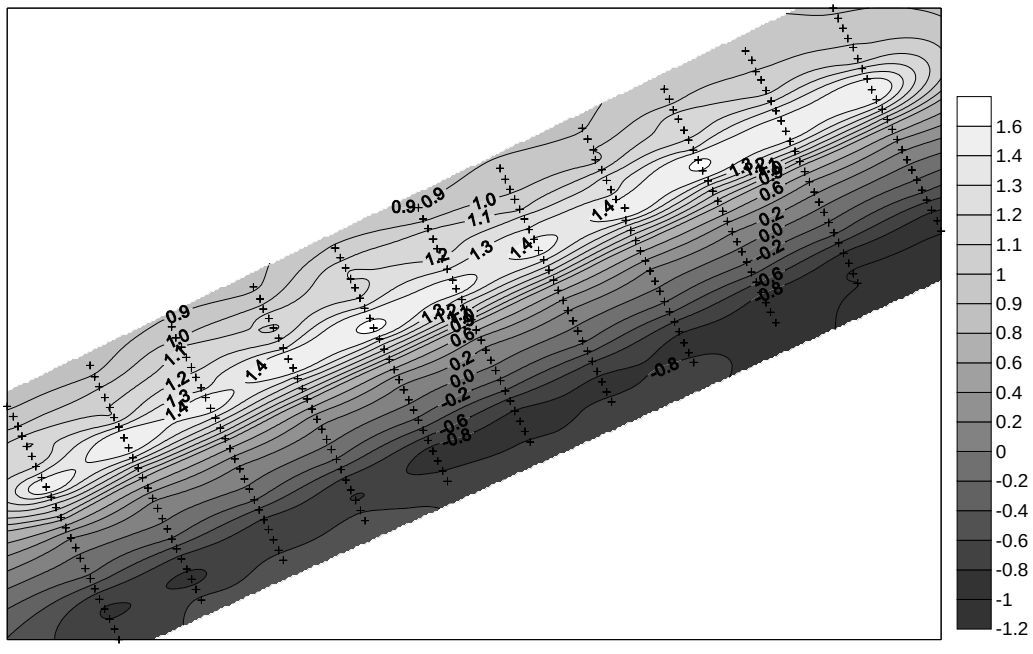


**Fig. 3.29. Contour of survey result on August 18, 2004 (Unit: meter).**

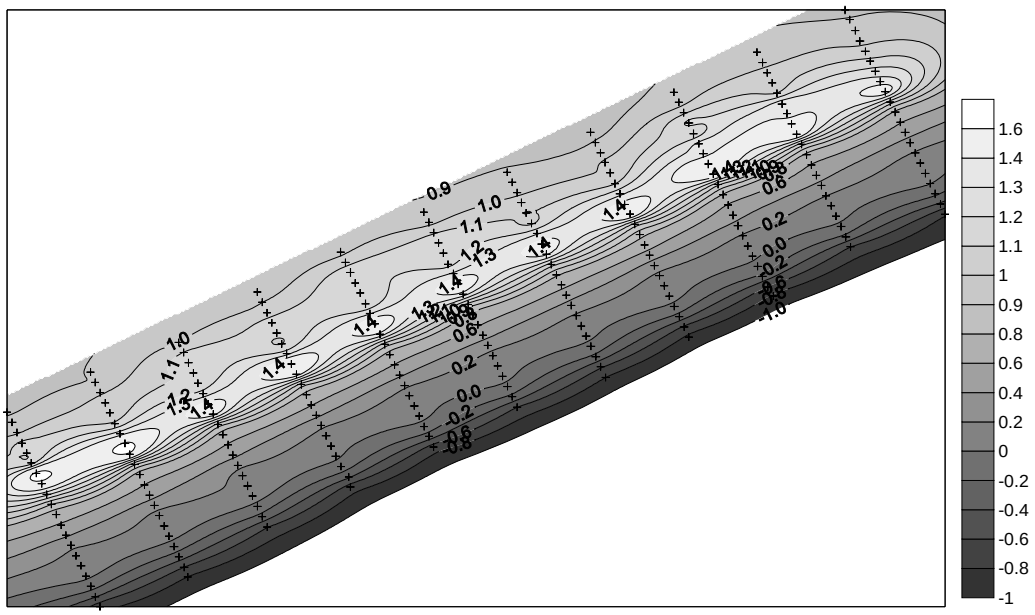


**Fig. 3.30. Contour of survey result on September 22, 2004 (Unit: meter).**

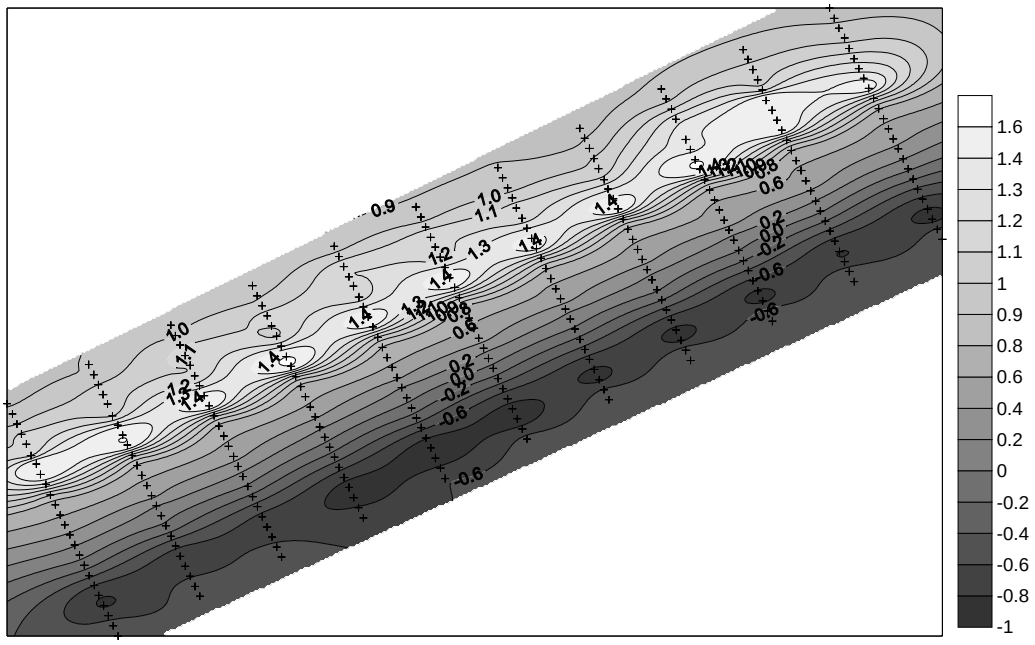


**Fig. 3.31. Contour of survey result on October 3, 2004 (Unit: meter).**

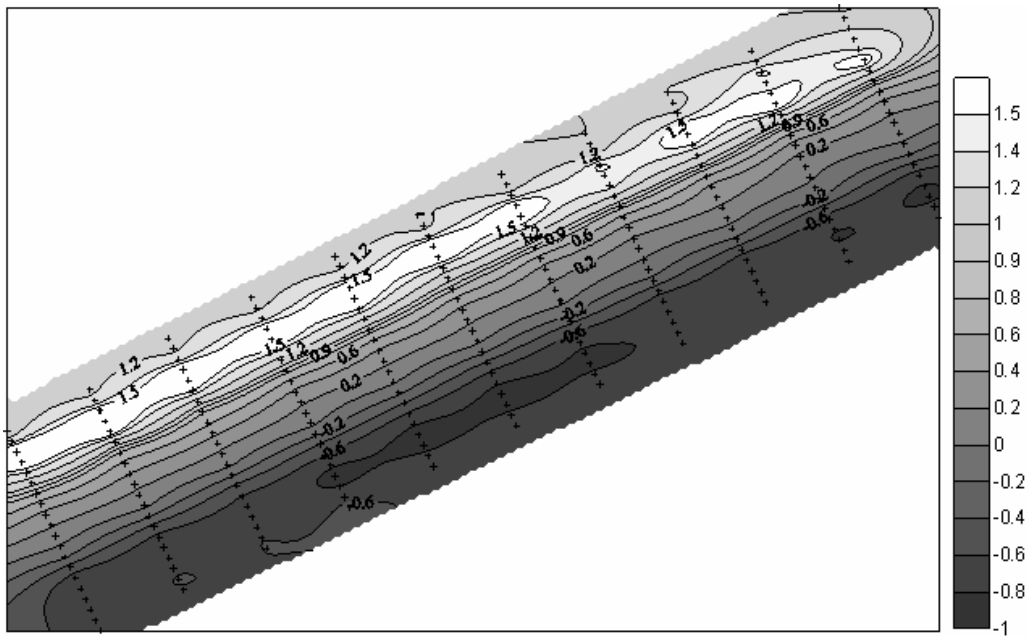


**Fig. 3.32. Contour of survey result on September 21, 2005 (Unit: meter).**

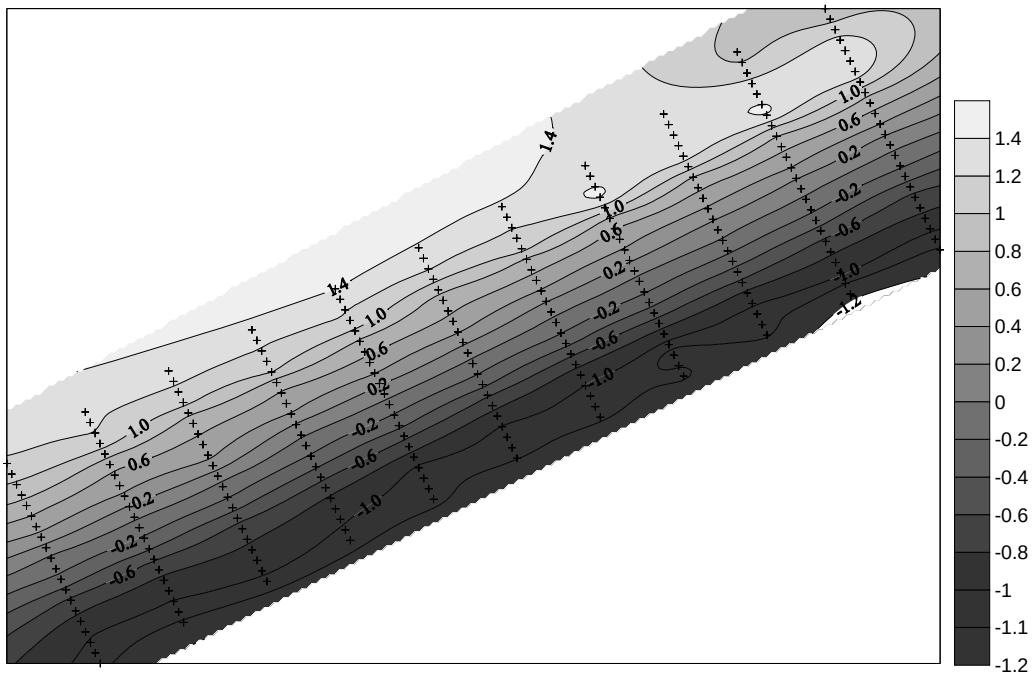


**Fig. 3.33. Contour of survey result on September 29, 2005 (Unit: meter).**

### 3.9.2. Cross-Shore Beach Profiles at Each Line

The cross-shore beach profiles were measured in 11 lines and the distance between them was 40.0 meters in longshore direction. The elevation data had a data point every 5.0 meters in cross-shore direction. The survey line T1 and T11 were compared to the previous survey results since 1999 (Fig. 3.34 to Fig. 3.44). They showed that the coastline was retreated by about 20 meters for six years. Apparent massive erosion by overwash at landfall of hurricane Rita was shown in each line. The dune was destroyed completely and it became flat. The eroded sand was transported and deposited behind the previous berm. The breach in the berm by tropical storm Ivan was observed and the berm was lower and flat by hurricane Rita (Fig. 3.45).

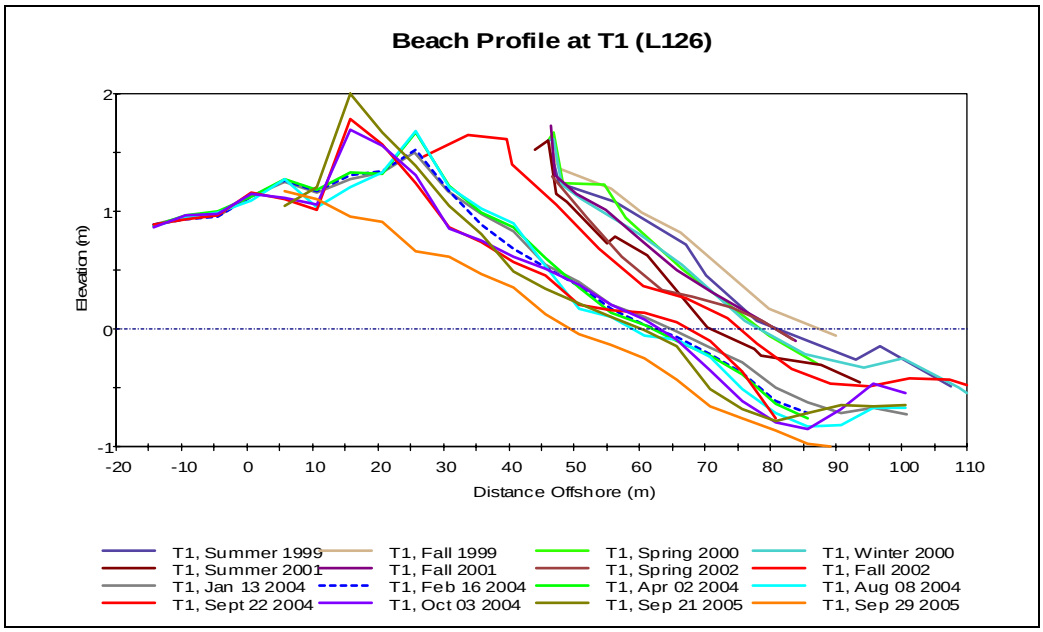


**Fig. 3.34. The cross-shore beach profile at T1 (L126) since 1999.**

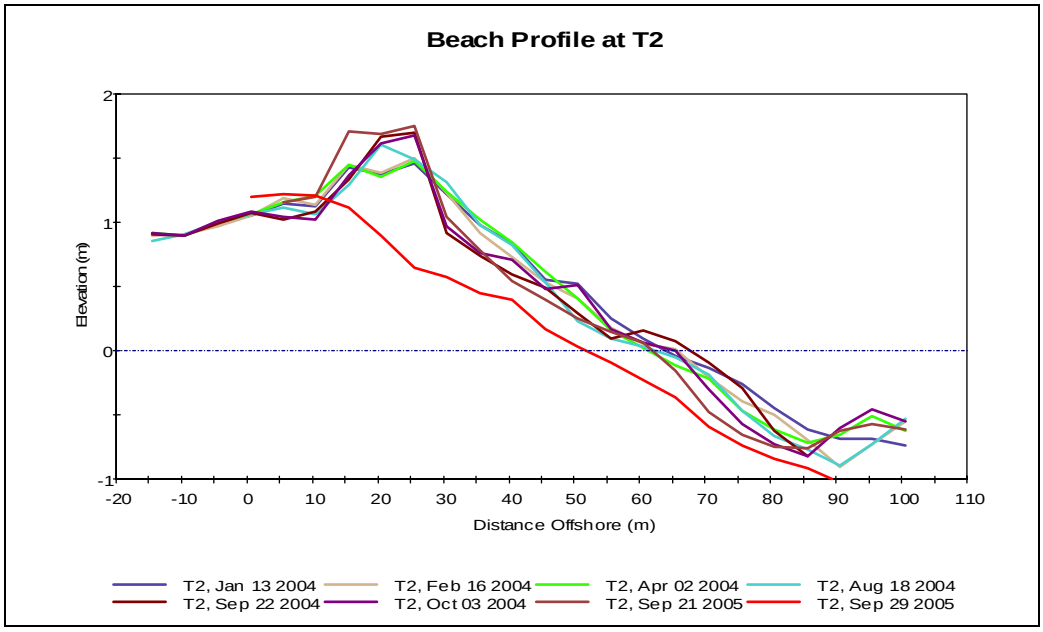


**Fig. 3.35. The cross-shore beach profile at T2 since January 2004.**

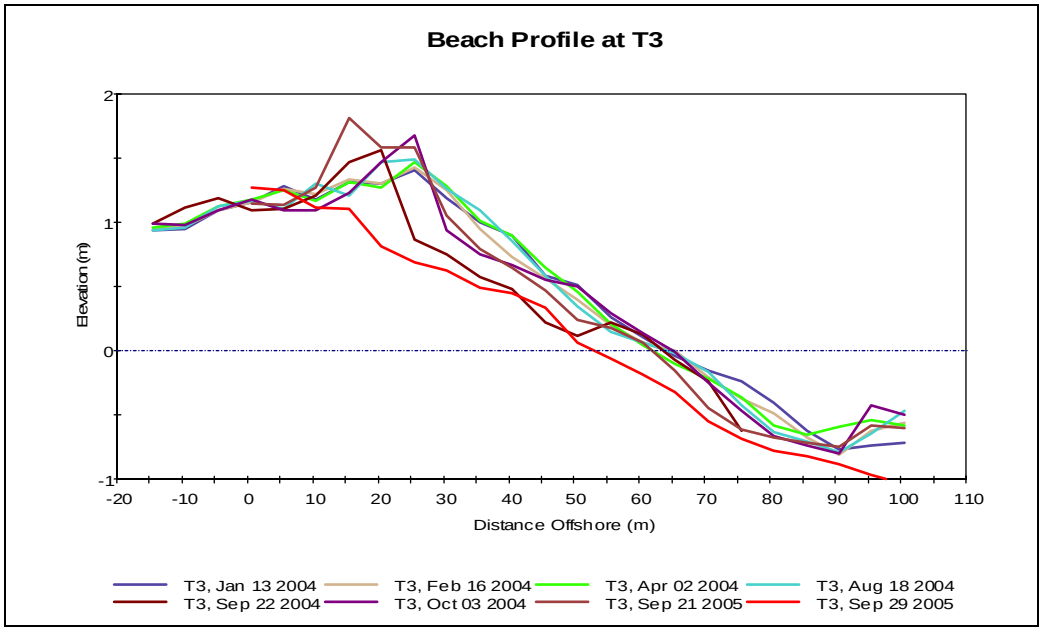


**Fig. 3.36. The cross-shore beach profile at T3 since January 2004.**

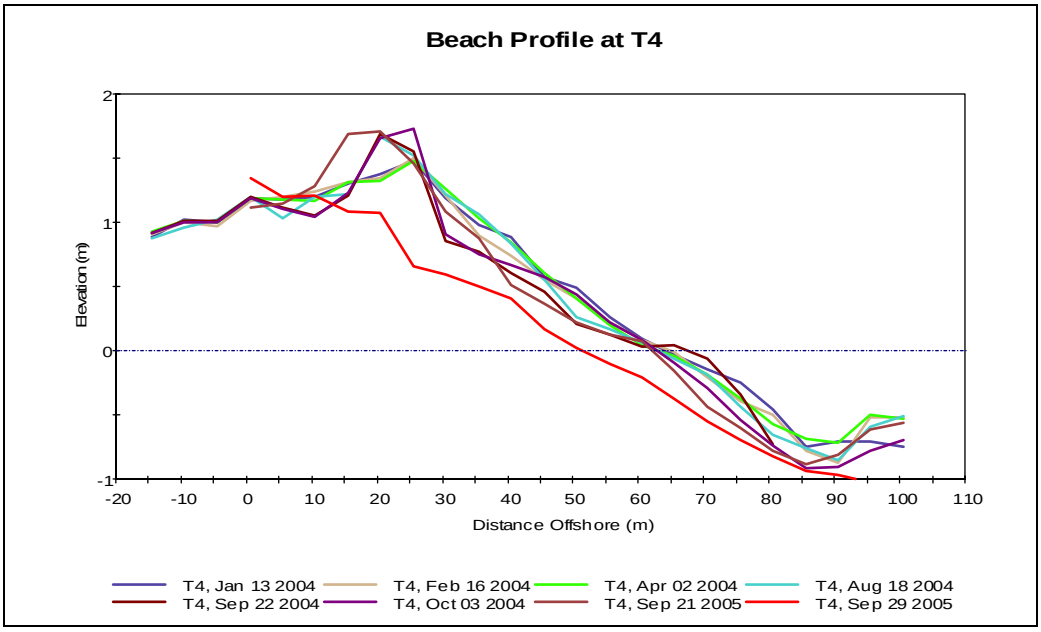


**Fig. 3.37. The cross-shore beach profile at T4 since January 2004.**

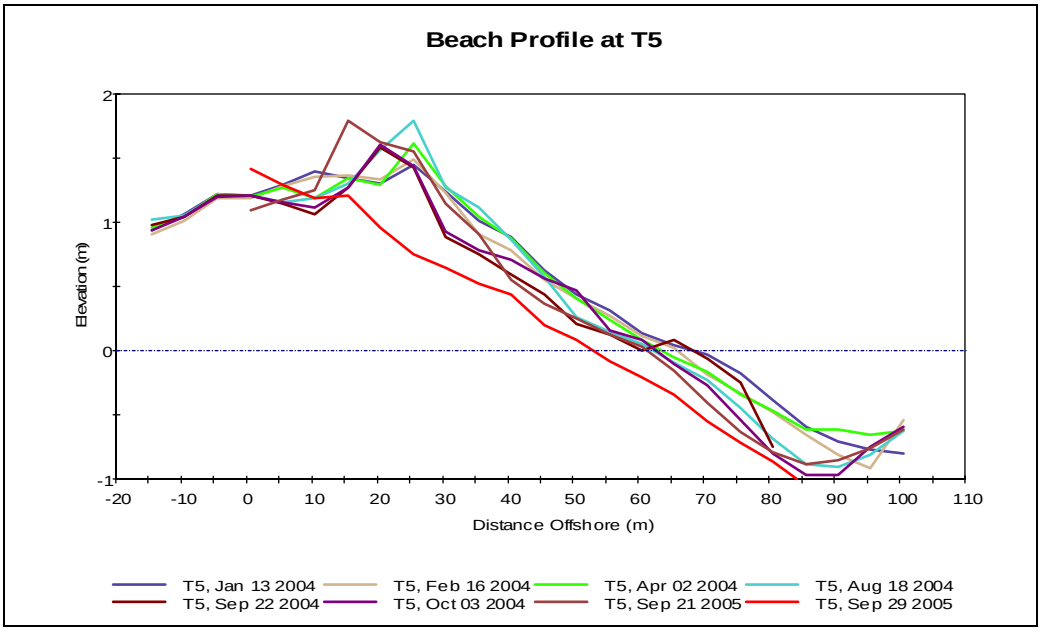


**Fig. 3.38. The cross-shore beach profile at T5 since January 2004.**

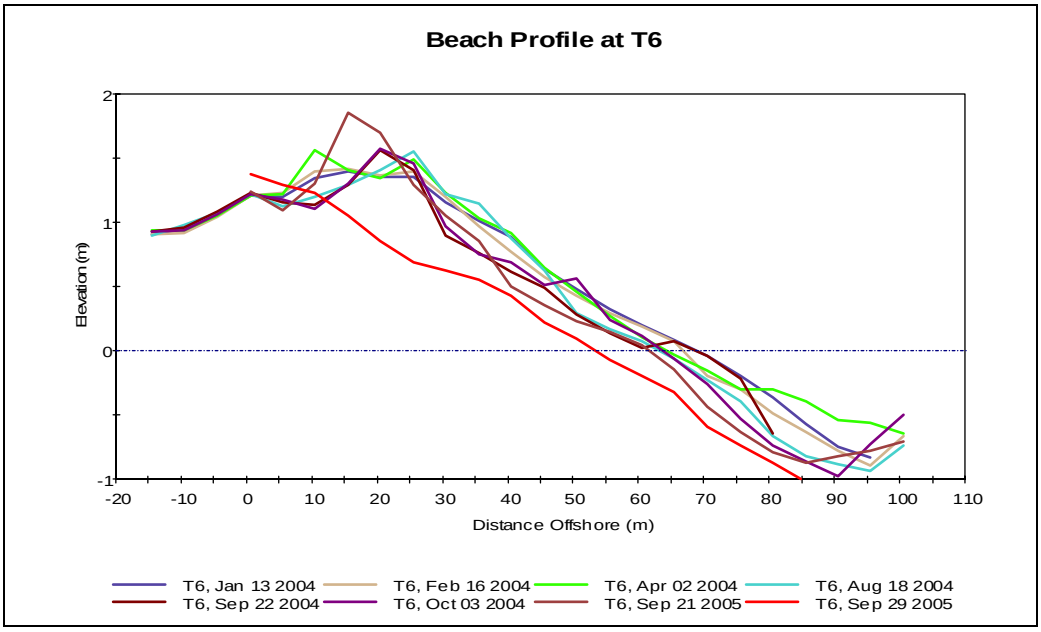


**Fig. 3.39. The cross-shore beach profile at T6 since January 2004.**

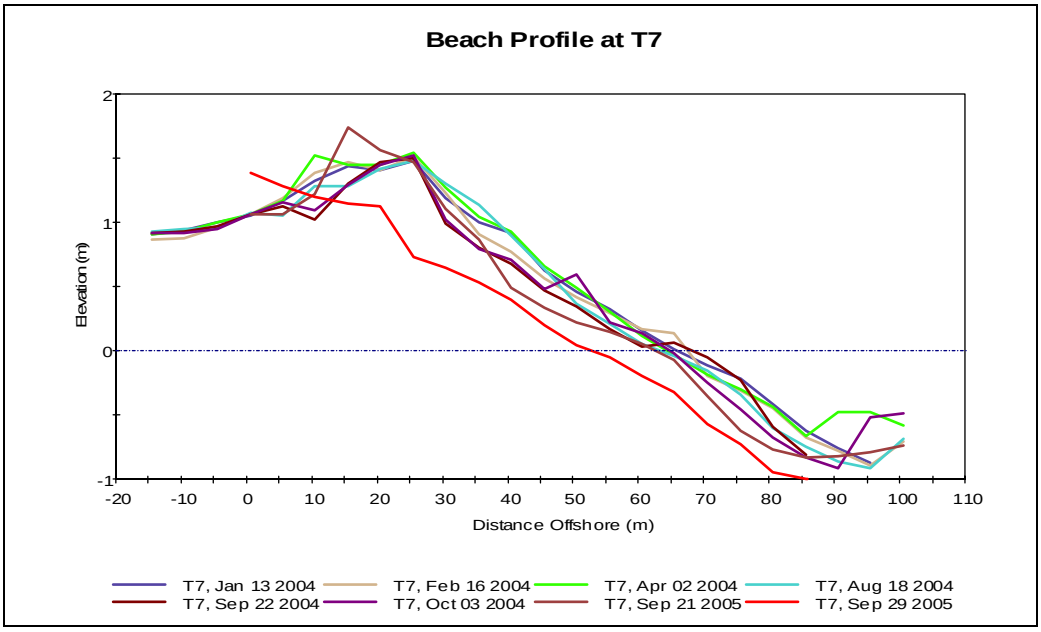


**Fig. 3.40. The cross-shore beach profile at T7 since January 2004.**

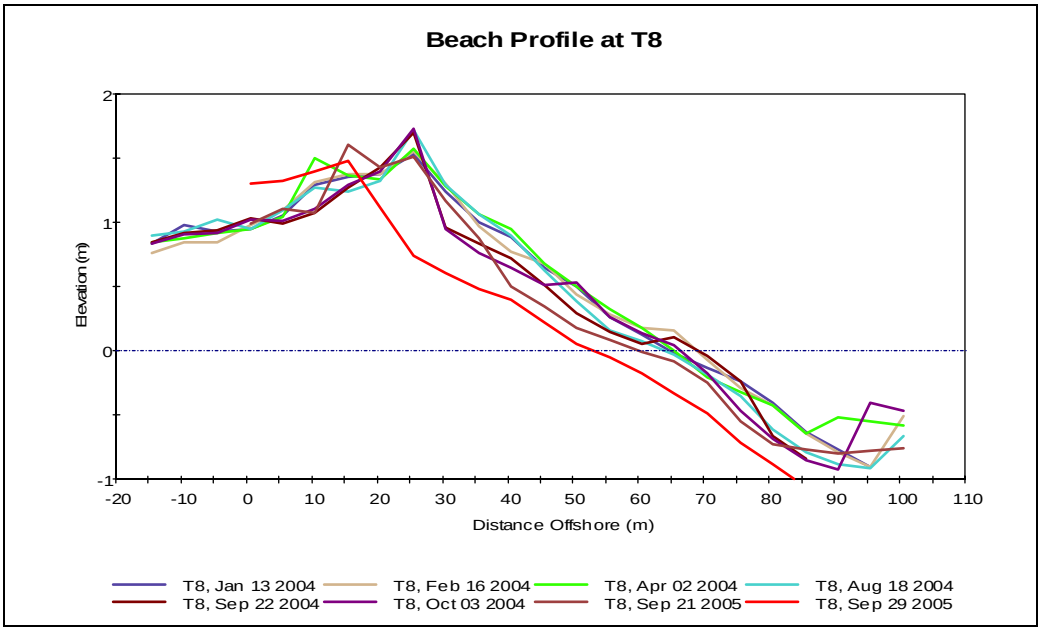


**Fig. 3.41. The cross-shore beach profile at T8 since January 2004.**

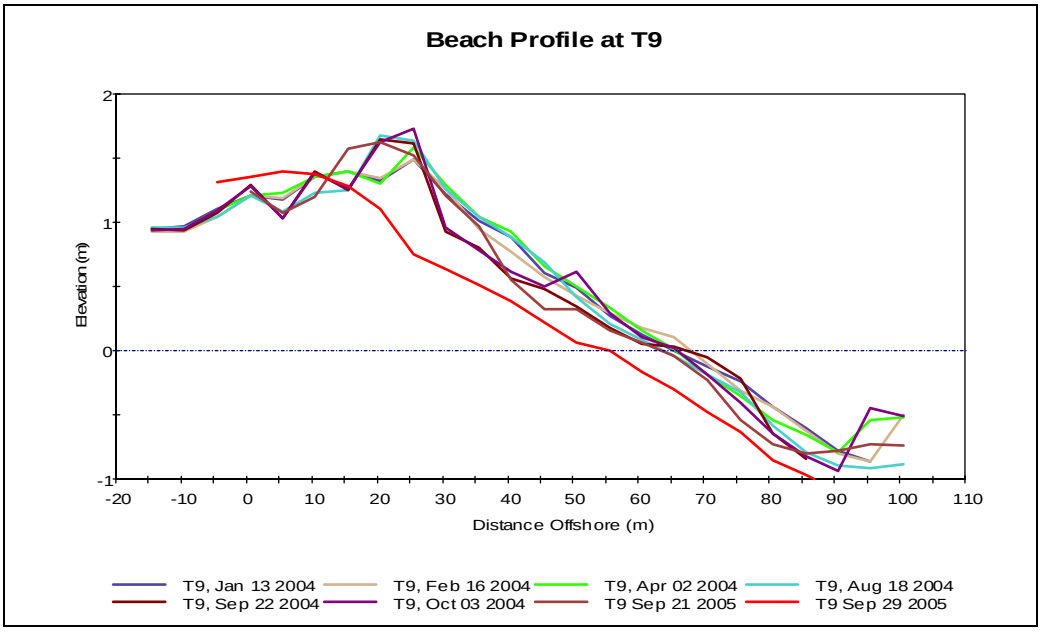


**Fig. 3.42. The cross-shore beach profile at T9 since January 2004.**

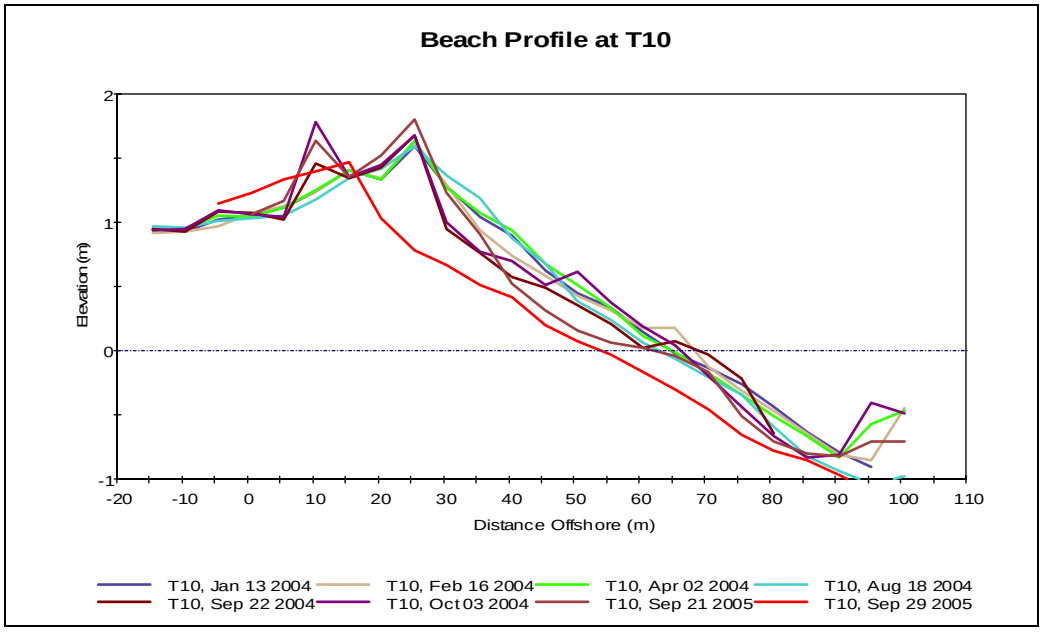


**Fig. 3.43. The cross-shore beach profile at T10 since January 2004.**

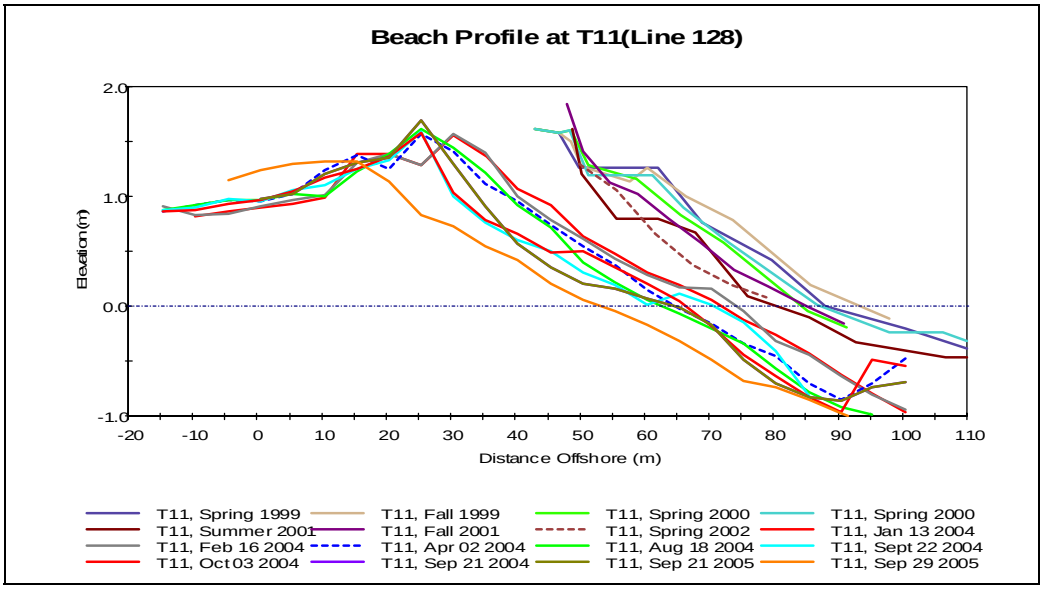


**Fig. 3.44. The cross-shore beach profile at T11 (L128) since 1999.**

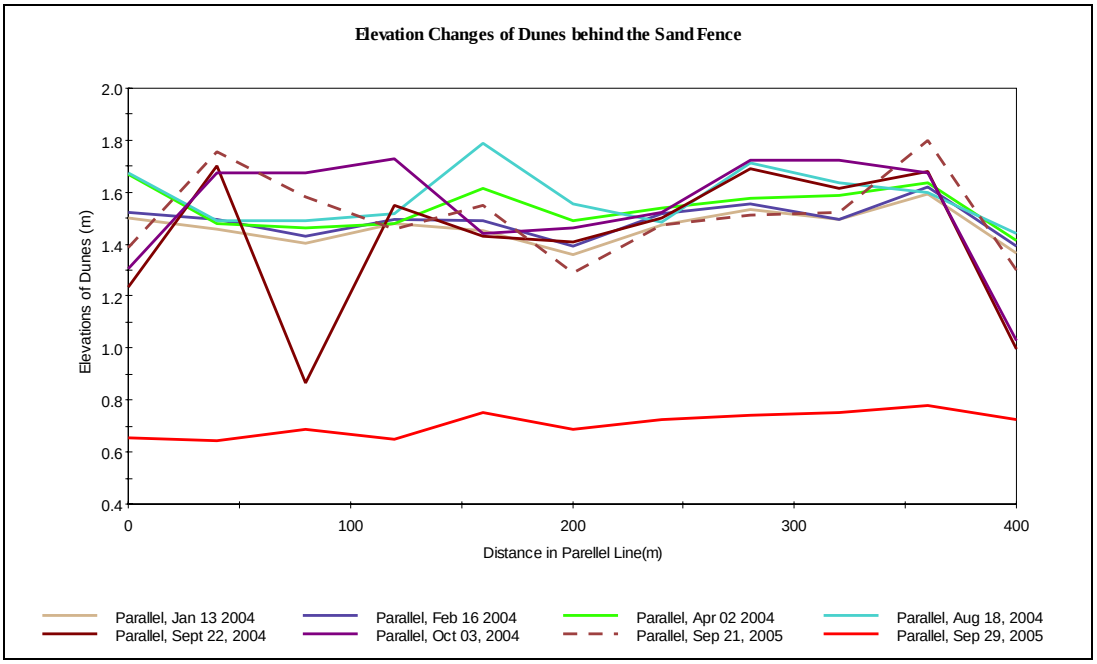


**Fig. 3.45. The change of peak berm height in the longshore direction since January 2004.**

### 3.10. Data Analysis

The volumetric beach changes were calculated at spatial and temporal scales from the survey measurements (Table 3.6). The deposition was apparent between February and April and it was assumed to be done by southerly or southeasterly wind. Erosion and deposition processes could be checked from 2D and 3D view of beach profiles. The erosion near to the previous top of berm was intensive between August and September by tropical storm Ivan. A suspected incision by tropical storm Ivan was observed in Table 3.6 a minor overwash fan was observed at the right side of survey area in (Fig. 3.47 and Fig. 3.52).

The berm was eroded completely by overwash at landfall of hurricane Rita (category 3) and the sediment processes by overwash was shown apparently in Fig. 3.49. The top of berm and foreberm were totally demolished and became flat after landfall of hurricane Rita (Fig. 3.56 and Fig. 3.57). The averaged volume of erosion for 11 lines was 26.24 $m^3/m$ before and after landfall of hurricane Rita.

**Table 3.6. Incremental volumetric changes ($m^3/m$) at each profile in 2004. Each change was computed by subtracting from the previous measurement.**

| Line | Jan | Feb | Apr | Aug | Sep | Oct |
|---|---|---|---|---|---|---|
| **T1(L126)** | - | -2.2 | 2.6 | -3.5 | -0.8 | -0.8 |
| **T2** | - | -1.9 | 0.8 | -1.7 | -0.9 | -0.3 |
| **T3** | - | -1.8 | 1.3 | -0.2 | -11.3 | 7.9 |
| **T4** | - | -2.5 | 1.2 | -0.7 | -4.0 | 1.3 |
| **T5** | - | -3.4 | 0.9 | -0.2 | -7.1 | 1.2 |
| **T6** | - | -2.0 | 2.3 | -3.9 | -4.1 | 0.9 |
| **T7** | - | -1.5 | 2.9 | -4.1 | -4.8 | 0.7 |
| **T8** | - | 0.0 | 1.4 | -2.4 | -4.4 | 0.1 |
| **T9** | - | -0.6 | 2.4 | -2.2 | -4.1 | 2.0 |
| **T10** | - | -0.6 | 1.5 | -2.0 | -3.2 | 4.6 |
| **T11(L128)** | - | - | -3.3 | -3.1 | -5.2 | 1.4 |

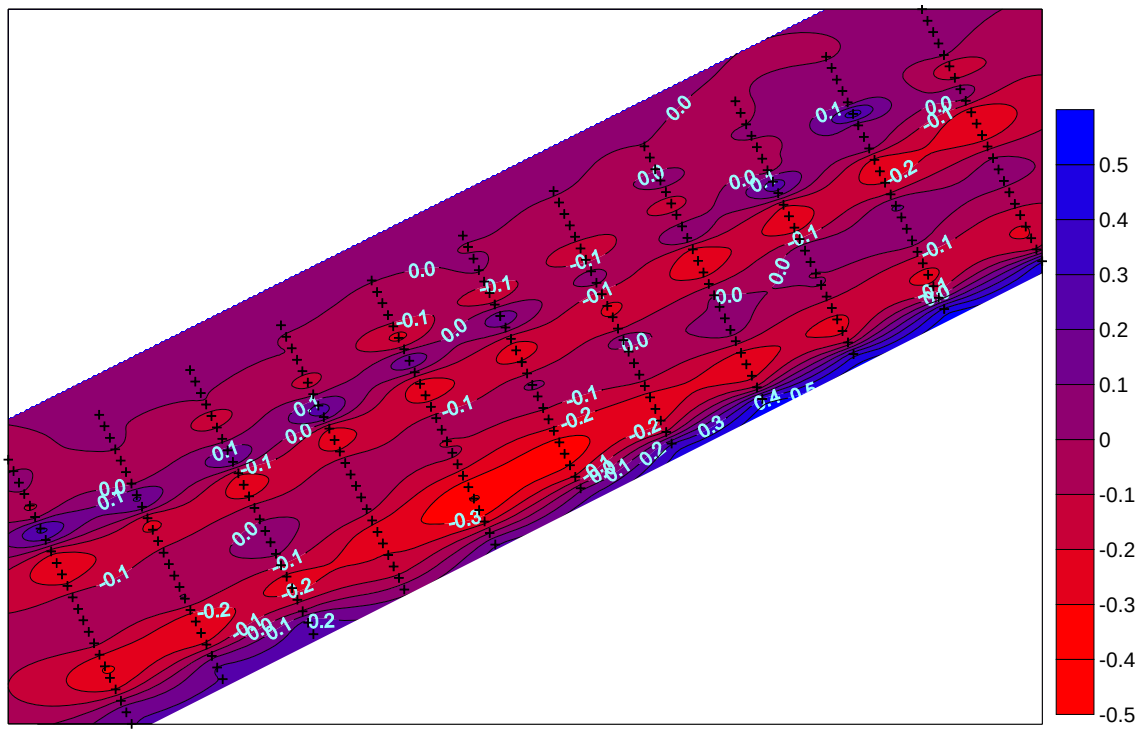


**Fig. 3.46. The elevation changes between January 13, 2004 and October 3, 2004. Blue and red colors represent deposition and erosion respectively (Unit: meter).**

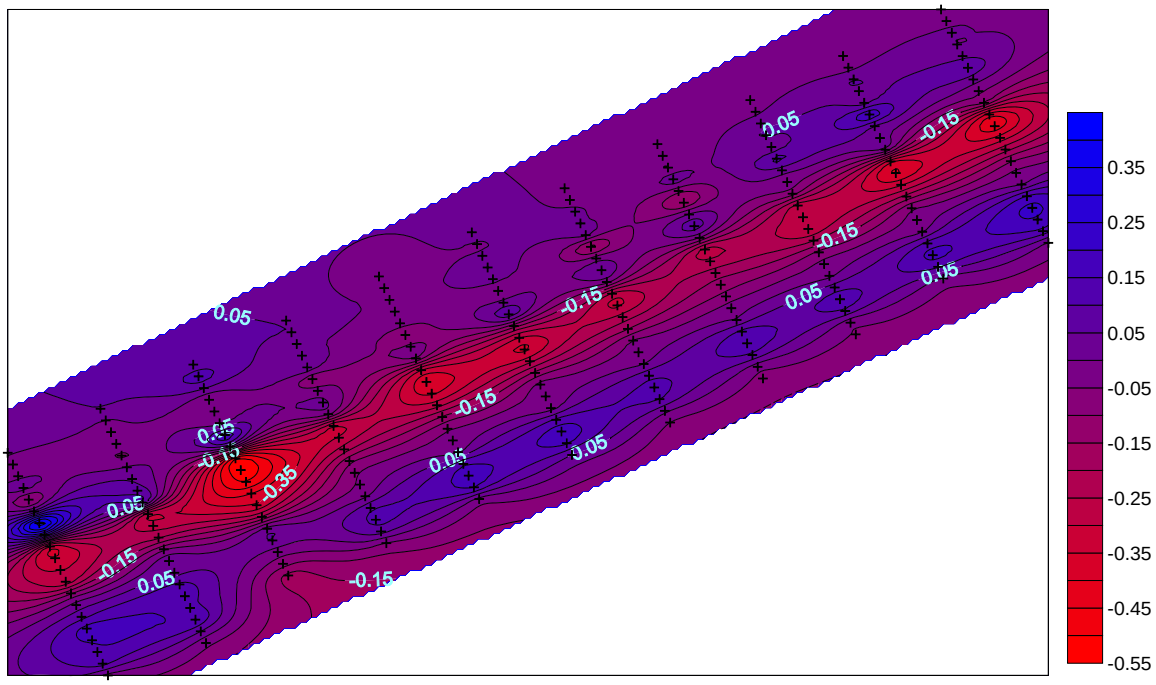


**Fig. 3.47. The elevation change between August 18, 2004 and September 22, 2004, before and after landfall of tropical storm Ivan. Blue and red colors represent deposition and erosion respectively (Unit: meter).**

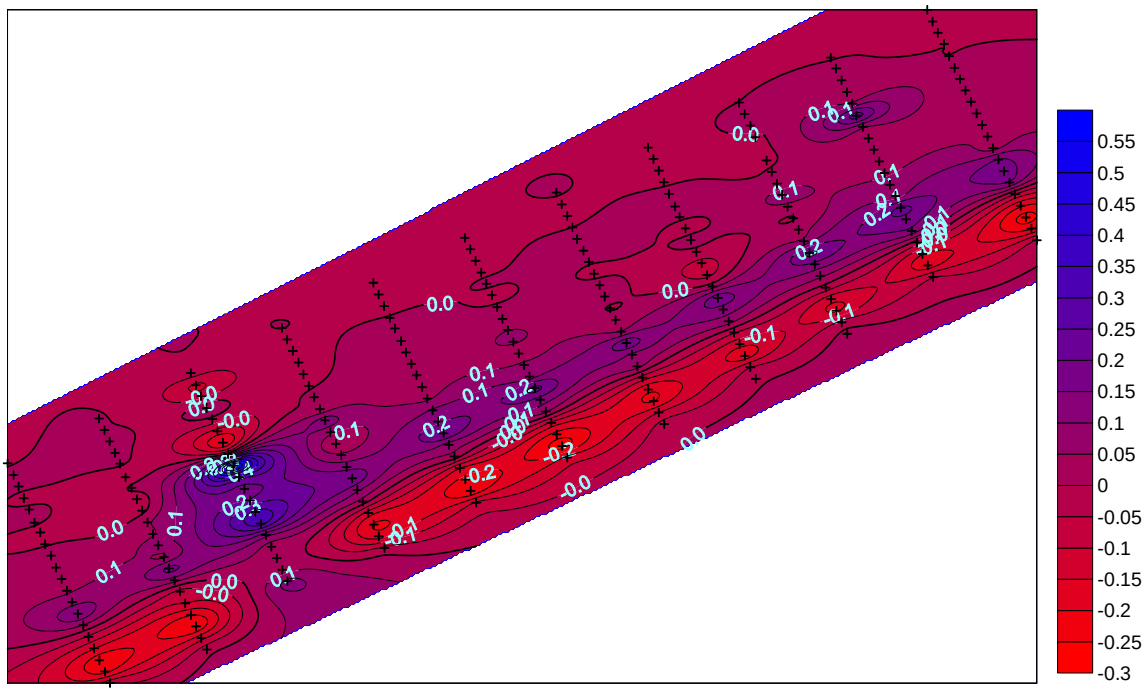


**Fig. 3.48. The elevation difference between September 22, 2004 and October 3, 2004. Blue and red colors represent deposition and erosion respectively.**

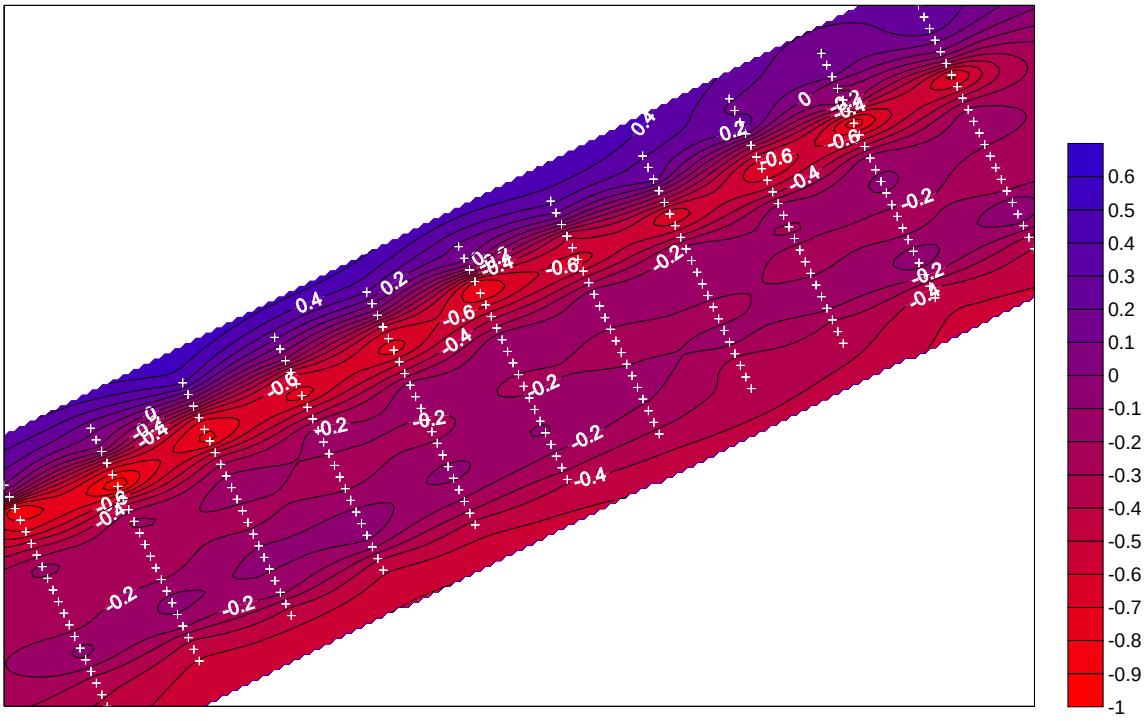


**Fig. 3.49. The elevation change between September 21, 2005 and September 29, 2005, before and after landfall of hurricane Rita. Blue and red colors represent deposition and erosion respectively (Unit: meter).**

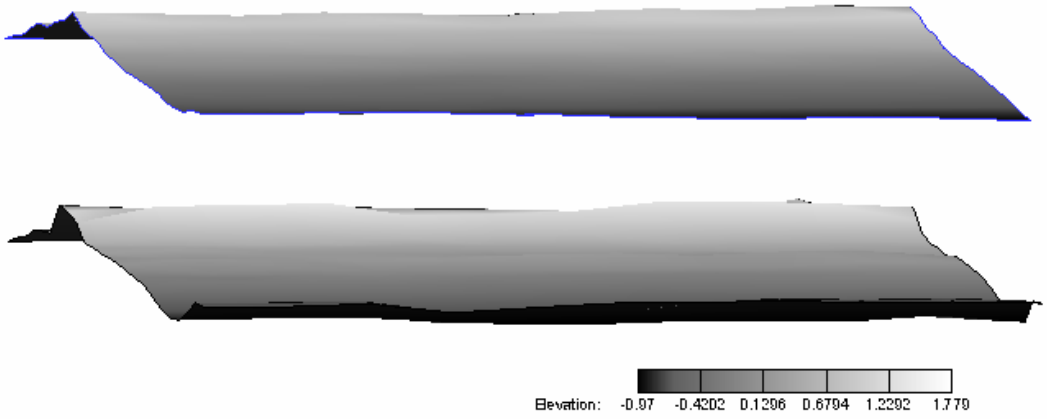


**Fig. 3.50. The front view of beach profiles (upper one was measured on January 13, 2004 and lower one was measured on October 3, 2004 (Unit: meter)).**

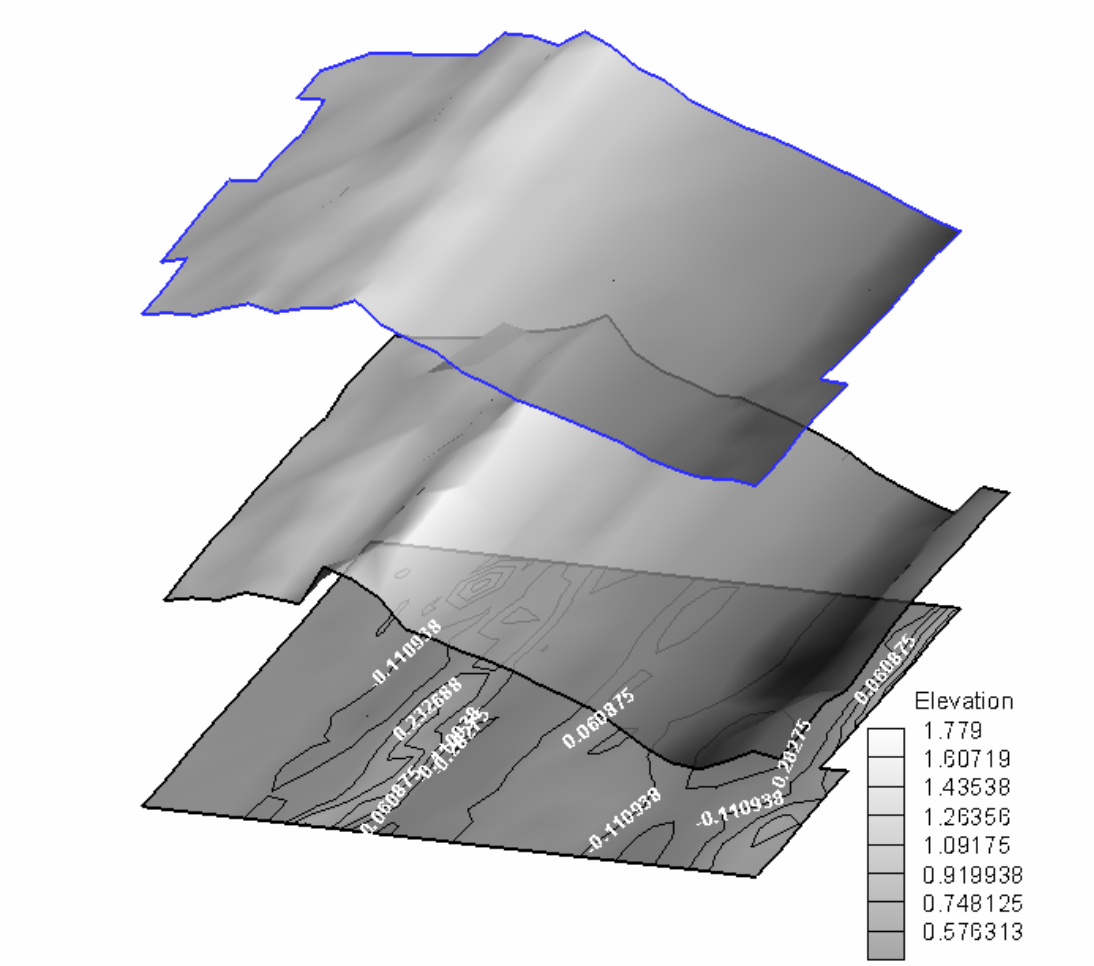


**Fig. 3.51. The oblique view of beach profiles (each one from the top showed the result on January 13, 2004, on October 3, 2004 and the change of elevation between them (Unit: meter)).**

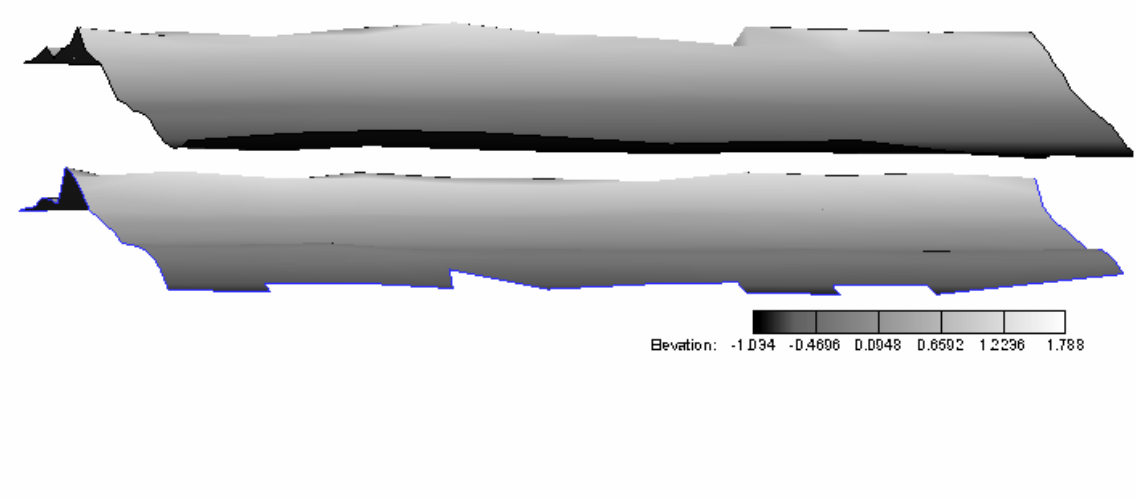


**Fig. 3.52. The front view of beach profiles (upper one was measured on August 18, 2004 and lower one was measured on September 22, 2004, before and after landfall of tropical storm Ivan (Unit: meter)).**

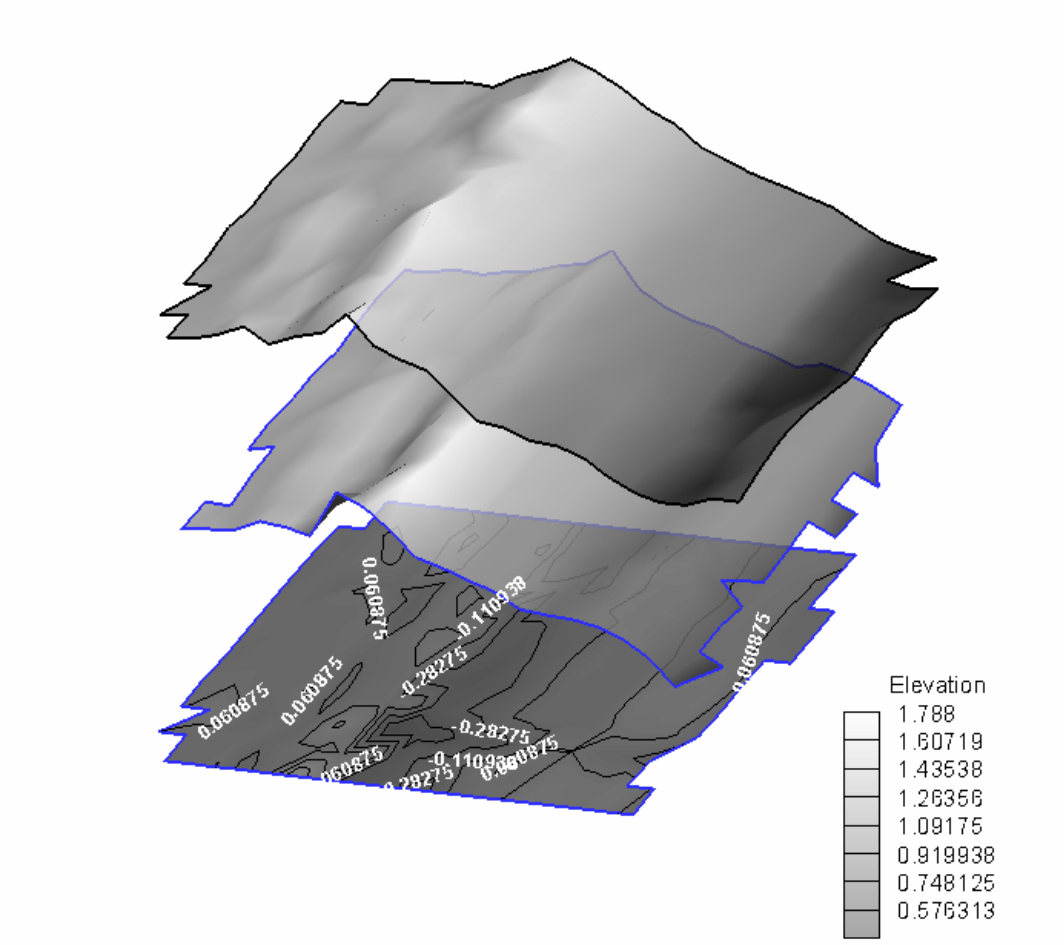


**Fig. 3.53. The oblique view of beach profiles (each one from the top showed the result on August 18, 2004, on September 22, 2004 and the elevation change between them before and after landfall of tropical storm Ivan (Unit: meter)).**

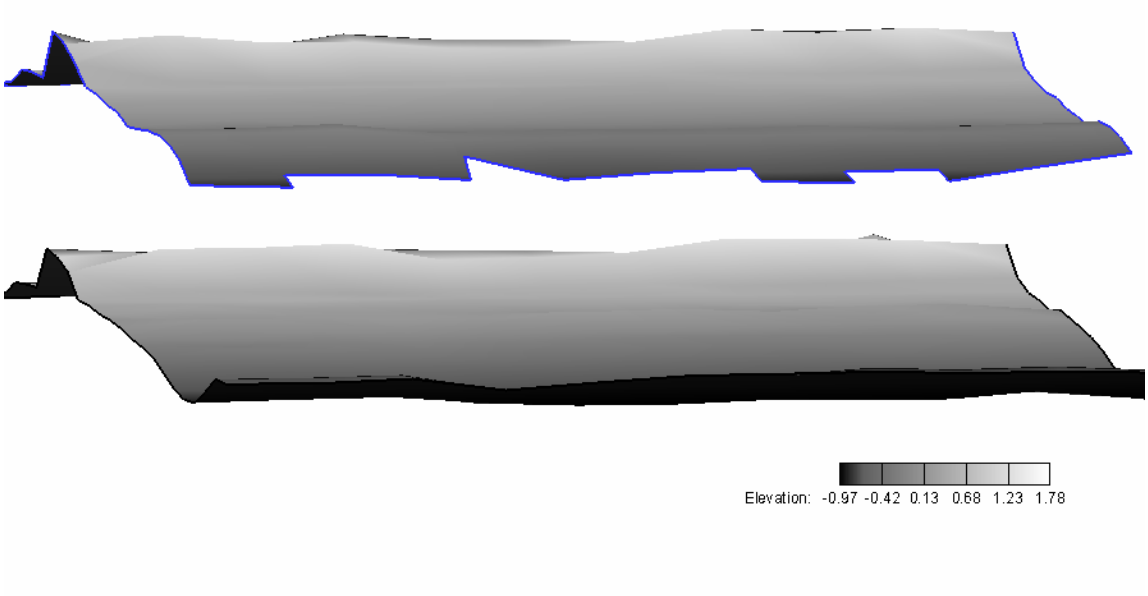


**Fig. 3.54. The front view of beach profiles (upper one was measured on September 22, 2004 and lower one was measured on October 3, 2004 (Unit: meter)).**

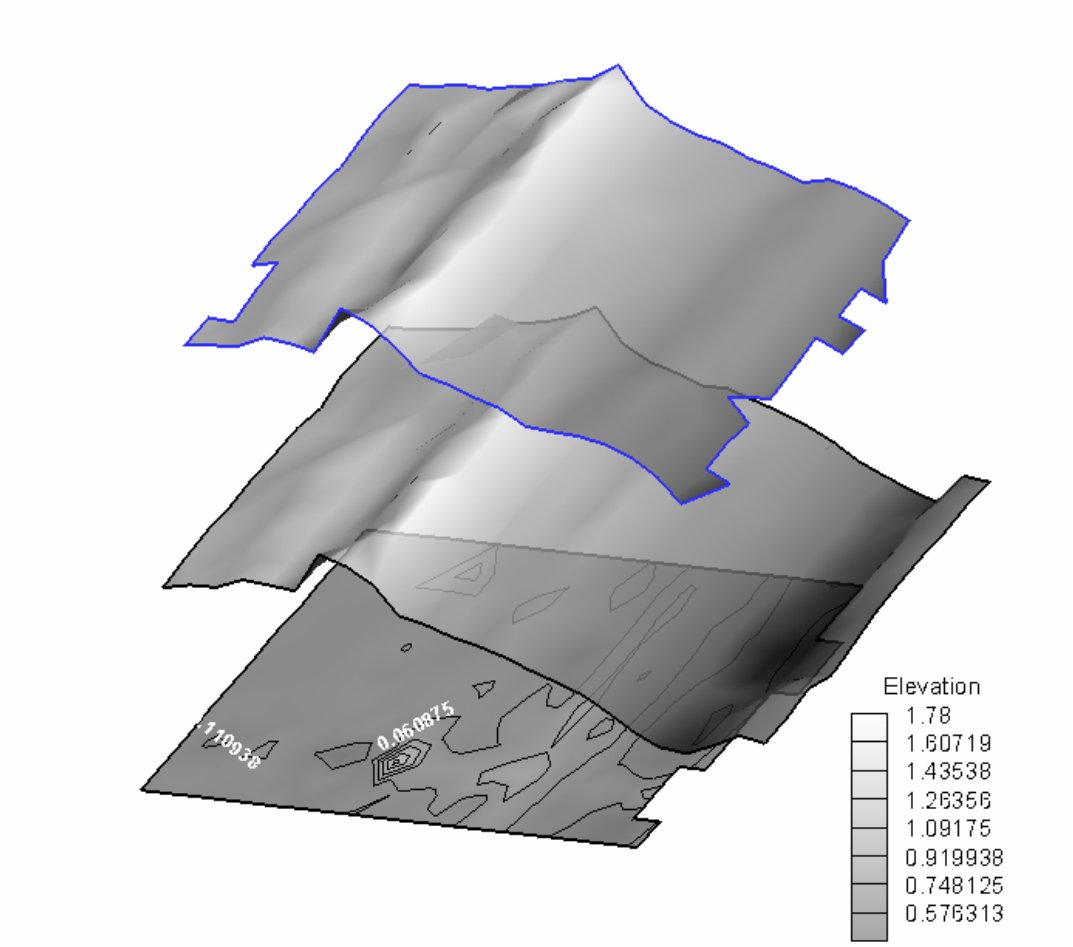


**Fig. 3.55. The oblique view of beach profiles (each one from the top showed the result on September 22, 2004, on October 3, 2004 and the change of elevation between them (Unit: meter)).**

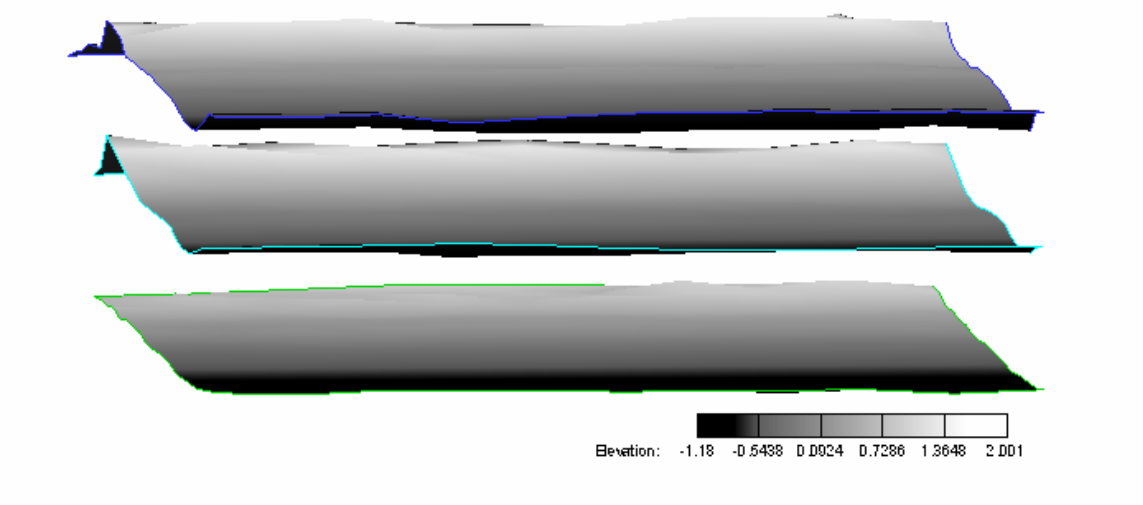


**Fig. 3.56. The front view of beach profiles (upper one was measured on October 3, 2004, and lower two was measured on September 21, 2005 and September 29, 2005 before and after landfall of hurricane Rita). The berm was lost completely and became flat bottom by hurricane Rita (Unit: meter).**

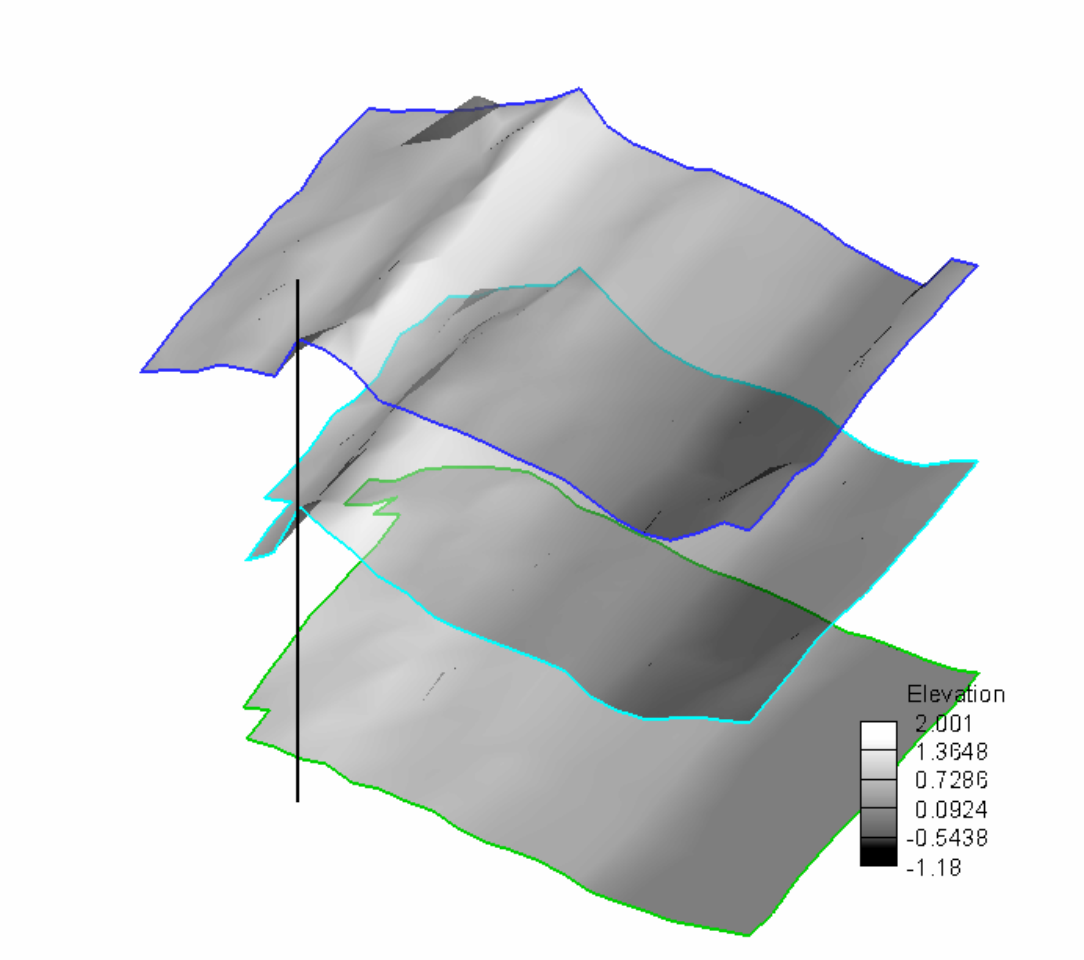


**Fig. 3.57. The oblique view of beach profiles (upper one was measured on October 3, 2004, and lower two was measured on September 21, 2005 and September 29, 2005 before and after landfall of hurricane Rita (Unit: meter)).**

### 3.11. Summary and Discussion

When potential of overwash was calculated based on equation (3.3), there were three overwash events from January, 2004 to October, 2004. They happened on September 15, 2004, September 22, 2004 and October 8, 2004 (Table 3.4). Among them, the first two events were generated by hurricane Ivan and final one was done by tropical storm Matthew. Because the overwash measured on September 22 was likely to be generated by Ivan's first pass through the Gulf of Mexico, the September, 2004 survey was assumed to be done after overwash by tropical storm Ivan. The overwash in September 15 was done by swell that had a long period. Even though the wave conditions in January and February had similar values to other overwash events, there was no overwash evidence by hindcast. Storm surge combined with tide elevation acted an important role in estimating potential of overwash.

The morphology of beach change can be understood by volumetric changes in Table 3.1. It also showed that there were two overwash events on September 15 and September 22, 2004 (Fig. 3.22) based on calculation of maximum runup height and intensive beach erosion was found in volume change between August and September, 2004 from field measurement. It meant the study area was affected by hurricane Ivan and its overwash processes. Fig. 3.46 and Fig. 3.48 show erosion and deposition of sediment between January and October, and pre and post landfall of Tropical Strom Ivan in 2004 respectively. Much erosion occurred in the toe of beach face and some sand moved behind the top of berm along the shoreline in Fig. 3.46. The pattern of beach erosion in 2004 was plotted in Fig. 3.50 and Fig. 3.51. It showed the beach erosion was still progressing. The erosion by

storm waves was apparent in Fig. 3.52 and Fig. 3.53 and the post-storm sand deposition was represented in Fig. 3.54 and Fig. 3.55.

The most severe damages by overwash were measured before and after hurricane Rita in 2005 (Fig. 3.49). The result showed that the average volume of erosion for 11 lines was 26.24 $m^3$/m. It became a good reference to make a comparison with empirical model.

The deposition between February and April (Table 3.6) was considered as part of results of eolian processes by southerly and southeasterly wind after installation of sand fences in January, 2004. The deposition between September and October was produced by transport of eroded sand from beach face by overwash. Storm frequency may be an important factor to generate beach erosion in the study area. This appears when the recovery period is longer than the period between storms as mentioned by Morton et al (1995).

The calibration and verification between field measurement and empirical equation are presented in Chapter IV.

# CHAPTER IV

# LABORATORY EXPERIMENTAL WORKS

## 4.1. Introduction

### 4.1.1. Objectives and Scope

The interaction between the waves and beach is necessary for understanding erosion processes. Storms accompanied by large waves and sea level rise can cause overtopping the berm. During overtopping, a large amount of sand is transported landward. Available field data are very difficult to obtain during a storm due to severe weather condition on the beach, so laboratory data are favorable to analyze overwash.

So, the purpose of this aspect of the study was to conduct experiments and understand the mechanism of overwash and its important parameters that were difficult to obtain from field measurements. This experiment investigated the response of the berm to overwash and the long term beach erosion at the beach face and top of beach with wave interactions.

Mid-scale experiments were conducted in Hydrolab at Texas A&M University to overcome the limitation caused by scale effect from small-scale experiment. The slope of foreberm was 1:27 in the field, whereas the slope of foreberm was 1:4 and 1:5 in the experiments. The bigger mid-scale experiment is necessary for beach erosion or sediment transport in laboratory tests using sand. The size of sediment material becomes smaller than sand and it cannot by simulating with clay. The limit of boundary between non-

cohesive sand and cohesive silts and clays is 0.074 mm. These materials have completely different characteristics.

The experiments were conducted with regular and irregular waves using the TMA spectrum with a flap type wave maker. The wave period and height were measured by resistance type wave gages. The speed of overtopping bore was measured by two wave gages located in a known distance with each other on the top of berm. Initial and final beach profiles after experiment were measured by laser equipment. The rates of sediment transport were calculated from volumetric changes between initial and final profiles.

The sensitivity analysis of correlations was done for different slopes of beach faces, speed of bores, wave heights and wave periods. The empirical formulas from these laboratory experiments were used for developing of numerical model in Chapter V.

### 4.1.2. Literature Review

Many laboratory experiments have been done for berms but experiment for overwash is very rare among them. Some researchers conducted experiments under storm conditions in different scales as shown in Table 4.1. Experiments by Saville (1957) during 1956-1957 were carried out for almost prototype-scale in a tank that had 194 m long, 6.1 m deep. Their research was carried for the study of foreshore erosion at storm conditions. Williams (1978) conducted a small scale laboratory test and mentioned that overwash for steep slopes tended to transport much greater distances. His remarks agreed with experiment results by this study. Hughes and Chiu (1981) conducted experiments in small-scale and tried to find and develop the relationships of movable-bed modeling for laboratory

experiment and evaluate the relative importance of the main factors in storm conditions. Vellinga (1983) made a comparison between small, large-scale experiment results, numerical model results and field measurements. He compared his experiment results with filed measurements in applying the similitude law. Hughes and Fowler (1990) made a comparison between their physical model and prototype experiments in Germany using scale effects.

Hancock (1994) conducted an experiment for simulation of overwash. He measured beach profiles and estimated concentrations for irregular wave conditions. His results needed to be compared with other experiment results. He used a small scale model and a relatively large sand size. Kobayashi et al. (1996) developed empirical equations for overwash rate of sand and wave reflections from Hancock (1994) experiment. Kobayashi et al. (1996) did experiments for overwash in a small-scale with irregular waves based on the TMA spectrum. They were focused on the concentration of sediment in water column at each overwash over a sand berm and measuring wave reflection coefficient from a berm. Because they did experiments in small-scale wave tank, it had restrictions to compare with field measurements. Tega and Kobayashi (2000) found that the average volumetric sediment concentration ratio between overtopping water and sand was equal to 0.038 in overtopping flow from their laboratory experiments. They created CBREAK, a numerical model for simulation of time-dependent sediment transport by overwash.

**Table 4.1. The comparison between laboratory experiment results.**

| | | Saville | Hughes & Chiu | Vellinga | Kobayashi et al. | TAMU |
|---|---|---|---|---|---|---|
| **Year** | | 1957 | 1981 | 1983 | 1996 | 2006 |
| **Purpose** | | Foreberm erosion at storm conditions | Foreberm erosion at storm conditions | Foreberm erosion at storm conditions | Sediment transport by overwash | Sediment transport by overwash |
| **Experiment scale** | | Large-scale | Small-scale | Small & Large-scale | Small-scale | Mid-scale |
| **Sand size ($d_{50}$, mm)** | **Prototype** | - | 0.262 | 0.225 | - | - |
| | **Model** | 0.22 | 0.147 | 0.095-0.225 | 0.38 | 0.15 |
| **Wave type** | | Regular | Regular | Irregular | Irregular | Regular & Irregular |
| **Wave period (sec)** | **Prototype** | 11.0 | 11.0 | 12.0 | - | - |
| | **Model** | 3.75-11.33 | 1.07 | 1.31-2.35 | 1.2-2.0 ($T_p$) | 1.2-2.0 ($T_p$) |
| **Wave height (m)** | | 1.52-1.68 | 0.104 | 1.5 ($Hs$) | 0.118-0.128 ($H_s$) | 0.20 & 0.25 ($H_s$) |
| **Duration** | | - | 30 min. | 40 hrs. | 325 sec. | 327 sec |
| **Beach size (m)** | | Height : 6.1 Length : 194 | Height : 0.24 Length : 1.52 | Height : 1.2 Length : 100 | Height : 0.65 Length : 8.1 | Height : 1.4 Length : 25.0 |
| **Slope (H : V)** | **Foreberm** | 1 : 0.5-1.0 | 1 : 1.03 | 1 : 3.12-11.7 | 1 : 0.19-0.38 | 1 : 0.20 & 1 : 0.25 |
| | **Surf zone** | 1 : 0.15 | 1 : 0.21 | - | 1 : 0.043 | 1 : 0.10 |

## 4.2. Experimental Setup

### 4.2.1. Wave Tank

The laboratory experiments were conducted in a 2D wave tank in a floor concrete open channel 28.0 m long, 1.5 m wide and 3.0 m high at Texas A&M University. A computer controlled wave generator generated waves of user defined amplitude and period. It is installed near one end of the tank and an experimental structure is at the opposite end of the tank. A wooden false bottom (Fig. 4.1) was built beneath the paddle of the wave generator to prevent loss of wave energy during generation of wave. The hinged flap type wave board was located at 1.1 m above bottom of the wave tank. The false bottom was extended on a slope of 1:10 to the laboratory beach and a sand berm. A sand collector of 4.7 $m^3$ was constructed just behind the sand berm to measure the amount of transported sand during an experiment.

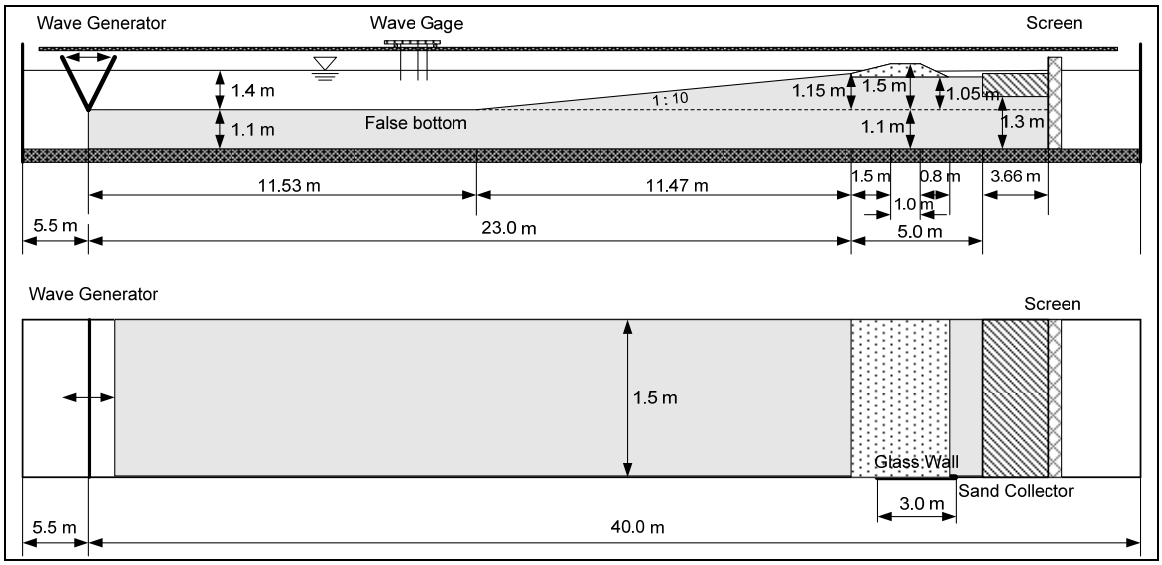


**Fig. 4.1. Layout of experiment facility in wave tank at Texas A&M University.**

### 4.2.2. Characteristics of Sand Used in Experiment

The poorly distributed sand (that had uniform size) was used for the beach and berm. A small sand size was selected for the experiment for sediment transport. The "Ottawa sand" that is famous for high quality and uniform size was used for this experiment. The $d_{50}$ size and specific gravity of the sand 0.15 mm and 2.65 respectively and the particle size distribution is shown in Fig. 4.2. The settling velocity of sand was obtained from Hallermeier (1981) and it was 1.7 cm/s (20 ˚C). The experimental berm was built with about 2.5 $m^3$ sand for this laboratory test. The same sand was used in all experiments.

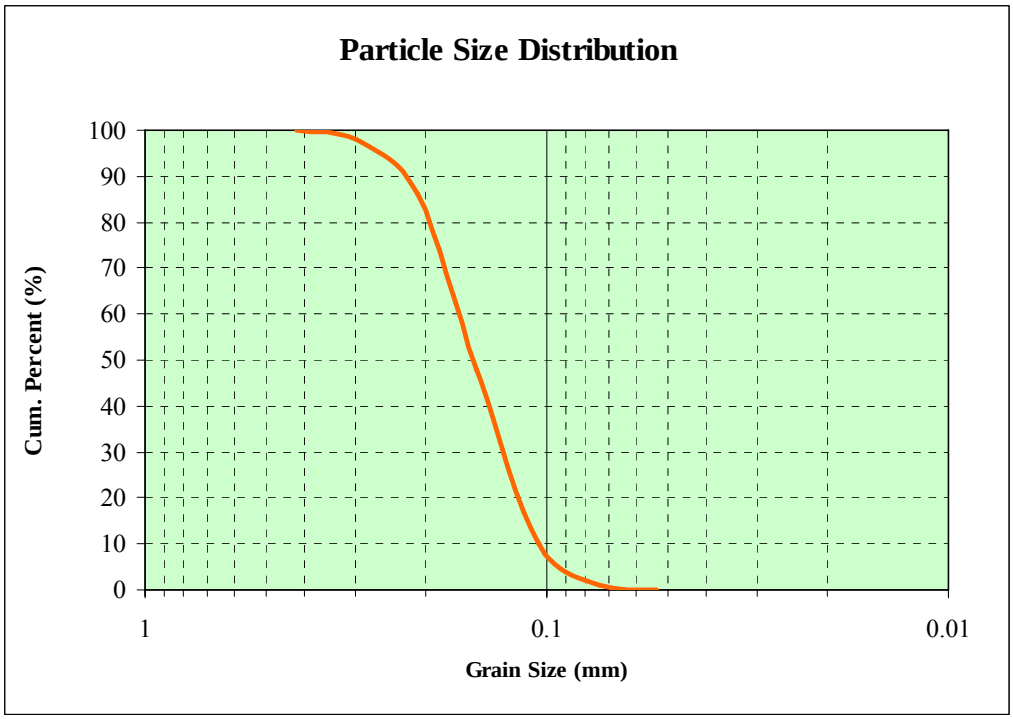


**Fig. 4.2. Cumulative size distribution of sand used in experiment.**

### 4.2.3. Wave Generator

The wave generator is flap type and has a paddle, 1.5 m wide and 1.9 m high. A paddle is hinged at the wall 1.1 m above bottom of the tank and is driven by the MTS (Model 458.10) hydraulic actuator. It is able to generate waves, 0.25 m high and 2.0 seconds period. A National Instruments board (AT-MIO-16E-10), installed in an IBM compatible computer, generates electric voltages ranged up to +/– 10 volts that control hydraulic actuator by varying themselves in wave generator. The relationship between period, displacement of paddle and voltage is obtained from calibration curves in Fig. 4.3. The voltage generation program based on the obtained relationship is developed with LabVIEW programming language.

The flap type wave generator theory for a generated wave height with a displacement of paddle is described by Dean and Dalrymple (1991) in the equation (4.1) and the result is shown in Fig. 4.4

$$\frac{H}{S} = 4\left(\frac{\sinh k_p h}{k_p h}\right)\frac{k_p h \sinh k_p h - \cosh k_p h + 1}{\sinh 2k_p h + 2k_p h} \tag{4.1}$$

where $H$ is wave height, $S$ is stroke, $k_p$ is wave number of progressive wave and $h$ is water depth.

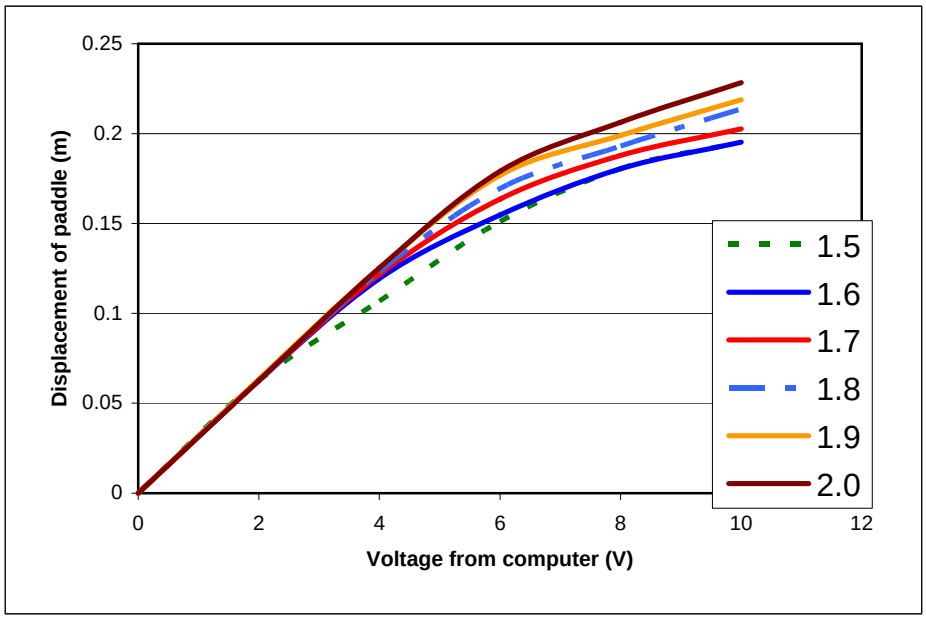


**Fig. 4.3. The relationship between wave period, voltage and displacement of paddle.**

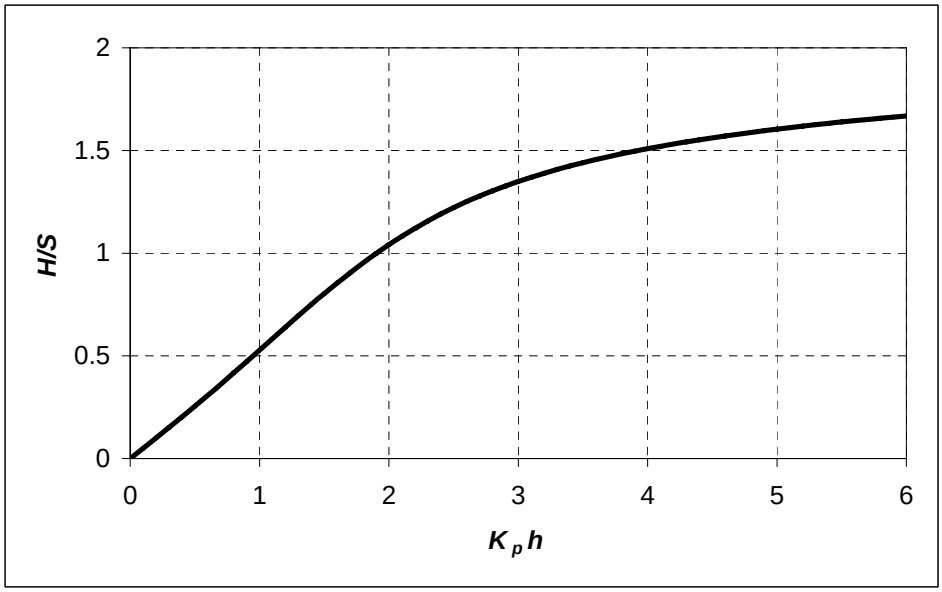


**Fig. 4.4. Wave height to stroke ratio versus relative depths for flap type.**

### 4.2.4. Wave Gages and Data Acquisition

Wave gages of electrical resistance type are used for measuring wave height and speed of bore by overwash. The free surface oscillation is calculated by the variation of resistance based on a calibration curve. Calibration curves are obtained from the relationships between the voltage and displacement at each gage before the laboratory test. A National Instruments board (AT-MIO-16E-10) is used to measure the variation of voltage from each gage and the data acquisition program is developed with LabVIEW programming language. The acquired analog voltage signals from each wave gage are converted to digital signals by the circuit board and the free surface elevations calculated from them based on a calibration curve are restored in computer memory storage by the data acquisition program.

### 4.2.5. Measuring Equipment of Beach Profile

The eye safe laser was used to measure the beach profile in the experiments. The measured profile was displayed in Fig. 4.5 by Surfer which is a program for a contouring and 3D surface mapping. The resolution of laser was 0.02 to 0.5 mm and it depended on the distance between the light source and the target. The laser profiler was installed on the bottom of the rails along the sides of the tank and moved in x and y directions with accuracy of 1 mm per 1 m in Fig. 4.6. The operation program installed in an IBM compatible computer controlled the movements of the laser and stored the obtained data in the computer. The range of scanning was 5.0 m and 3.0 m in x and y direction, respectively,

and it took about 15 minutes to measure the whole area every 5 mm in x and 20 mm y directions. It could measure the beach profiles under the clear water and its range was almost 1.0 meter. The most important ability of laser profiler was to measure the time series of changes in water surfaces or beach profiles during experiments, because it did not need to touch objects unlike conventional sand profilers.

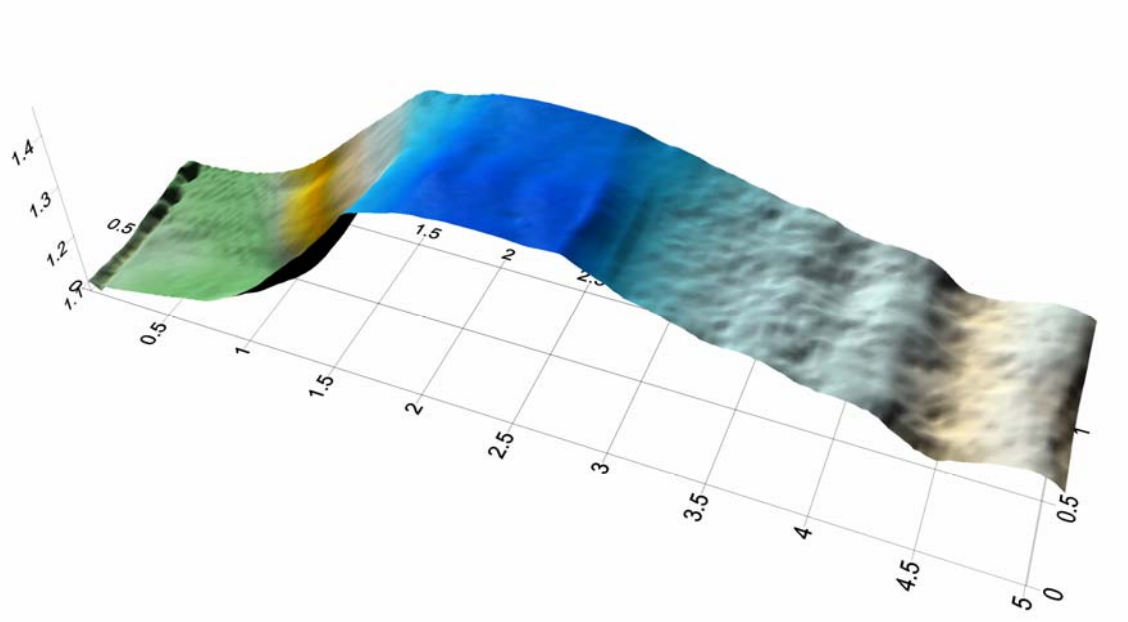


**Fig. 4.5. The plot of sand profile by a laser profile after a beach erosion test.**

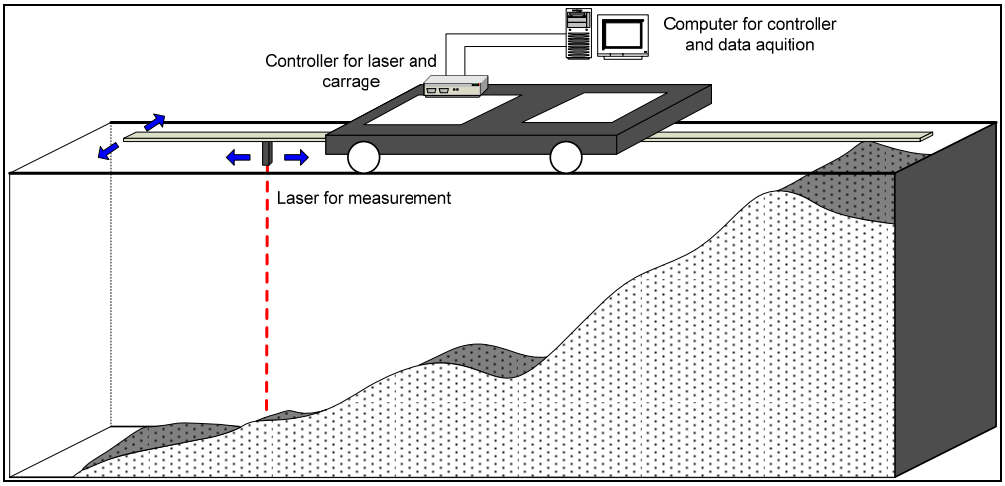


**Fig. 4.6. Laser profiler for scanning of sand profile in the experiment.**

## 4.3. Procedure of Experiment

### 4.3.1. Schedule of Procedures

The procedures to conduct experiment are shown in Fig. 4.7.

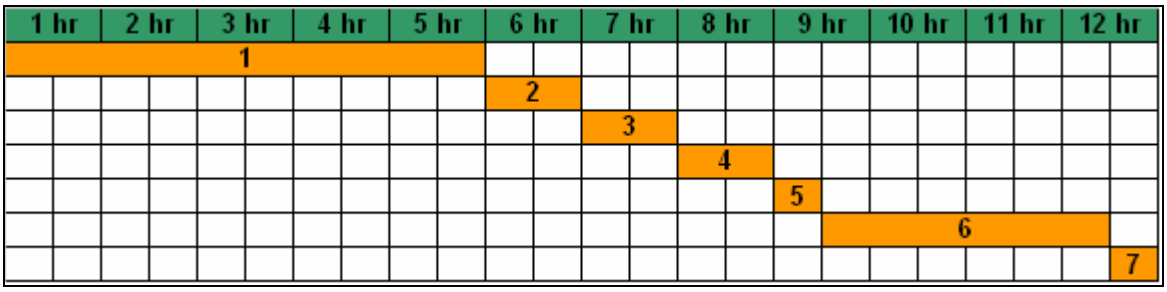


**Fig. 4.7. The schedule of procedures for overwash experiment.**

The identifications of the procedures are:

1. To build and measure the initial beach (5 hours).
2. To fill the water tank up to the top of the berm (1 hour).
3. To wait for saturation of sand (1 hour).
4. To drain the water up to the experiment level and setup the sensors (1 hour).
5. To start experiment (0.5 hours).
6. To drain the water (3 hours). It is necessary for the removal of suspended material.
7. To measure the eroded beach (0.5 hours).

Thus each experiment required approximately twelve hours to conduct.

### 4.3.2. Wave Generation and Data Acquisition

Two National Instruments circuit boards (AT-MIO-16E-10) installed in an IBM compatible computer were used for wave generation and data acquisition respectively. Regular and irregular waves were generated for this experiment. Each test consisted of series of waves that had intervals of 0.02 seconds and its duration was 327 seconds. The test duration was determined from average periods where exposed berm was eroded and its elevation was lower than water level by overwash. Two different wave heights of 0.14 and 0.17 m and four different wave periods of 1.4, 1.6, 1.8 and 2.0 seconds were selected for the regular and two different $H_{mo}$ of 0.10 and 0.15 m and four different wave periods of 1.4, 1.6, 1.8 and 2.0 seconds were selected for the irregular waves in Table 4.2.

The TMA spectrum was used to generate irregular waves and it was transformed by the transformation factor developed by Bouws et al. (1985) from approximate form of the JONSWAP spectrum by Goda (1985) in equation (4.2).

$$S(f)=\alpha H_{1/3}{}^{2}T_{p}{}^{-4}f^{-5}\exp\left[-1.25(T_{p}f)^{-4}\right]\gamma^{\exp\left[-(T_{p}f-1)^{2}/2\sigma^{2}\right]} \tag{4.2}$$

where

$$\alpha\approx\frac{0.0624}{0.230+0.0336\gamma-0.185(1.9+\gamma)^{-1}} \tag{4.3}$$

$$\sigma=\begin{cases}\sigma_a : f\le f_p\\ \sigma_b : f\ge f_p\end{cases}$$

$$\gamma=1\sim 7 \quad (\text{mean of } 3.3), \quad \sigma_a\approx 0.07,\ \sigma_b\approx 0.09 \tag{4.4}$$

The TMA spectrum of equation (4.6) was an extension of the JONSWAP spectrum to apply to wind-generated seas in finite water depth and it was generated by the transformation factor by Kitaigorodskii et al. (1975) in equation (4.5).

$$\phi(\omega_h)=\left[\frac{\left(k(\omega,h)\right)^{-3}\frac{\partial}{\partial\omega}k(\omega,h)}{\left(k(\omega,\infty)\right)^{-3}\frac{\partial}{\partial\omega}k(\omega,\infty)}\right] \tag{4.5}$$

$$S(f)=\left[JONSWAP\ spectrum(f)\right]\bullet\phi(\omega_h)$$

$$\omega_h=2\pi f\sqrt{h/g} \tag{4.6}$$

A simple approximation form of the transformation factor developed by Thompson and Vincent (1985) is

$$\phi(\omega_h)=\begin{cases}\frac{1}{2}\omega_h^2 & for\ \ \omega_h\le 1\\ 1-\frac{1}{2}\left(2-\omega_h\right)^2 & for\ \ \omega_h\ge 1\end{cases} \tag{4.7}$$

The time series of random waves were obtained from the TMA spectrum by the stochastic integral equation (4.8) developed by Pierson (1955).

$$\eta(x,y,t)=\int_{-\pi}^{\pi}\int_0^{\infty}\cos\left\{\frac{\omega^2}{g}\left(x\cos\theta+y\sin\theta\right)-\omega t+\varepsilon(\omega,\theta)\right\}\bullet\sqrt{2S(\omega,\theta)d\omega\,d\theta} \tag{4.8}$$

where $\eta$ is free surface elevation, $\omega$ is frequency in rps, $\theta$ is direction of waves, $\varepsilon$ = phase and $S(\omega,\theta)$ is a directional spectral density function. An example of an obtained the TMA spectrum and time series of random waves are displayed in Fig. 4.8.

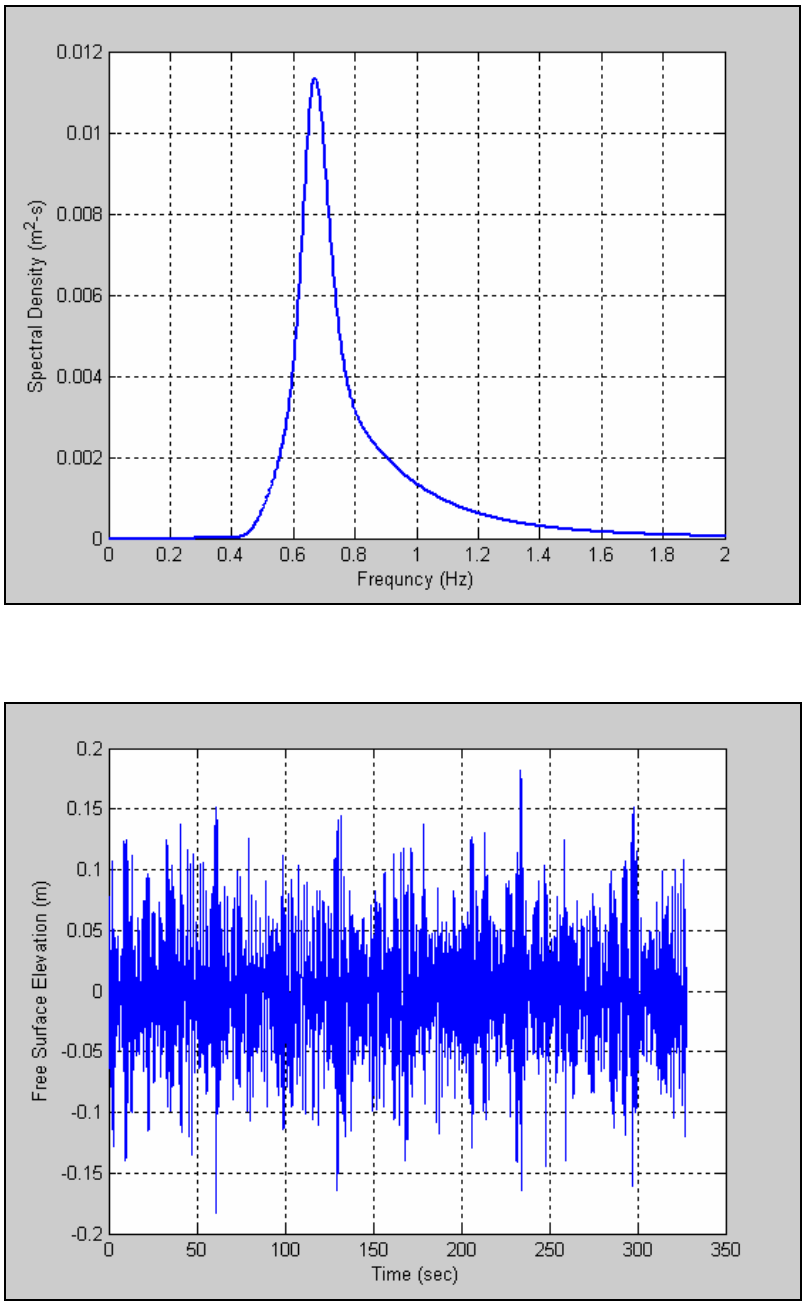


**Fig. 4.8. The computed TMA spectrum (top) and time series of random waves (bottom) at condition of $H_s$ = 0.2 m and $T_p$ = 1.5 seconds.**

**Table 4.2. Test cases for regular and irregular waves.**

| | | Regular waves | | Irregular waves | |
|---|---|---|---|---|---|
| **Test No.** | **Slope of foreberm** | **Wave height $H$ (m)** | **Wave Period $T$ (sec)** | **Wave height $H_{mo}$ (m)** | **Wave period $T_p$ (sec)** |
| **1** | 1: 4 | 0.14 | 1.4 | 0.10 | 1.4 |
| **2** | 1: 4 | 0.14 | 1.6 | 0.10 | 1.6 |
| **3** | 1: 4 | 0.14 | 1.8 | 0.10 | 1.8 |
| **4** | 1: 4 | 0.14 | 2.0 | 0.10 | 2.0 |
| **5** | 1: 4 | 0.14 | 1.4 | 0.10 | 1.4 |
| **6** | 1: 4 | 0.14 | 1.6 | 0.10 | 1.6 |
| **7** | 1: 4 | 0.14 | 1.8 | 0.10 | 1.8 |
| **8** | 1: 4 | 0.14 | 2.0 | 0.10 | 2.0 |
| **9** | 1: 5 | 0.17 | 1.4 | 0.15 | 1.4 |
| **10** | 1: 5 | 0.17 | 1.6 | 0.15 | 1.6 |
| **11** | 1: 5 | 0.17 | 1.8 | 0.15 | 1.8 |
| **12** | 1: 5 | 0.17 | 2.0 | 0.15 | 2.0 |
| **13** | 1: 5 | 0.17 | 1.4 | 0.15 | 1.4 |
| **14** | 1: 5 | 0.17 | 1.6 | 0.15 | 1.6 |
| **15** | 1: 5 | 0.17 | 1.8 | 0.15 | 1.8 |
| **16** | 1: 5 | 0.17 | 2.0 | 0.15 | 2.0 |

### 4.3.3. Beach and Berm

Sand with a median diameter of 0.15 mm was selected and about 2.5 $m^3$ sand was used to build a laboratory berm on a false bottom. The slope of beach in swash zone was 1:10 on a wooden false bottom and the slope of the sand beach face had ratios of 1:4 (vertical: horizontal, $\theta$ = 14.04 °) and 1:5 ($\theta$ = 11.31 °) (Fig. 4.9). The berm was measured before and after each test and it was used to compute the volume of beach erosion and deposition by overwash. To satisfy scale requirement based on the average sand size (Table 4.3) from the field, the sand size in laboratory experiment had to be smaller than the limit of sand size. Cohesive and non-cohesive sediment have totally different characteristics and they are distinguished at a size of 0.076 mm.

**Table 4.3. The sand sizes measured in 2003 near the survey area (Lee, 2003).**

| Line No. | Berm (mm) | Beach (mm) | Average (mm) |
|---|---|---|---|
| 75 | 0.217 | - | - |
| | 0.228 | - | 0.223 |
| 80 | 0.186 | 0.147 | - |
| | 0.193 | 0.157 | **0.171** |
| 85 | 0.151 | 0.169 | - |
| | 0.148 | 0.180 | 0.162 |
| Average | 0.187 | 0.163 | 0.175 |

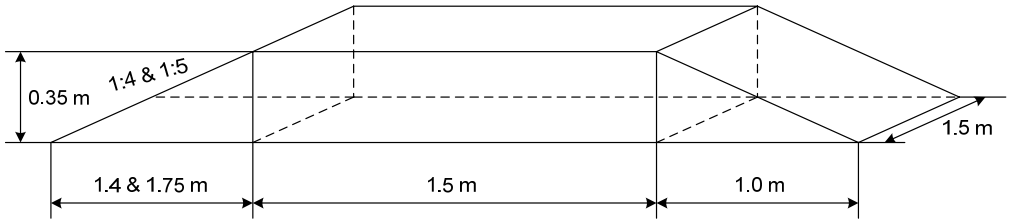


**Fig. 4.9. The shape of initial sand beach for the experiments.**

### 4.3.4. Measurement of Speed of Bore

The speed of bore during overwash is a very important parameter in determining the washover. When the bore touched the top of berm, the speed was measured by two wave gages by monitoring of the change of signals (Fig. 4.10). When wave period was 1.4 sec and wave height was 0.14 m on 1:4 slope, the speed of bore was 0.896 m/s by equation 4.9.

$$\text{Speed of bore} = \frac{\text{Distance between two gages}}{\text{Time to reach from } 1^{st} \text{ gage to } 2^{nd} \text{ gage}} \qquad (4.9)$$

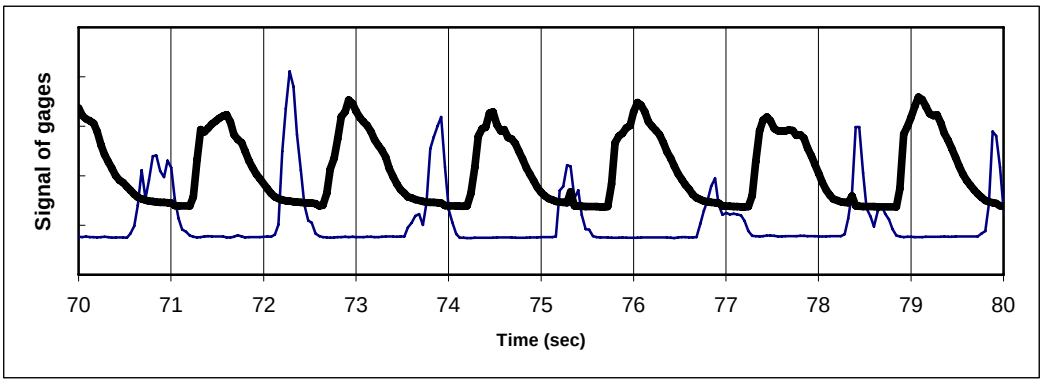


**Fig. 4.10. An example of measuring of the speed of bore by two wave gages.**

### 4.3.5. Measurement of Beach Profile

Beach profiles were measured by the eye safe laser with 0.5 mm accuracy in Fig. 4.6. Sampling spaces were 5 mm and 20 mm in x and y directions, respectively, and x, y and z data were used to analyze erosion and deposition. The range of measurement was 7.0 m in cross-shore direction and 1.0 m in longshore direction. The beach profiles were measured three ways for each case. The initial beach was measured at the beginning of experiment and the time series of beach changes were measured over the center of berm back and forth during experiment at every 15 seconds and the final beach was measured after draining of water in the wave tank. The data were averaged in longshore direction and a representative cross-shore profile was generated. The measurement was begun 25 cm away from both side walls for the purpose of reducing the sidewall effects.

## 4.4. Experimental Results

### 4.4.1. Measured Wave Data

Regular and irregular waves were generated in the experiments in two different slope of foreberm (1:4 and 1:5). Two different wave heights ($H$ = 0.14 m and 0.17 m) and four different wave periods ($T$ = 1.4, 1.6, 1.8 and 2.0) were used for the regular waves. Two different wave heights ($H_{mo}$ = 0.10 m and 0.15 m) and four different wave periods ($T_p$ = 1.4, 1.6, 1.8 and 2.0) were used for the irregular waves in the experiments, so there were sixteen cases in both regular and irregular waves (Table 4.4 and Table 4.5).

The coefficients of reflection were calculated by the method of three wave gages (Suh et al., 2001) and the result showed they were proportion to wave periods. The coefficient of reflection became small at the longer period of waves, because the transmission by overwash was increased at longer period waves.

**Table 4.4. The reflection coefficient and comparison between the target and measured wave height for regular waves.**

| Slopes of fore berm | Wave height (m) | Wave period (sec) | Regular waves | | |
|---|---|---|---|---|---|
| | | | Reflection coefficient | Target $H$ (m) | Measured $H$ (m) |
| 1 : 4 | 0.14 | 1.4 | 0.383 | 0.140 | 0.135 |
| | | 1.6 | 0.528 | 0.140 | 0.144 |
| | | 1.8 | 0.593 | 0.140 | 0.137 |
| | | 2.0 | 0.386 | 0.140 | 0.133 |
| | 0.17 | 1.4 | 0.415 | 0.170 | 0.162 |
| | | 1.6 | 0.520 | 0.170 | 0.166 |
| | | 1.8 | 0.485 | 0.170 | 0.165 |
| | | 2.0 | 0.353 | 0.170 | 0.162 |
| 1 : 5 | 0.14 | 1.4 | 0.376 | 0.140 | 0.133 |
| | | 1.6 | 0.563 | 0.140 | 0.139 |
| | | 1.8 | 0.535 | 0.140 | 0.139 |
| | | 2.0 | 0.513 | 0.140 | 0.133 |
| | 0.17 | 1.4 | 0.381 | 0.170 | 0.171 |
| | | 1.6 | 0.498 | 0.170 | 0.165 |
| | | 1.8 | 0.547 | 0.170 | 0.162 |
| | | 2.0 | 0.504 | 0.170 | 0.161 |

**Table 4.5. The comparison between the target and measured wave heights and periods for irregular waves.**

| Slopes of fore berm | Wave height (m) | Wave period (sec) | Irregular waves | | | |
|---|---|---|---|---|---|---|
| | | | Target $H_{mo}$ (m) | Measured $H_{mo}$ (m) | Target $T_p$ (m) | Measured $T_p$ (m) |
| 1 : 4 | 0.10 | 1.4 | 0.10 | 0.098 | 1.40 | 1.42 |
| | | 1.6 | 0.10 | 0.106 | 1.60 | 1.57 |
| | | 1.8 | 0.10 | 0.107 | 1.80 | 1.73 |
| | | 2.0 | 0.10 | 0.104 | 2.00 | 1.93 |
| | 0.15 | 1.4 | 0.15 | 0.149 | 1.40 | 1.42 |
| | | 1.6 | 0.15 | 0.153 | 1.60 | 1.59 |
| | | 1.8 | 0.15 | 0.149 | 1.80 | 1.72 |
| | | 2.0 | 0.15 | 0.151 | 2.00 | 1.92 |
| 1 : 5 | 0.10 | 1.4 | 0.10 | 0.961 | 1.40 | 1.43 |
| | | 1.6 | 0.10 | 0.103 | 1.60 | 1.56 |
| | | 1.8 | 0.10 | 0.099 | 1.80 | 1.73 |
| | | 2.0 | 0.10 | 0.098 | 2.00 | 1.90 |
| | 0.15 | 1.4 | 0.15 | 0.157 | 1.40 | 1.43 |
| | | 1.6 | 0.15 | 0.152 | 1.60 | 1.54 |
| | | 1.8 | 0.15 | 0.153 | 1.80 | 1.72 |
| | | 2.0 | 0.15 | 0.149 | 2.00 | 1.89 |

### 4.4.2. Beach Profile

The profiles were measured in two ways and the first was the time series of beach changes during the experiments and the second was the final shape of beach after the experiments. Time series of beach changes were measured at each test case but some produced useless data. In same cases the laser beam was reflected from the water surface which was turbid from breaking waves and suspended sand and the lens of laser was contaminated by extremely breaking waves accidentally.

The ranges of measurement were 7.0 m in cross-shore and 1.0 m in alongshore, because there was little deposition beyond 7.0 m seaward. The profile data every 20 mm in longshore direction was averaged and the result became a representative line in cross-shore direction at each test case.

The long term changes for 1635 (5 × 327 seconds) seconds by irregular waves were measured and shown in Fig. A.33. There were some volume changes on the top of foreberm and submerged bar but little change behind the berm. The submerged bar was being built up in almost the same location and the rate of deposition was decreasing with time. Half of the total retreat of foreberm occurred in the first 327 seconds and the rates of retreat were 51.85 %, 22.22%, 9.26 %, 9.26 % and 7.41 % at every 327 second from the beginning of experiment Fig. 4.11. The ratio of sediment transport between landward and seaward was 30.84 % to 69.16 % from the experiments (the table on page 125) and it meant that most of sand eroded by waves was transported seaward in this case. All measured beach profiles were shown in Appendix A.

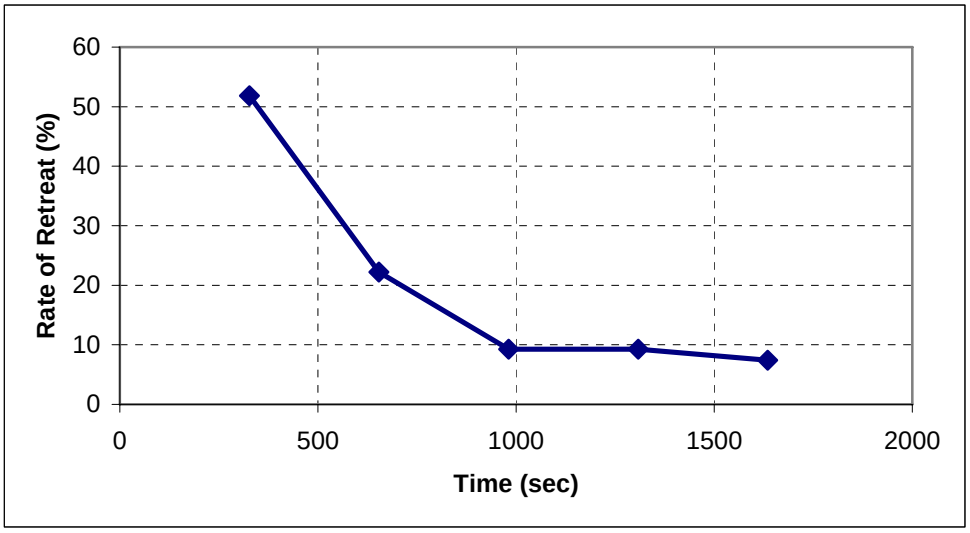


**Fig. 4.11. The change of rate of retreat over a running time.**

### 4.4.3. Comparison by Different Wave Heights for Regular Waves

To find and understand the factors that cause overwash was important to conduct laboratory experiments. In this study, three major factors such as wave height, period and slope were selected and the correlation between overwash events was studied from experiment results.

The impact of wave height and slope of foreberm was displayed here. Each graph from Fig. 4.12 to Fig. 4.18 shows the different amount of erosion by different wave heights. The comparison by different slope of beach face was made between Fig. 4.12 and Fig. 4.13. Erosion and transportation on the berm were much stronger with increasing of wave height.

The impact of slope was apparently shown in Fig. 4.18 and Fig. 4.19. Though the experiments were conducted at the same wave height and period, the berm was eroded completely at steeper slope.

These factors of overwash are strongly correlated with wave runup and overtopping. The sensitivity analysis was conducted in this chapter and it was used to develop empirical formulas.

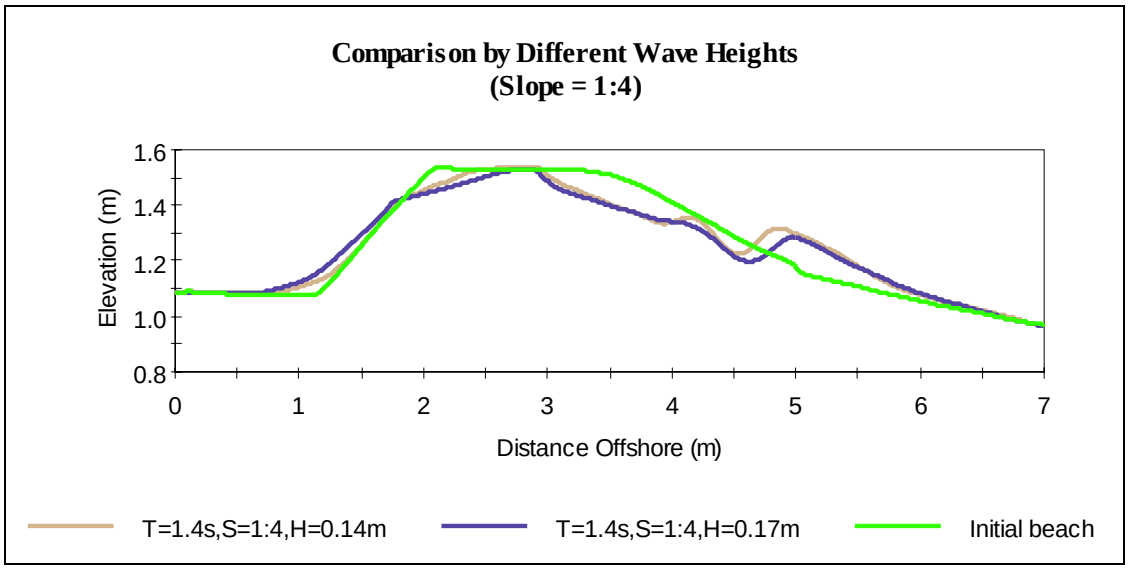


**Fig. 4.12. Comparison by different wave heights for regular waves (period = 1.4 s, slope = 1:4).**

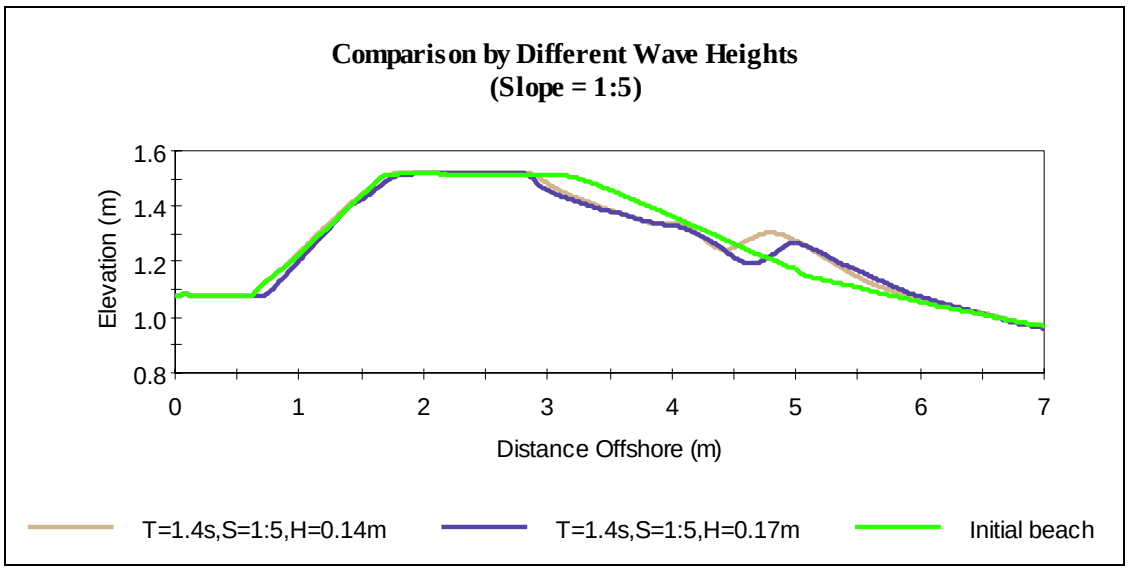


**Fig. 4.13. Comparison by different wave heights for regular waves (period = 1.4 s, slope = 1:5).**

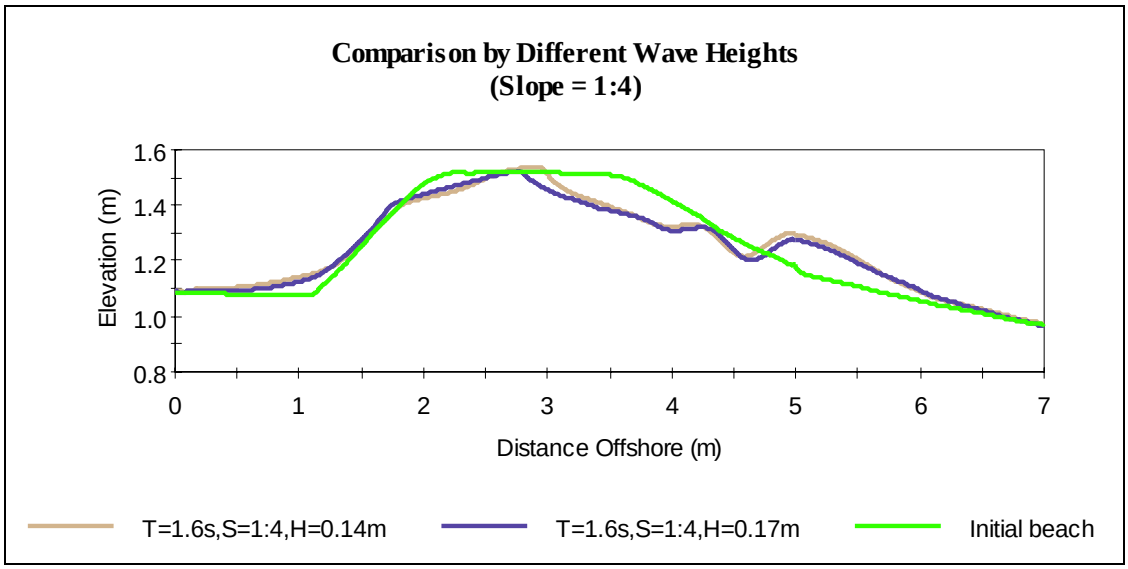


**Fig. 4.14. Comparison by different wave heights for regular waves (period = 1.6 s, slope = 1:4).**

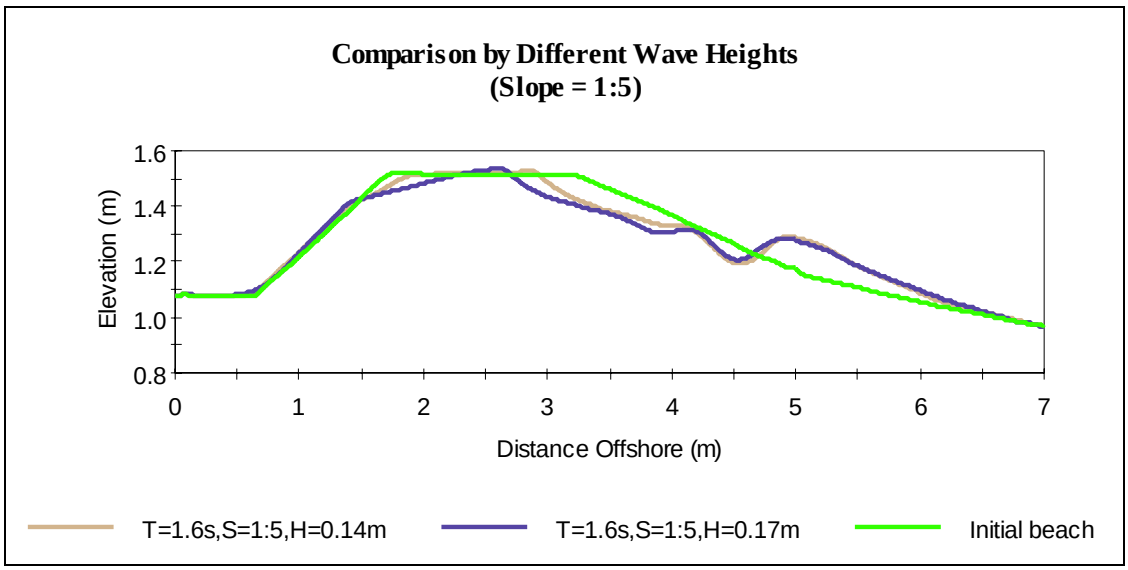


**Fig. 4.15. Comparison by different wave heights for regular waves (period = 1.6 s, slope = 1:5).**

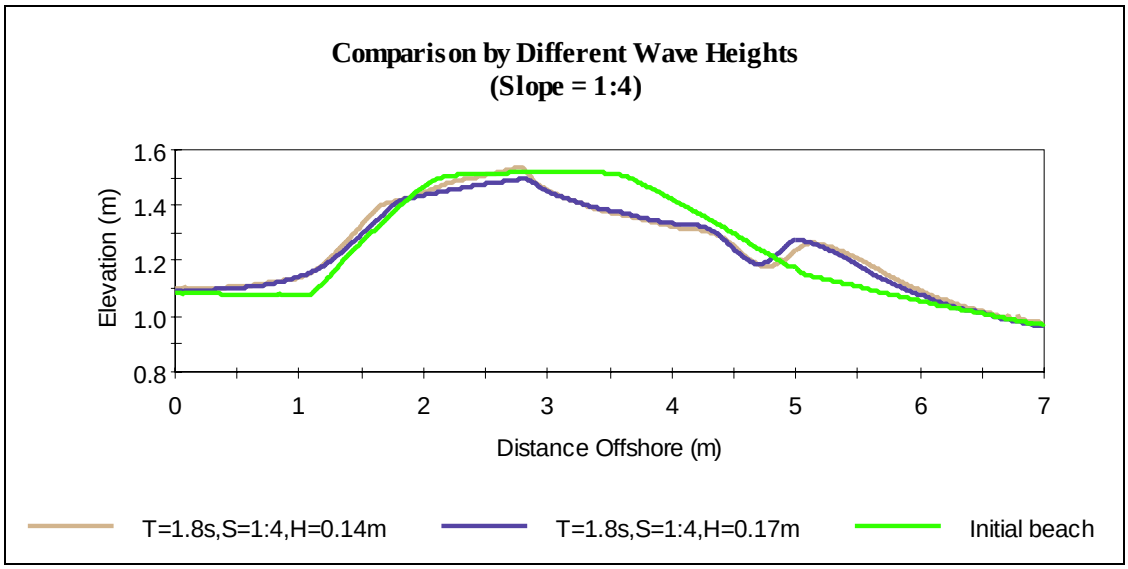


**Fig. 4.16. Comparison by different wave heights for regular waves (period = 1.8 s, slope = 1:4).**

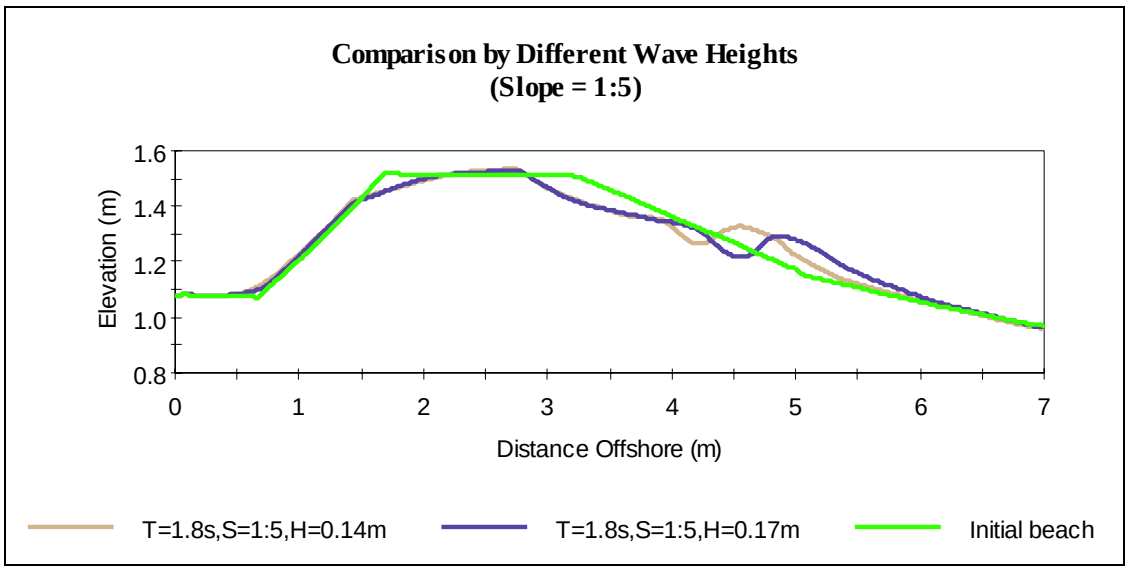


**Fig. 4.17. Comparison by different wave heights for regular waves (period = 1.8 s, slope = 1:5).**

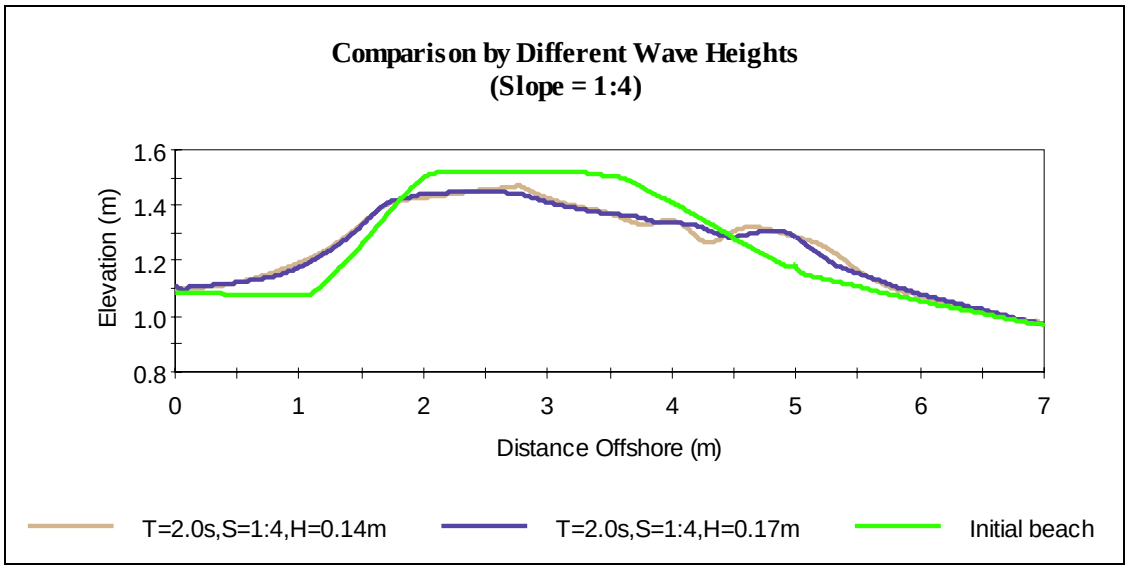


**Fig. 4.18. Comparison by different wave heights for regular waves (period = 2.0 s, slope = 1:4).**

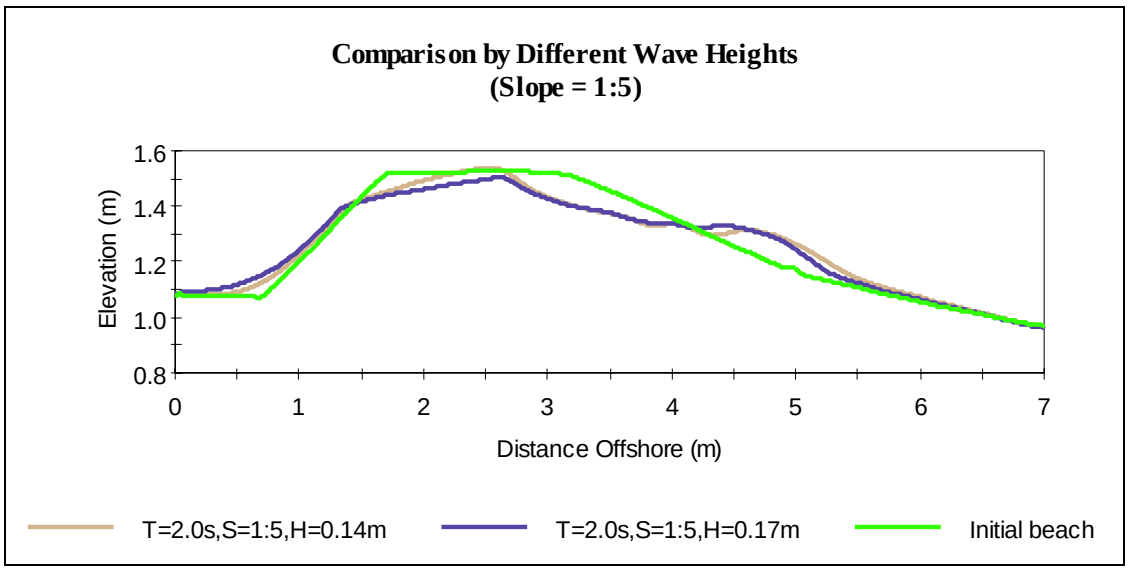


**Fig. 4.19. Comparison by different wave heights for regular waves (period = 2.0 s, slope = 1:5).**

### 4.4.4. Comparison by Different Wave Periods for Regular Waves

When wave period became longer, a submerged bar was located further offshore. This relation was valid up to wave period of 1.8 sec but it was different at 2.0 sec. Much sand was eroded and transported behind the berm after wave period of 2.0 sec, because erosion of berm was increased with longer wave.

When we compare the results in Fig. 4.20 and Fig. 4.21, erosion was more sensitive to change of wave period than wave height. Less sand was eroded in Fig. 4.22 and Fig. 4.23 due to milder slope than 1:4 slope cases.

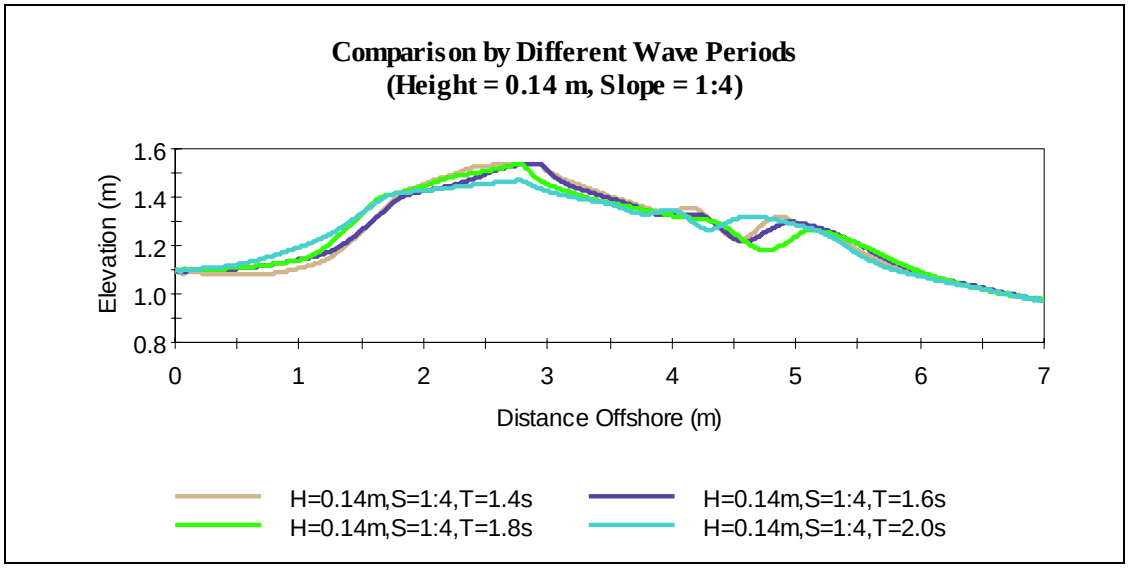


**Fig. 4.20. Comparison by different wave periods for regular waves (height = 0.14 m, slope = 1:4).**

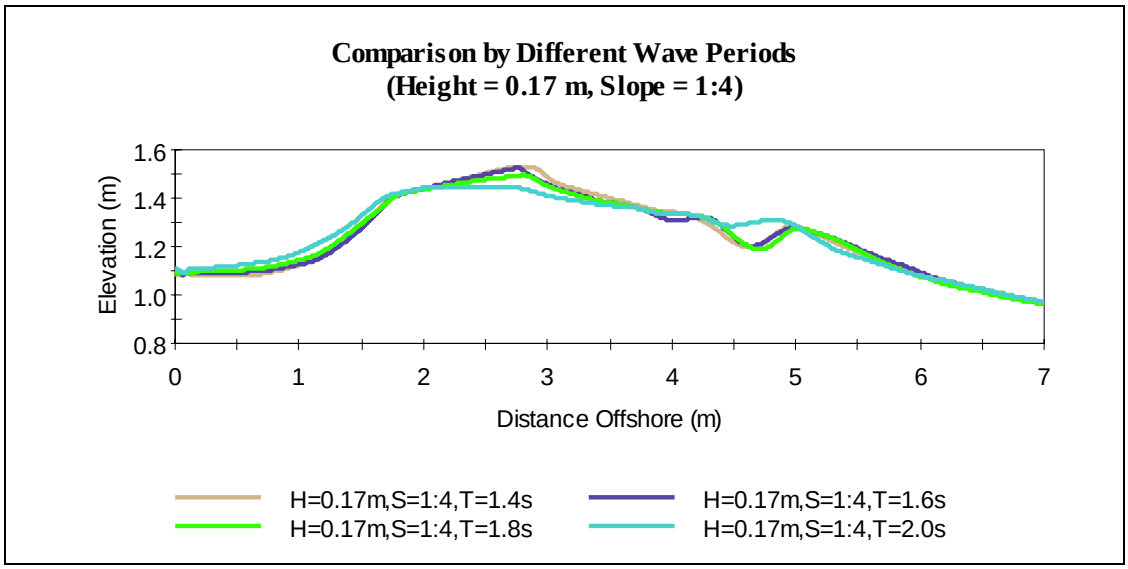


**Fig. 4.21. Comparison by different wave periods for regular waves (height = 0.17 m, slope = 1:4).**

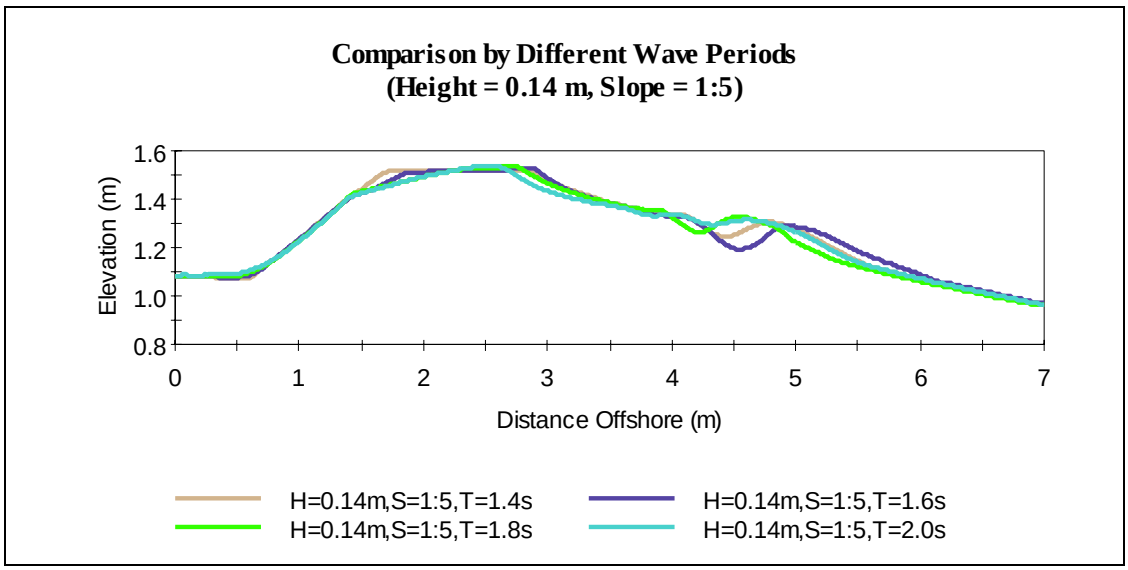


**Fig. 4.22. Comparison by different wave periods for regular waves (height = 0.14 m, slope = 1:5).**

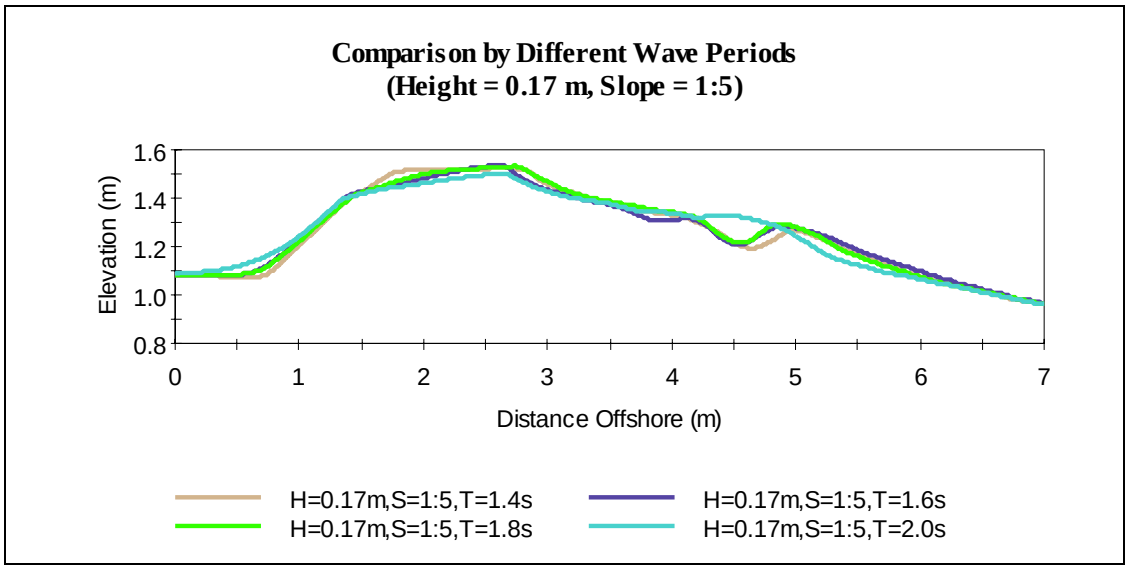


**Fig. 4.23. Comparison by different wave periods for regular waves (height = 0.17 m, slope = 1:5).**

### 4.4.5. Comparison for Irregular Waves

Erosion by irregular waves was not big enough to figure out the impact of factors at each case in Fig. 4.24 to Fig. 4.27. The difference by factors may be appeared, when the experiment was conducted for long enough like Fig. A.33.

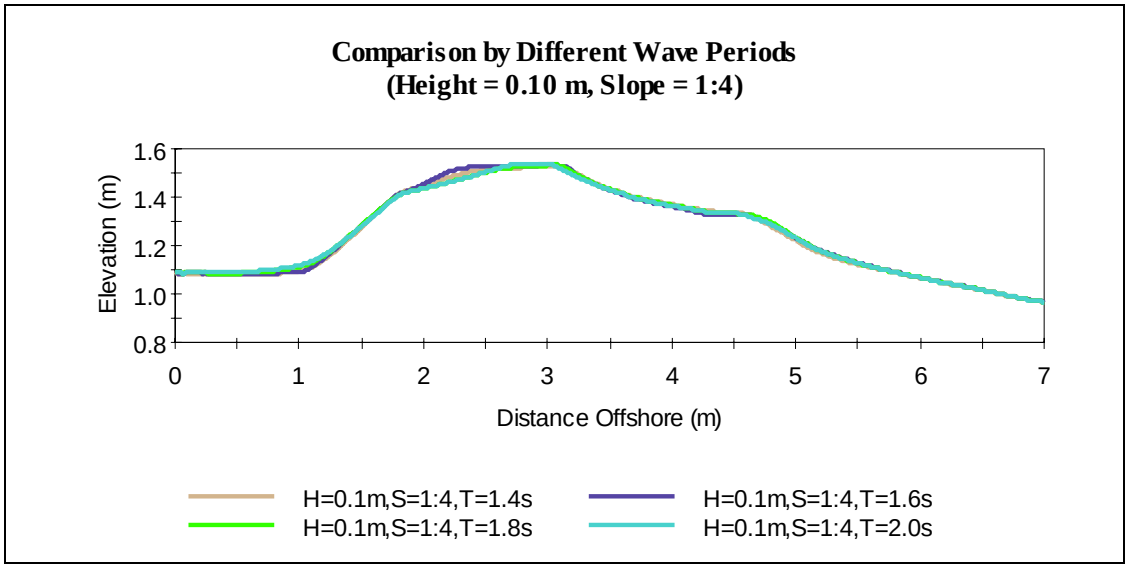


**Fig. 4.24. Comparison by different wave periods for irregular waves (height = 0.10 m, slope = 1:4).**

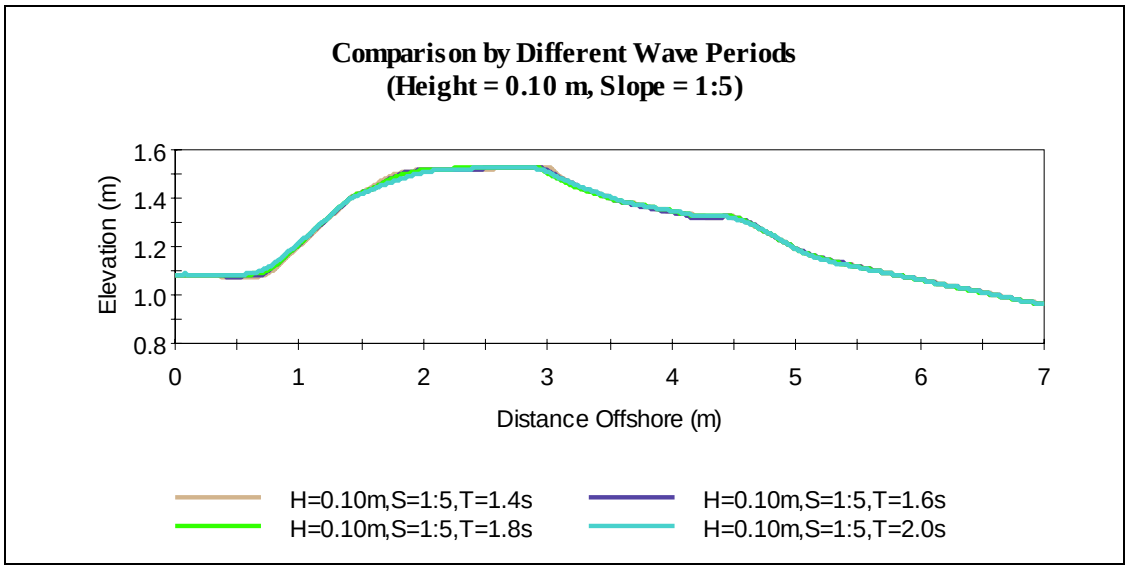


**Fig. 4.25. Comparison by different wave periods for irregular waves (height = 0.10 m, slope = 1:5).**

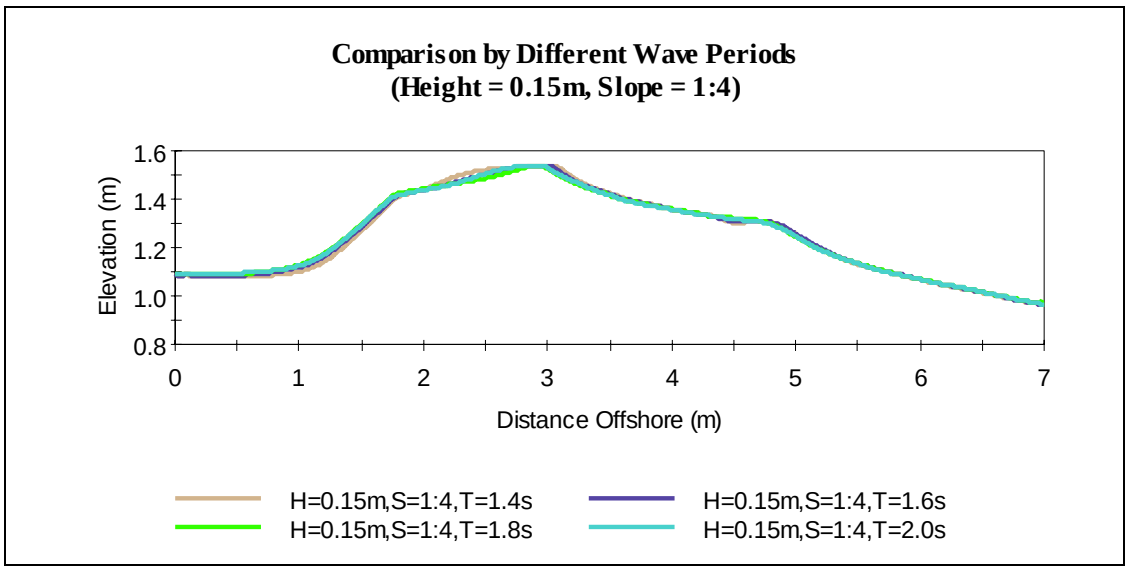


**Fig. 4.26. Comparison by different wave periods for irregular waves (height = 0.15 m, slope = 1:4).**

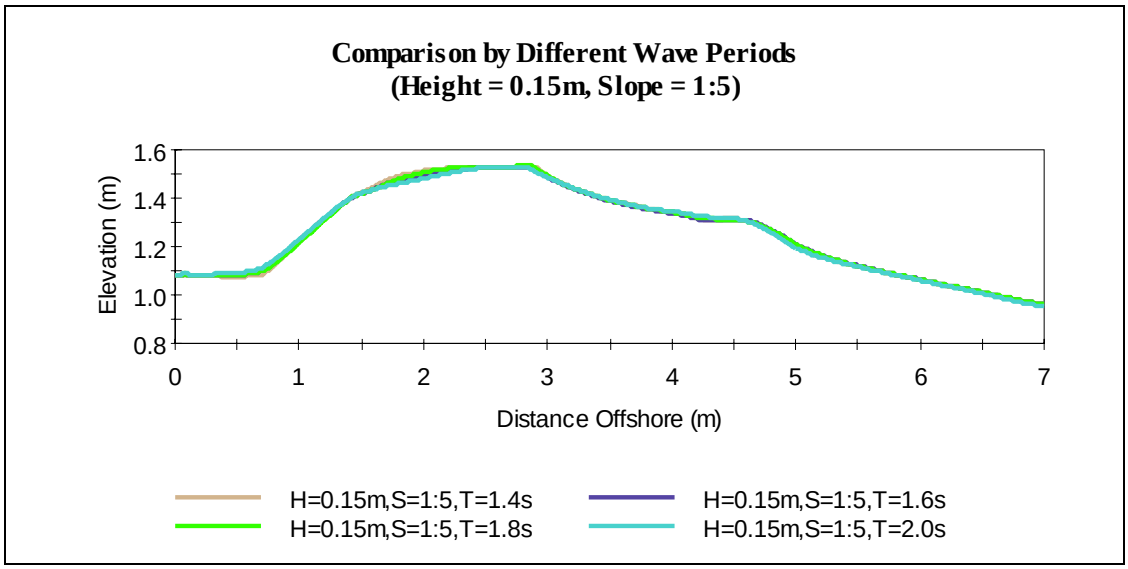


**Fig. 4.27. Comparison by different wave periods for irregular waves (height = 0.15 m, slope = 1:5).**

## 4.5. Analysis of Results

### 4.5.1. Mechanics of Sediment Transport

The eroded sand in swash zone was transported landward and seaward and each arrow shows the transport of sand in Fig. 4.28. An objective was made for this research to focus on the effect of overwash, because much erosion and deposition happens by waves in swash zone simultaneously. A point was selected from the change of sand volume in cross-shore direction, called the zero-point, as shown in Fig. 4.28. It was assumed that all sand on the right side of the zero-point was moved offshore and the other in the left side of the zero-point was related to overwash. The changes of eroded and deposited sand were integrated from offshore to the berm and the location where the net volume was zero was selected as the zero-point. The zero-point was located in swash zone in most of cases and its location showed a relationship between overwash and wave periods.

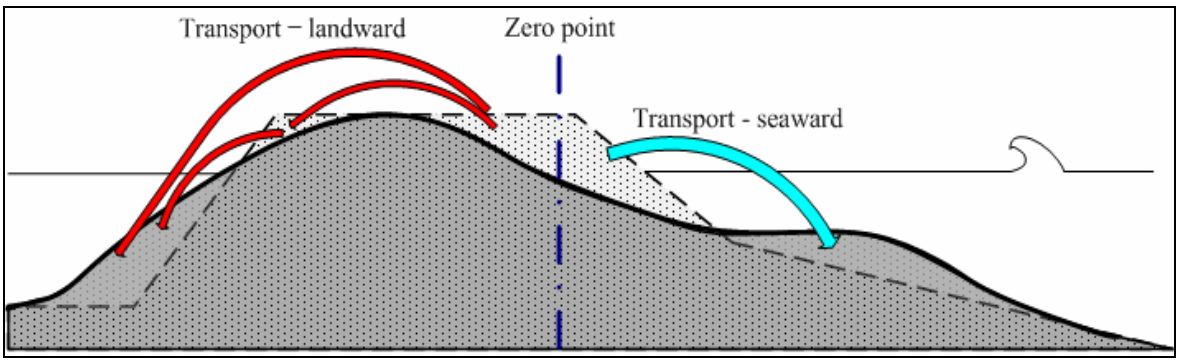


**Fig. 4.28. Morphological profile changes and mechanics of sediment transport by overwash.**

### 4.5.2. Sediment Transport

The data in Table 4.6 and Table 4.7 were obtained based on the result of profiles and small sand in sand collector behind the berm. Some of the sand eroded by waves from swash zone was transported offshore and became a submerged bar and the rest of sand were transported over the berm and deposited in the top of berm and behind the berm in Fig. 4.28. The overtopping bore made erosion on the top of berm. The eroded sand was transport behind the berm and deposited there.

The ratios of volume of transported sand between landward and seaward were calculated based on the zero-point of each case. The volume showed that much sand was transported landward by overwash, when wave height was bigger, wave period was longer and slope of foreberm was steeper like the characteristics of overtopping. It agreed with the result that much sand was eroded and deposited landward after the attack of extreme waves by hurricane and the beach was never fully recovered. This is an explanation why much of sand was eroded and transported landward by Hurricane Rita in the field measurement.

The numbers of waves that overwash were counted and they were used for getting the average volume of overwashed sand per each overwash. The average volume of overwashed sand per each overwash was proportional to wave height and period but it was inversely proportional to slope of foreberm. The number of overwash events was exactly proportioned to the inverse of wave period, because overwash occurred by overtopping at each wave runup. When it was considered that overwash happened for several hours during landfall of hurricane, about two hundred overwash events in a laboratory could be a good reference for one hour-overwash in beach.

**Table 4.6. The volume of overwashed sand by regular waves.**

| Slopes of fore berm | Wave height (m) | Wave period (sec) | Zero point (m) | Ratio of transport landward and seaward | | Number of Overwash Events | Volume of overwash transport ($cm^3/cm$) | Average volume of sand per overwash ($cm^3/cm$) |
|---|---|---|---|---|---|---|---|---|
| | | | | Land ward (%) | Sea Ward (%) | | | |
| 1 : 4 | 0.14 | 1.4 | 2.95 | 16.67 | 83.33 | 117 | 230.00 | 1.97 |
| | | 1.6 | 3.00 | 29.89 | 70.11 | 125 | 550.00 | 4.40 |
| | | 1.8 | 3.53 | 49.62 | 50.38 | 132 | 876.42 | 6.64 |
| | | 2.0 | 3.23 | 49.80 | 50.20 | 163 | 1200.53 | 7.37 |
| | 0.17 | 1.4 | 3.31 | 33.11 | 66.89 | 164 | 490.00 | 2.99 |
| | | 1.6 | 3.27 | 37.64 | 62.36 | 204 | 670.00 | 3.28 |
| | | 1.8 | 3.44 | 53.89 | 46.11 | 181 | 1040.00 | 5.75 |
| | | 2.0 | 3.32 | 52.91 | 47.09 | 163 | 1180.00 | 7.24 |
| 1 : 5 | 0.14 | 1.4 | 2.85 | 10.00 | 90.00 | 46 | 100.00 | 2.17 |
| | | 1.6 | 2.91 | 15.33 | 84.67 | 59 | 210.00 | 3.56 |
| | | 1.8 | 3.31 | 44.55 | 55.45 | 181 | 490.00 | 2.71 |
| | | 2.0 | 2.65 | 26.31 | 73.69 | 163 | 360.53 | 2.21 |
| | 0.17 | 1.4 | 3.23 | 23.58 | 76.42 | 105 | 250.00 | 2.38 |
| | | 1.6 | 2.77 | 20.65 | 79.35 | 181 | 312.32 | 1.73 |
| | | 1.8 | 2.77 | 19.46 | 80.54 | 181 | 222.32 | 1.23 |
| | | 2.0 | 3.07 | 46.98 | 53.02 | 163 | 700.00 | 4.29 |

**Table 4.7. The volume of overwashed sand by irregular waves.**

| Slopes of fore berm | Wave height $H_{mo}$ (m) | Wave period $T_p$ (sec) | Zero point (m) | Ratio of transport landward and seaward | | Number of Overwash Events | Volume of overwash transport ($cm^3/cm$) | Average volume of sand per overwash ($cm^3/cm$) |
|---|---|---|---|---|---|---|---|---|
| | | | | Land ward (%) | Sea Ward (%) | | | |
| 1 : 4 | 0.10 | 1.4 | 3.13 | 17.86 | 82.14 | 44 | 250.00 | 5.68 |
| | | 1.6 | 3.16 | 13.42 | 86.58 | 52 | 200.00 | 3.85 |
| | | 1.8 | 3.15 | 31.69 | 68.31 | 65 | 412.84 | 6.35 |
| | | 2.0 | 3.18 | 27.83 | 72.17 | 71 | 466.68 | 6.57 |
| | 0.15 | 1.4 | 3.12 | 22.05 | 77.95 | 56 | 280.00 | 5.00 |
| | | 1.6 | 3.22 | 26.49 | 73.51 | 73 | 400.00 | 5.48 |
| | | 1.8 | 3.15 | 36.28 | 63.72 | 86 | 506.68 | 5.89 |
| | | 2.0 | 3.18 | 32.19 | 67.81 | 91 | 498.47 | 5.48 |
| 1 : 5 | 0.10 | 1.4 | 3.04 | 14.29 | 85.71 | 26 | 150.00 | 5.77 |
| | | 1.6 | 2.98 | 13.43 | 86.57 | 31 | 180.00 | 5.81 |
| | | 1.8 | 3.03 | 28.92 | 71.08 | 49 | 248.21 | 5.07 |
| | | 2.0 | 2.97 | 20.98 | 79.02 | 56 | 268.21 | 4.79 |
| | 0.15 | 1.4 | 2.92 | 21.36 | 78.64 | 40 | 220.00 | 5.50 |
| | | 1.6 | 3.03 | 20.12 | 79.88 | 59 | 302.32 | 5.12 |
| | | 1.8 | 2.98 | 22.84 | 77.16 | 63 | 272.32 | 4.32 |
| | | 2.0 | 3.20 | 30.84 | 69.16 | 79 | 352.32 | 4.46 |

### 4.5.3. Sensitivity Analysis for Regular Waves

The seven parameters from the experiment were used to develop the empirical formulas of overwash in equation (4.10).

$$Q_s = f_1(H, T, S, h, w, U, \xi, R) \tag{4.10}$$

where $Q_s$ = total sediment transport rate in unit width ($m^3/m \cdot s$), $H$ = wave height (m), $T$ = wave period (sec), $S$ = slope of foreberm ($tan\theta$), $h$ = water depth (m) in deep water, $w$ = settling velocity of sand (m/s), $U$ = speed of bore (m/s), $\xi$ = Iribarren number ( $S / \sqrt{H_0 / L_0}$ ) and wave runup height. The total sediment transport could be determined by these dominant seven variables based on a probabilistic and regression approaches.

The basic form of sediment transport can be expressed with combination of the seven dominant variables in equation (4.11).

$$U = C\sqrt{gR} \tag{4.11}$$

where $U$ = speed of bore, $C$ = constant and $g$ = gravitational acceleration

The factors of slope, Iribarren number, Shield parameter and settling velocity divided by speed of bore were more dominant than any other from the results of sensitivity analysis in Fig. 4.29.

Runup and thickness of bore on top of berm are also important factors to understand the mechanics of overwash but this experiment failed to measure them due to the incapability of equipments. However, runup height can be estimated by equation (4.11).

A new functional relationship of sediment transport with dimensionless terms was derived by using dimensional analysis as

$$\frac{Q_s}{\sqrt{gH^3}} = f_2\left(S, \frac{H}{L}, \xi, \frac{w}{U}, \frac{H}{wT}, \frac{U^2/g}{H}, \frac{U^2}{(s-1)gd_{50}}\right) \tag{4.12}$$

Wave steepness was important to express the characteristics of wave and the Iribarren number showed better relationship with sediment transport. Only Iribarren number was used to develop the formula, because Iribarren number was composed of slope of foreberm and wave steepness in itself.

The settling velocity was related to vertical movement of sediment and the speed of bore was related to the horizontal movement of sediment. It meant the characteristics of overwash had the similar mechanics of transport as an open channel. The bed load transport could be more dominant than suspended load transport in this case. Because the settling velocity of sand was a function of size of sand, the final empirical equation by the factors of settling velocity could represent the effects of different sand size. The wave runup height from equation (4.11) was a function of wave height and the relationship between these factors was shown in Fig. 4.29. The final form of the equation could be expected to be similar to equation (4.13) based on above relationships between the factors.

$$\frac{Q_s}{\sqrt{gH^3}} = a_0\, \xi^{a_1}\left(\frac{U^2}{(s-1)gd_{50}}\right)^{a_2} \tag{4.13}$$

where $a_0$, $a_1$, and $a_2$ = parameters.

The sensitivity analyses of each factor were displayed in Fig. 4.29. Because the experiment for the effect of slope was conducted in only two different slopes, the relationship between sediment transport and slopes of foreberm needed to be displayed in two different slopes which have the same wave conditions. They showed good relationship with sediment transport rate.

When the natural logarithms of both sides of equation (4.10) are applied, a linear multiple form could be derived as follows,

$$\ln\left(\frac{Q_s}{\sqrt{gH^3}}\right)=\ln(a_0)+a_1\ln\left(\xi\right)+a_2\ln\left(\frac{U^2}{(s-1)gd_{50}}\right) \tag{4.14}$$

The main problem of regression by least squares method was also sensitive to extreme values which called outliers. The robust regression (Rousseeuw and Van Driessen, 1998) was used for multiple regression and elimination of outliers in developing of sediment transport formula.

The computed values from 16 measured data were as follows,

$$a_0 = \quad e^{-10.2813} = 3.427\times10^{-5}$$

$$a_1 = \quad 2.5849$$

$$a_2 = \quad 0.4223$$

The new empirical equation of sediment transport rate with these values was given as

$$Q_s = 3.427\times10^{-5}\,\xi^{2.5849}\left(\frac{U^2}{(s-1)gd_{50}}\right)^{0.4223}\sqrt{gH^3}\quad\left(m^3/m\cdot s\right) \tag{4.15}$$

The values from the empirical equation (4.15) were compared to the values from the laboratory experiments for verification of the new equation in Fig. 4.30. R-squared value of linear regression was an indicator of how the model fit the data and it meant a perfect correlation with data when the value was 1.0. The R-squared value for regular waves was 0.8791 and it meant that 87.9 % correlation could be explained by this new equation.

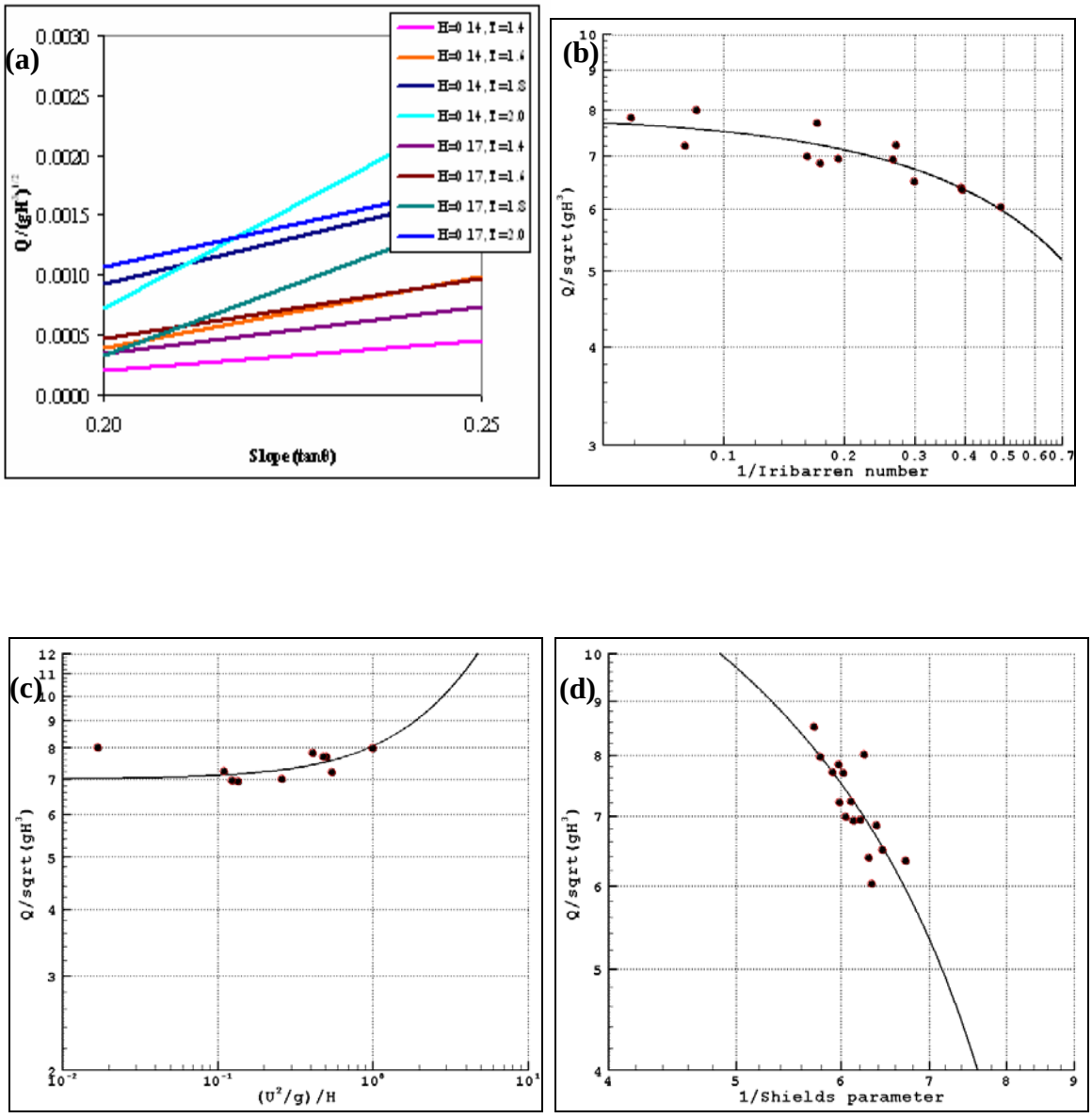


**Fig. 4.29. Relationships between total sediment transport and (a) slope, (b) 1 / Iribarren number, (c) square root of speed of bore / gravitational acceleration / wave height and (d) 1 / Shields parameter in regular waves.**

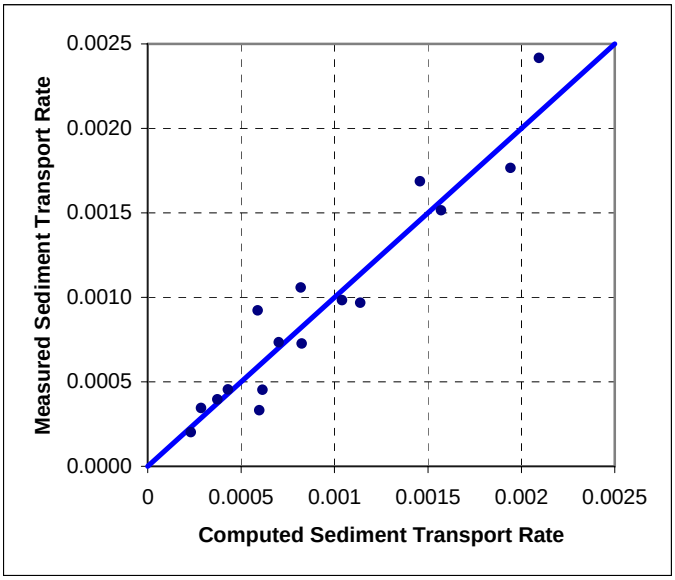


**Fig. 4.30. The comparison between computed and measured sediment transport rate by regular waves for verification.**

### 4.5.4. Sensitivity Analysis for Irregular Waves

The same methods as those in regular waves were applied to get an empirical formula for irregular waves. However, the speeds of bores are different to each incoming waves in irregular waves, so a different factor included the settling velocity was used. The factors in this equation were determined from sensitivity analysis in Fig. 4.31.

$$\frac{Q_s}{\sqrt{gH^3}} = a_0 \left(\xi\right)^{a_1} \left(\frac{H}{wT}\right)^{a_2} \tag{4.16}$$

The calculated values were as follows,

$$a_0 = \mathrm{e}^{-7.8993} = 3.71\times10^{-4}$$

$$a_1 = 2.0175$$

$$a_2 = 0.0603$$

The Equation (4.17) of sediment transport rate for irregular waves was obtained from above values.

$$Q_s = 3.71\times10^{-4}\ \xi^{2.0175} \left(\frac{H_s}{wT_p}\right)^{0.0603} \sqrt{gH_s^{\,3}} \quad \left(m^3/m\cdot s\right) \tag{4.17}$$

The comparison between computed and measured values was shown in Fig. 4.32. The R-squared value for irregular waves was 0.8531 and it was less than the result by regular waves. The results of irregular waves could be improved by increasing the running time of experiment, because the number and intensity of overwash were different at each case during a relatively short running time.

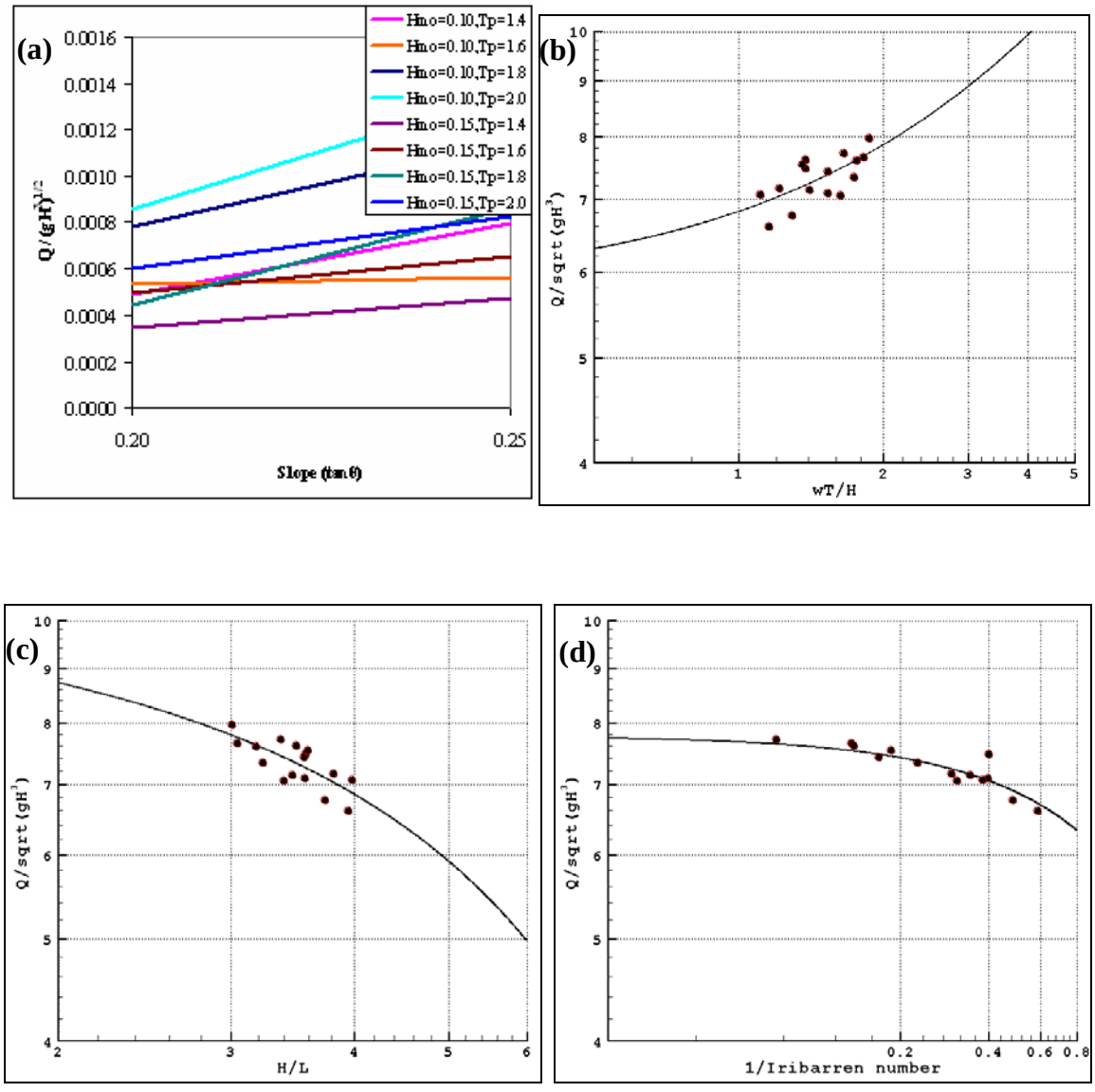


**Fig. 4.31. Relationships between total sediment transport and (a) slope, (b) (settling velocity · wave period) / wave height, (c) wave height / wave length in deep water and (d) 1 / Iribarren number in irregular waves.**

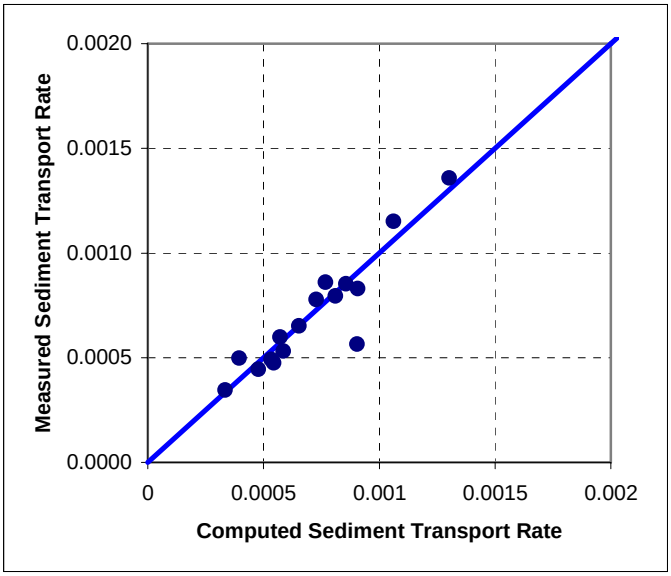


**Fig. 4.32. The comparison between computed and measured sediment transport rate by irregular waves for verification.**

### 4.5.5. The Energy Loss by the Uprush of the Waves and Rundown

A lot of energy was dissipated by the collision of the uprush of the waves and rundown during overwash and the result showed some differences to estimate speed of bore in existing theories. It may make a difficulty to develop an empirical formula and a numerical model, because there is no reference for this collision phenomenon.

The photos of collision are shown in Fig. 4.33. The wave breaking is shown in the first photo and the collision began to generate in the second photo. The intensity of collision was not able to measure in the experiment but the energy dissipation by collision seemed to be stronger than wave breaking by the photos.

The collision could be another mechanism to explain overwash and washover. The strong intensity of turbulence by wave breaking and collision generated erosion and suspension in the foreberm and suspended sand was then transported over the berm by overtopping.

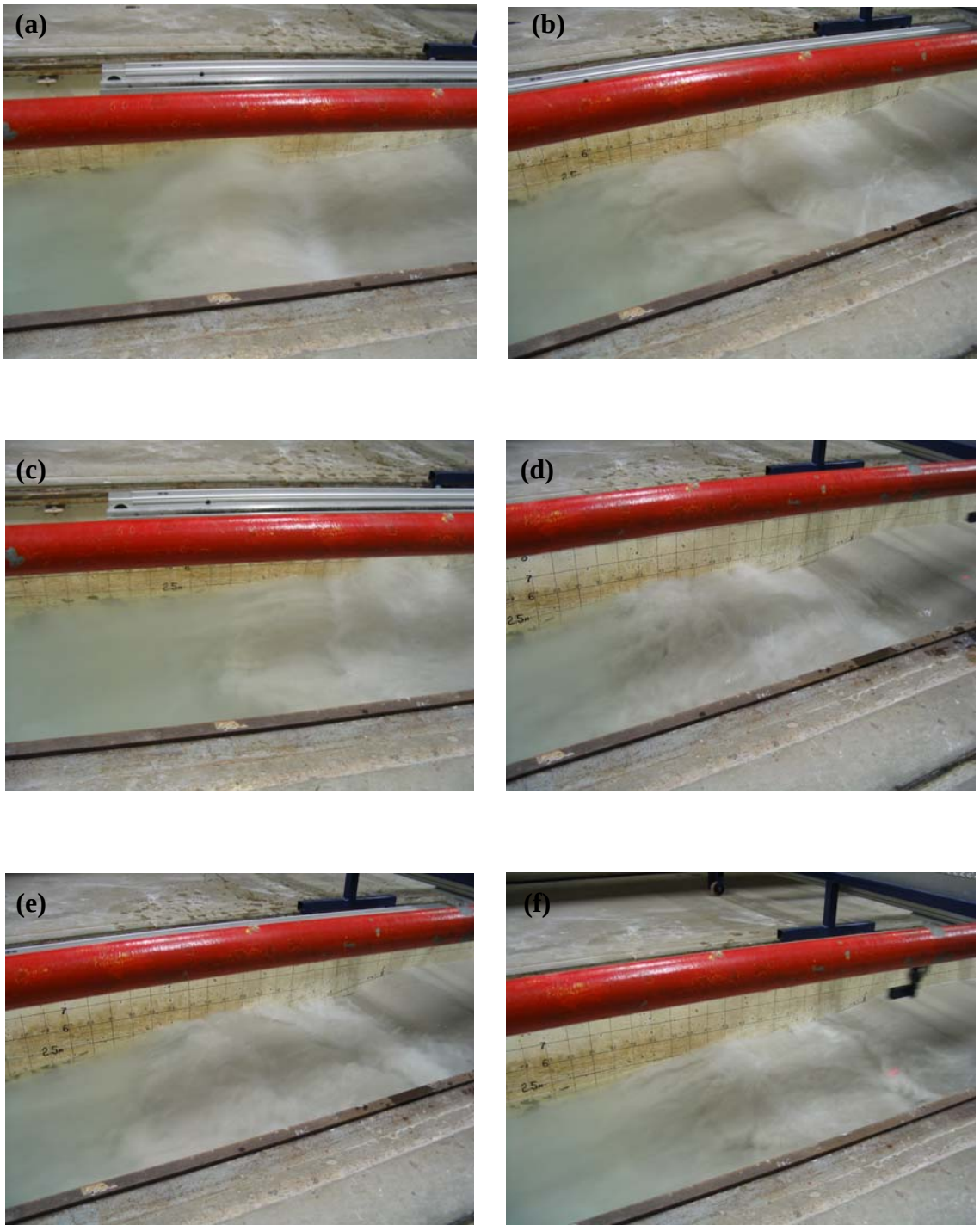


**Fig. 4.33. The energy loss by the crash between the uprush of waves and rundown.**

## 4.6. Comparison with the Field Measurement (Study Area)

The field measurement with the most significant overwash event was conducted before and after landfall of Hurricane Rita in 2005 and the measured data were shown in Chapter III. The survey included eleven lines and the beach conditions in each line were averaged as follows,

- Average slope of beach face : 0.0368 (1:27.174, 2.108 degree)
- Average sand size : 0.171 mm
- Settling velocity by sand size : 0.019 m/s
- Average volume of erosion for eleven lines : 26.24 $m^3/m$

$$Q_s = 3.71\times10^{-4}\,\xi^{2.0175}\left(\frac{H_s}{wT_p}\right)^{0.0603}\sqrt{gH_s^{\,3}}\quad\left(m^3/m\cdot s\right) \tag{4.18}$$

The equation (4.18) developed from the laboratory experiments for irregular waves was used to estimate the total sand volume of erosion by overwash. Only $H_s$ and $T_p$ were changed with the wave conditions in Fig. 4.34 and the Iribarren number and settling velocity were determined from the beach conditions. Because these $H_s$ and $T_p$ were representative values at each hour, it was assumed that $H_s$ and $T_p$ did not change for an hour and the different $H_s$ and $T_p$ were applied at every hour. The wave heights from the buoy was not available 4 hours before landfall of Hurricane Rita, it was assumed that the last measured wave height was continued during unavailable time.

The start and end of overwash were determined by the calculation of overtopping in Chapter III. The calculation was done by summation of storm surge, tides and maximum runup by waves. Overwash started at 2 am in September 23, 2005 and it ended at 3 am in

September 24, 2005. Overwash lasted for 26 hours by above information. The total computed volume of erosion by overwash was 28.97 $m^3/m$ in Table 4.8 and the result was close to the result by the field measurement (26.24 $m^3/m$). However, the impact of storm surge was not included in the estimation by the empirical equation (4.18).

The pattern of erosion by overwash is shown in Table 4.8 as computed. The erosion by long period swells was much greater than the erosion before landfall, whereas the wave height was peak at the time of landfall.

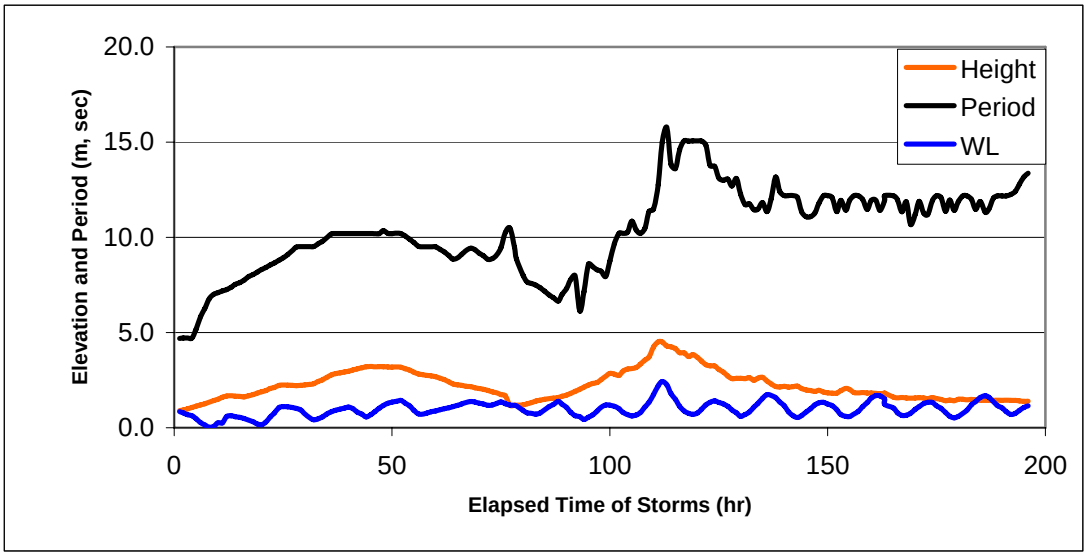


**Fig. 4.34. Wave conditions and water level (NAVD 88) in Ocean city before and after storms (Larson et at., 2004).**

**Table 4.8. The computed volume of erosion by overwash in the study area during landfall of hurricane Rita.**

| Year | Month | Day | Hour | $H_s$ (m) | $T_p$ (sec) | Tides & Surge (m) | Volume ($m^3/m$) |
|---|---|---|---|---|---|---|---|
| 2005 | 9 | 23 | 2 | 2.41 | 9.65 | 0.707 | 1.460 |
| 2005 | 9 | 23 | 3 | 2.84 | 10.42 | 0.687 | 1.857 |
| 2005 | 9 | 23 | 4 | 2.73 | 10.09 | 0.672 | 1.706 |
| 2005 | 9 | 23 | 5 | 2.78 | 8.42 | 0.595 | 1.210 |
| 2005 | 9 | 23 | 6 | 3.10 | 8.21 | 0.610 | 1.223 |
| 2005 | 9 | 23 | 7 | 3.32 | 7.82 | 0.614 | 1.154 |
| 2005 | 9 | 23 | 8 | 3.44 | 7.84 | 0.662 | 1.183 |
| 2005 | 9 | 23 | 9 | 3.50 | 7.84 | 0.730 | 1.194 |
| 2005 | 9 | 23 | 10 | 3.36 | 7.41 | 0.818 | 1.046 |
| 2005 | 9 | 23 | 11 | 3.51 | 7.86 | 0.870 | 1.202 |
| 2005 | 9 | 23 | 12 | 3.97 | 8.31 | 0.874 | 1.435 |
| 2005 | 9 | 23 | 13 | 3.63 | 7.16 | 0.759 | 1.020 |
| 2005 | 9 | 23 | 14 | 3.68 | 7.20 | 0.802 | 1.039 |
| 2005 | 9 | 23 | 15 | 3.60 | 7.10 | 0.802 | 0.999 |
| 2005 | 9 | 23 | 16 | 4.16 | 7.22 | 0.744 | 1.118 |
| 2005 | 9 | 23 | 17 | 4.21 | 7.31 | 0.757 | 1.153 |
| 2005 | 9 | 23 | 18 | 4.32 | 7.42 | 0.706 | 1.204 |
| 2005 | 9 | 23 | 19 | 4.17 | 6.56 | 0.697 | 0.928 |
| 2005 | 9 | 23 | 20 | 4.40 | 6.72 | 0.681 | 1.002 |
| 2005 | 9 | 23 | 21 | 4.14 | 6.21 | 0.530 | 0.830 |
| 2005 | 9 | 23 | 22 | 4.07 | 6.06 | 0.676 | 0.784 |
| 2005 | 9 | 23 | 23 | 4.52 | 6.09 | 0.677 | 0.839 |
| 2005 | 9 | 24 | 0 | NA | 5.73 | 0.470 | 0.745 |
| 2005 | 9 | 24 | 1 | NA | 6.33 | 0.626 | 0.905 |
| 2005 | 9 | 24 | 2 | NA | 6.19 | NA | 0.866 |
| 2005 | 9 | 24 | 3 | NA | 6.19 | NA | 0.866 |

## 4.7. Comparison with the Field Measurement (Ocean City)

The comparison with field measurement in Ocean city was conducted by the same method used in previous comparison. The survey results from Larson et al. (2004) were used to estimate the volume of sand by overwash.

- Slope of beach face : 0.0719 (1:13.9)
- Average sand size : 0.20 mm
- Settling velocity by sand size : 0.025 m/s
- Volume of eroded sand from field measurement (Fig. 4.35) : 21.25 $m^3/m$

The start and end of overwash were determined by the calculation of overtopping in Chapter III. Overwash was expected for four hours between 111 and 114 hours in Fig. 4.34. The volume of eroded sand by the empirical formula from this research was 17.45 $m^3/m$.

Though this procedure cannot exactly estimate the volume of eroded sand by overwash, it may be a good reference for approximate expectation.

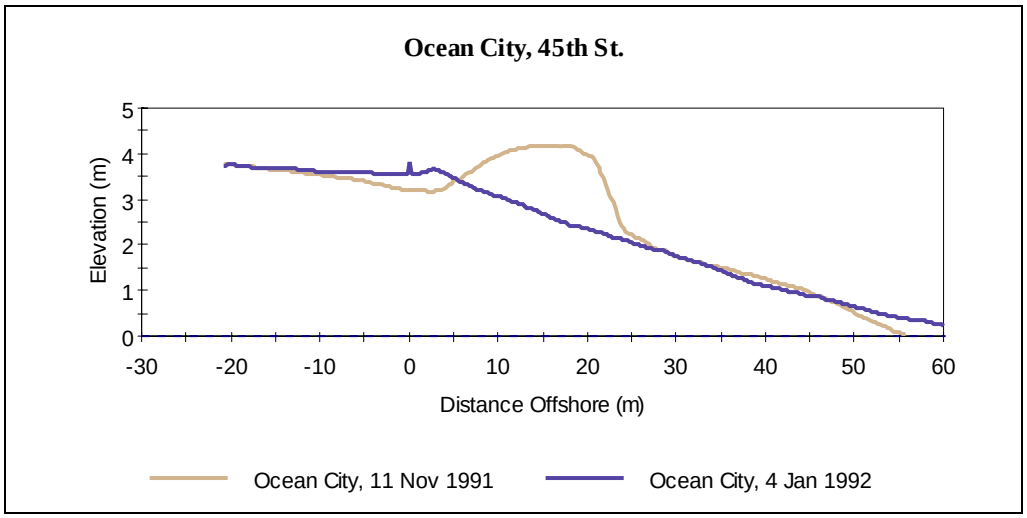


**Fig. 4.35. Survey results in Ocean city before and after storms (Larson et at., 2004).**

## 4.8. Summary and Discussion

The experiments of overwash with two different slopes of foreberm, two different wave heights and four different wave periods were conducted in regular and irregular waves. The incident and reflected waves were separated by the method of three wave gages and the computed coefficients of reflection were included in this study. A laser beach profiler was specially constructed to improve the accuracy and automation of measurements. The new equipment was also used to measure the time series of beach changes during the experiment, because the laser profiler did not need to touch the surface of object directly.

The sediment transport rates were computed from comparison between erosion and deposition by overwash. A new method was developed to calculate sediment transport rates only by overwash, because overwash was generated with other processes simultaneously. It was called the zero-point which divided swash zone by overwash and other processes. The calculated volumes of sand based on the zero-point had good relationships between each test case and they were used to develop the new empirical formulas of sediment transport rate.

The sensitivity analyses were conducted to find the factors in regular waves and irregular waves respectively and the factors which had good relationships with sediment transport were used to develop empirical equations. The regression coefficients for the selected factors were computed by multiple regression and the robust regression was used to eliminate the effect of outliers. The new empirical equation of sediment transport rates by regular and irregular waves were verified by comparison with measured data in this

chapter and they were used to develop a numerical model in next chapter.

An expected collision between runup and rundown was found in foreberm and seemed to cause enormous energy dissipation before overwash. It may be a difficulty to develop theories and numerical models of overwash by its own complexity.

# CHAPTER V

# CONCLUSIONS AND RECOMMENDATIONS

## 5.1. Conclusions

Overwash induced by storm conditions is an important factor causing loss of sand from the berm and littoral system on many beaches. The study of overwash was conducted in two ways, field measurement and laboratory experiment.

Field observations have been conducted since January 2004 that evidently show the beach erosion by overwash induced by storms in the study area. The severe damages by overwash were measured in the study area before and after landfall of hurricane Rita in 2005. The average volume of erosion for 11 lines was 26.24 $m^3/m$ by hurricane Rita. The eroded sand was transported and deposited landward and this measurement results show the characteristic of overwash. Five overwash events by storm were measured in the study area from January 2004 to October 2005 and the coastline was eroded by landfall of storm and swell of distant storms continuously. Hindcasting of overwash by calculation of maximum water level based on an empirical runup equation, tides and storm surge was verified by comparing to field survey and analysis of field data. The analyzed data were used for the estimation of start and end time of overwash. The measured volume of erosion was compared to the results from the empirical formulas developed in laboratory experiments.

The mid-scale laboratory experiment was designed to eliminate the scale effects in

small scale test by other researchers. The state of the art laser profiler was used to measure the changes of beach profiles in this study. It provided consistent accuracy and automation during experiments. The comparison between the results of regular and irregular waves could be a good approach to understand the influence of waves in overwash problems. When wave period was increased, the erosion rate by overwash was also increased and it meant the erosion was more sensitive to the wave length. It was also shown that the long period swells ahead of storms produced much more erosion than the erosion at landfall. The erosion rate by overwash is increased at higher wave height, longer wave period and steeper beach face. The sensitivity tests were conducted for slope of beach face, wave height and wave period by regular and irregular waves respectively.

The results were used to develop empirical formulas. The erosion rate was increased according to the increase of wave period but it was decreased after breach of the berm. The Iribarren number and the Shields parameter were selected for regular waves and the Iribarren number and the Dean's number were selected for irregular waves from the sensitivity tests. The impact of the Dean's number is much smaller than the Iribarren number for irregular waves but it improves the accuracy of the developed empirical formula. The Iribarren number is more dominant than the other factors in both empirical formulas for regular and irregular waves. The eroded sand volume by overwash was estimated simply by empirical formula for irregular waves within 15 % accuracy. The measured speed of bore by overwash represented good correlations with erosion rate but it did not agree with known theories due to collision between uprush and down rush of waves. The overwash is directly related to the speed of the bore to the 0.85 power. The zero-point method was devised to compute the volume of sediment transport only by overwash,

because a part of eroded sand was transported over the berm by overwash and the rest moved seaward by other causes. The erosion rate is changed according to the change of geometry by erosion and most of erosion (50 %) was conduction at the early of overwash (327 of 1635 sec). The rate is decrease with time.

## 5.2. Recommendations

The empirical formulas developed from the laboratory experiment were only focused on erosion by overwash and it could not simulate erosion in swash zone. Because the beach is continuous from offshore to onshore, the coupling of the overwash model and swash zone model has to be considered in erosion and deposition by sediment transport by overwash.

The empirical formulas were developed through dimensional analysis and resulted in known factors such as the Iribarren number and the Shields parameter but it could not explain the mechanism of overwash completely. New factors of sediment transport and fluid dynamics should be developed by dimensional analysis and they have to be proved by comparison with laboratory experiments.

The speed of bore is important to determine the magnitude of erosion by overwash and there is strong correlation between the speed of bore and runup height. It is difficult to estimate by the existing theories, because as the berm changes so does the hydrodynamics. Therefore, it needs to be formulated from careful laboratory experiments.

Because overwash is the major cause of beach erosion in the area studied here for short periods, the impacts of other factors such as rate of surge increase, wind,

precipitation and the sediment layers of different grain size, which was discussed in chapter II, are ignored. They need to be included to simulate the morphological changes completely in further studies.

# REFERENCES

Battjes, J. A., 1974. Surf Similarity. Proc. 14th Coastal Engineering Conference, ASCE, 466-479.

Bouws, E., Gunther, H., Rosenthal, W. and Vincent, C. L., 1985. Similarity of the Wind Wave Spectrum in Finite Depth Water: 1. Spectral Form. Journal of Geophysical Research 90 (C1), 975-986.

Dean, R. G. and Dalrymple, R. A., 1991. Water Wave Mechanics for Engineers and Scientists. World Scientific Publishing Co, Singapore.

Dean, R. G. and Dalrymple, R. A., 2002. Coastal Processes with Engineering Applications. Cambridge University Press, Cambridge, UK.

Dolan, R., 1972. Barrier Dune System along the Outer Banks of North Carolina: A Reappraisal. Science 176, 286-288.

Feagin, R. A., Sherman, D. J. and Grant, W. E., 2005. Coastal Erosion, Global Sea-Level Rise, and the Loss of Sand Dune Plant Habitats. Frontiers in Ecology and the Environment 3, 359-364.

Fisher, J. S., Leatherman, S. P. and Perry, F. C., 1974. Overwash Processes on Assateague Island. Proc. 14th Coastal Engineering Conference, ASCE, 1194-1212.

Goda, Y., 1985. Random Seas and Design of Maritime Structures. University of Tokyo Press, Japan.

Hallermeier, R. J., 1981. Terminal Settling Velocity of Commonly Occurring Sand Grains. Sedimentology 28, 859– 865.

Hancock, M. W., 1994. Experiments on Irregular Wave Overtopping and Overwash of Dunes. M.S. Thesis, University of Delaware, Newark, DE.

Holland, K. T., Holman, R. A. and Sallenger, A. H., 1991. Estimation of Overwash Bore Velocities Using Video Techniques. Proc. Coastal Sediments '91, ASCE, 489-497.

Holman, R. A., 1986. Extreme Value Statistics for Wave Run-Up on a Natural Beach. Coastal Engineering 9, 527-544.

Holman, R. A. and Sallenger, A. H., 1985. Setup and Swash on a Natural Beach. Journal of Geophysical Research 90, 945-953.

Hughes, S. A. and Chiu, T. Y., 1981. Beach and Dune Erosion during Severe Storms. UFL/COEL 99/001, Coastal and Oceanographic Engineering Department, University of Florida, Gainesville, FL.

Hughes, S. A. and Fowler, J. E., 1990. Midscale Physical Model Validation for Scour at Coastal Structures. Report Number: CERC-90-8, and Coastal Eng. Res. Cent. U. S. Army Engineer Waterways Experiment Station, Vicksburg, MS.

Kitaigorodskii, S. A., Krasitskii, V. P., and Zaslavskii, M. M., 1975. On Phillip's Theory of Equilibrium Range in the Spectra of Wind-Generated Gravity Waves. Journal of Physical Oceanography 5, 410-420.

Knutson, T. R. and Tuleya, R. E., 2004. Impact of CO2-Induced Warming on Simulated Hurricane Intensity and Precipitation: Sensitivity to the Choice of Climate Model and Convective Parameterization. Journal of Climate 17 (18), 3477-3495.

Kobayashi, N., Tega, Y. and Handcock, M. W., 1996. Wave Reflection and Overwash of Dunes. Journal of Waterway, Port, Coastal, and Ocean Engineering 122 (3), 150-153.

Komar, P. D., 1998. Beach Processes and Sedimentation. 2nd Ed., Prentice-Hall, Englewood Cliffs, NJ.

Kriebel, D. L., Dalrymple, R. A., Pratt, A. and Sakovich, V., 1997. A Shoreline Risk Index for Northeasters. Conf. Natural Disaster Reduction, 251-252.

Larson, M., Wise, R. A. and Kraus, N. C., 2004. Coastal Overwash, Part 2: Upgrade to SBEACH, ERDC/RSM-TN-15, U.S. Army Engineer Research and Development Center, Vicksburg, MS.

Le Méhauté, B., 1976. An Introduction to Hydrodynamics and Water Waves. Springer-Verlag, New York.

Leatherman, S.P., 1976. Barrier Island Dynamics: Overwash Processes and Aeolian Transport. Proc. 15th Coastal Engineering Conference, ASCE, 1958-1974.

Leatherman, S. P., 1977. Assateague Island: A Case Study of Barrier Island Dynamics. Proc. of the 1st Conference on Scientific Research in the National Parks, 769-775.

Leatherman, S. P., 1979. Beach and Dune Interactions during Storm Conditions. Journal of Engineering Geology 12, 281-290.

Leatherman, S. P., 1983. Barrier Dynamics and Landward Migration with Holocene sea-level rise. Nature 301, 415-417.

Leatherman, S. P., 1984. Coastal Geomorphic Responses to Sea Level Rise in and Around Galveston, Texas. In: M.C. Barth and J.G. Titus (Eds), Greenhouse Effect and Sea Level Rise: A Challenge for This Generation. Van Nostrand Reinhold, New York.

Lee, H. I., 2003. Shoreline Assessment of Jefferson County, Texas. M.S. Thesis, Texas A&M University, College Station, TX.

Morton, R. A., 1975. Shoreline Changes between Sabine Pass and Bolivar Roads – An Analysis of Historical Changes of the Texas Gulf Shoreline. Geological Circular, 75-6, Bureau of Economic Geology, the University of Texas at Austin.

Morton, R. A., 1997. Gulf Shoreline Movement between Sabine Pass and The Brazos River, Texas: 1974 to 1996. Geological Circular, 97-3, Bureau of Economic Geology, the University of Texas at Austin, Austin, TX.

Morton, R. A., 2002. Factors Controlling Storm Impacts on Coastal Barriers and Beaches-A Preliminary Basis for Near Real-time Forecasting. Journal of Coastal Research 18 (3), 486-501.

Morton, R. A., Gibeaut, J.C., and Paine, J.G., 1995. Meso-scale Transfer of Sand during and after Storms: Implications for Prediction of Shoreline Movement. International Journal of Marine Geology 126, 161-179.

Morton, R. A. and Sallenger, A.H., Jr., 2003. Morphological Impacts of Extreme Storms on Sandy Beaches and Barriers. Journal of Coastal Research 19 (3), 560-573.

Nelson, H. F. and Bray, E. E., 1970. Stratigraphy and History of the Holocene Sediments in the Sabine-High Island area, Gulf of Mexico. SEPM Special Publication 15. In: J. P. Morgan (Ed.) Tulsa, OK. Society for Sedimentary Geology, 48-77.

NOAA, 1999. About LIDAR Data. http://www.csc.noaa.gov/products/sccoasts/html/tutlid.htm.

NOAA, 2004a. Ivan Graphics Archive. http://www.nhc.noaa.gov/archive/2004/IVAN_graphics.shtml.

NOAA, 2004b. Matthew GraphicsArchive.http://www.nhc.noaa.gov/archive/2004/MATTHEW_graphics.shtml.

NOAA, 2005. Katrina Graphics Archive. http://www.nhc.noaa.gov/archive/2005/KATRINA_graphics.shtml.

NOAA, 2006a. Upper Texas Coast Tropical Cyclones in the 2000s. http://www.srh.noaa.gov/hgx/hurricanes/2000s_maps.htm.

NOAA, 2006b. The Saffir-Simpson Hurricane Scale. http://www.nhc.noaa.gov/aboutsshs.shtml.

NOAA, 2006c. Katrina Graphics Archive. http://www.nhc.noaa.gov/archive/2005/RITA_graphics.shtml.

NOAA, 2006d. Western Gulf of Mexico Recent Marine Data. http://www.ndbc.noaa.gov/maps/WestGulf.shtml.

Pierson, W. J., 1955. Wind Generated Gravity Waves. Advances in Geophysics 2, 93-178.

Rousseeuw, P. J. and Van Driessen, K., 1998. A fast Algorithm for the Minimum Covariance Determinant Estimator. http://support.sas.com/rnd/app/da/iml/sect1.htm.

Ruggiero, P., Komra, P. D., McDougal, W. G., Marra, J. J., and Beach, R. A., 2001. Wave Runup, Extreme Water Levels and the Erosion of Properties Backing Beach. Journal of Coastal Research 17 (2), 407-419.

Smith, J. and Leatherman, S. P., 2000. Erosion Anomaly on Eastern Jones Beach Island, NY: Genesis and Management Implications, SHORE AND BEACH 68, 29-32.

Sallenger, A.H. Jr., 2000. Storm Impact Scale for Barrier Islands. Journal of Coastal Research 16 (3), 890-895.

Saville, T., 1957. Scale Effects in Two Dimensional Beach Studies. Transactions from the 7th General Meeting of the International Association of Hydraulic Research.1, A3-1-A3-10.

Sonu, C. J., 1970. Beach Changes by Extraordinary Waves Caused by Hurricane Camille. Technical Report 77, Coastal studies institute, Louisiana State University, Baton Rouge, LA.

Suh, K. D., Park, W. S., and Park, B. S., 2001. Separation of Incident and Reflected Waves in Wave-Current Flumes. Coastal Engineering 43, 149-159.

TCOON, 2006. Station Overview. http://lighthouse.tamucc.edu/overview/126.

Tega, Y. and Kobayashi, N., 2000. Dune Profile Evolution due to Overwash. Proc. 27th Coastal Engineering Conference, ASCE, 2634-2647.

Thompson, E. F. and Vincent, C. L., 1985. Significant Wave Height for Shallow Water Design. Journal of the Waterway, Port, Coastal and Ocean Division 111 (5), 828-842.

Titus, J. G., 1990. Greenhouse Effect, Sea Level Rise, and Barrier Islands: Case Study of Long Beach Island, New Jersey. Coastal Management 18, 65-90.

Trimble Navigation Limited, 1999. 4700 Specifications. http://www.trimble.com.

U.S. Army Corps of Engineers, 1973. Shore Protection Manual, 2nd Ed. Research Center, U.S. Government Printing Office, Washington D.C.

USGS, 2004. Hurricane Ivan Impact Studies. http://coastal.er.usgs.gov/hurricanes/ivan/site-index.php?storm_id=9&site_id=21.

Vellinga, P., 1983. Predictive Computational Model for Beach and Dune Erosion during Storm Surges. Publication No. 294, Delft Hydraulics Laboratory, Netherlands.

Wamsley, T. V., 2000. Shoreline Monitoring Program on the Upper Texas Coast Utilizing a Real-Time Kinematic Differential Global Positioning System. M.S. Thesis, Texas A&M University, College Station, TX.

Williams, P., 1978. Laboratory Development of a Predictive Relationship for Washover Volume on Barrier Island Coastlines. M.S. Thesis, University of Delaware, Newark, DE.

Wright, L. D. and Short, A. D., 1983. Morphodynamics of Beaches and Surf Zones in Australia. Handbook of Coastal Processes and Erosion, CRC Press, Boca Raton, FL.

# APPENDIX A

## Beach profiles from laboratory experiments

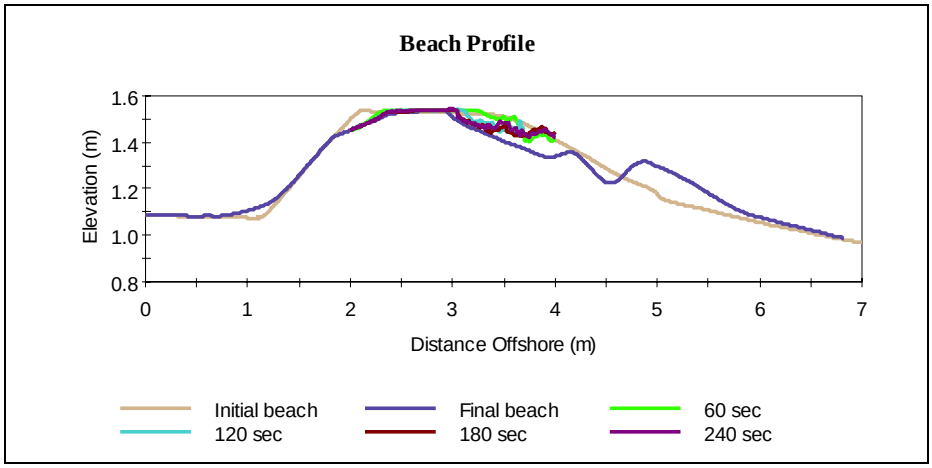


**Fig. A.1. The time series of beach profile changes by regular waves (height = 0.14 m, period = 1.4 sec, slope = 1:4).**

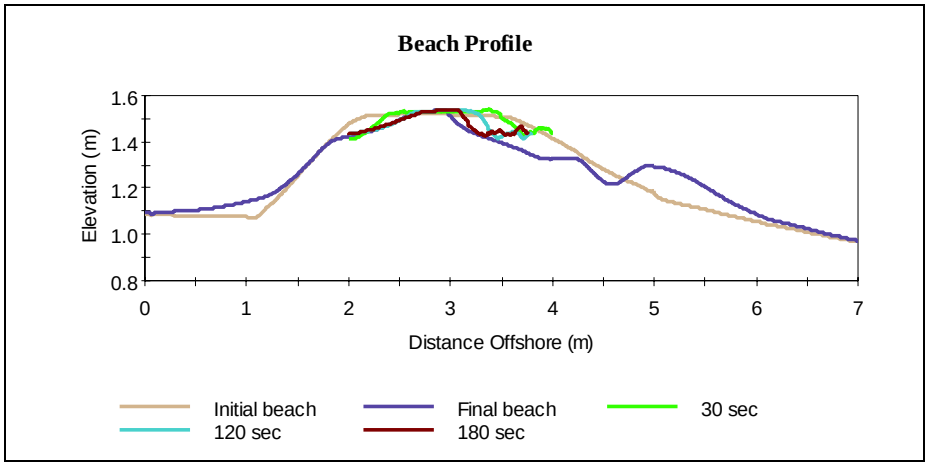


**Fig. A.2. The time series of beach profile changes by regular waves (height = 0.14 m, period = 1.6 sec, slope = 1:4).**

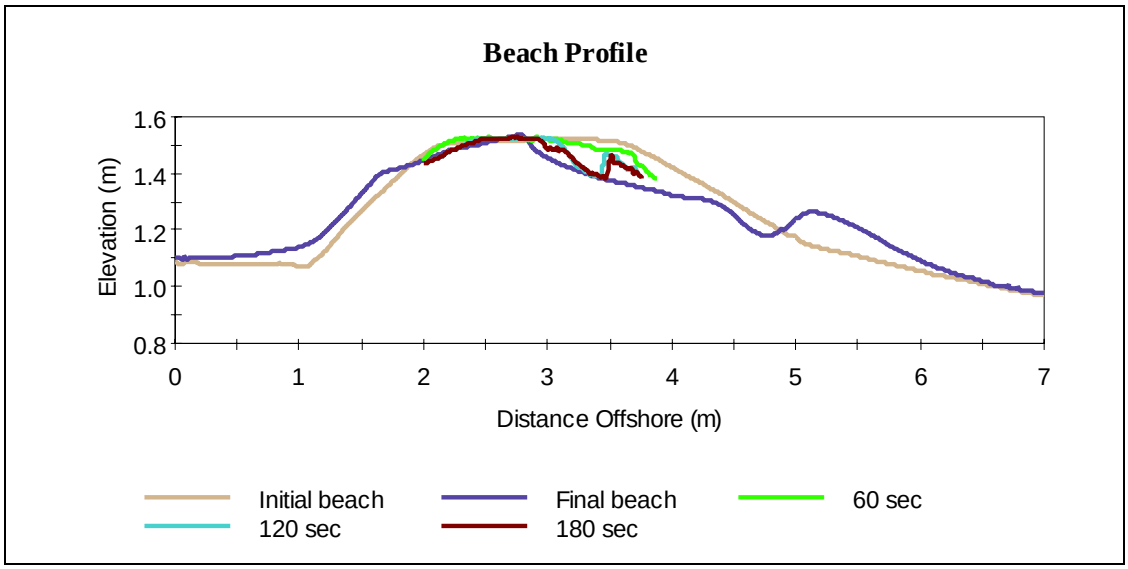


**Fig. A.3. The time series of beach profile changes by regular waves (height = 0.14 m, period = 1.8 sec, slope = 1:4).**

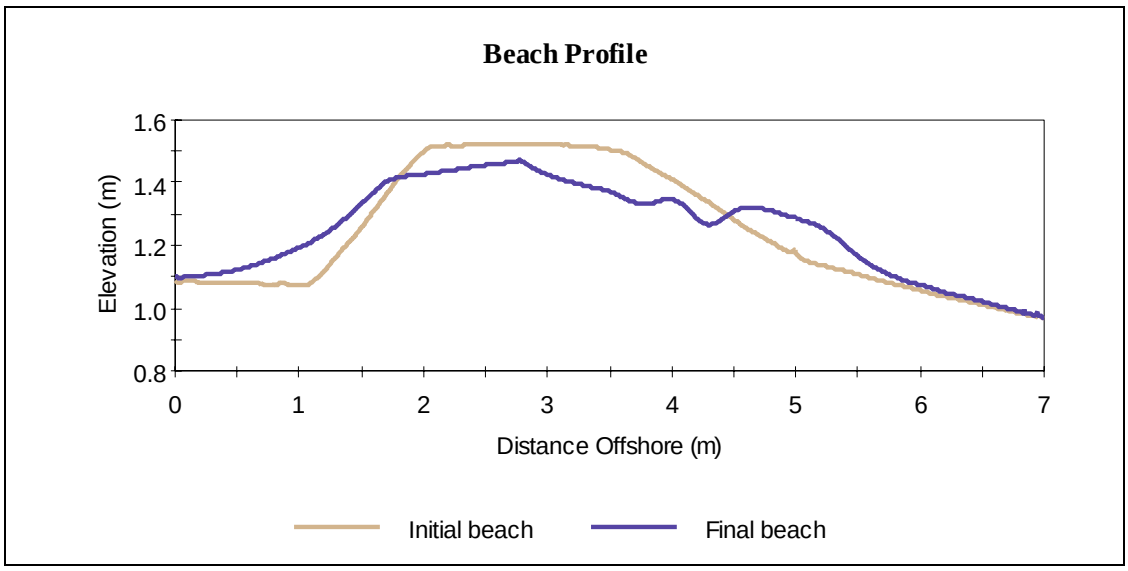


**Fig. A.4. The time series of beach profile changes by regular waves (height = 0.14 m, period = 2.0 sec, slope = 1:4).**

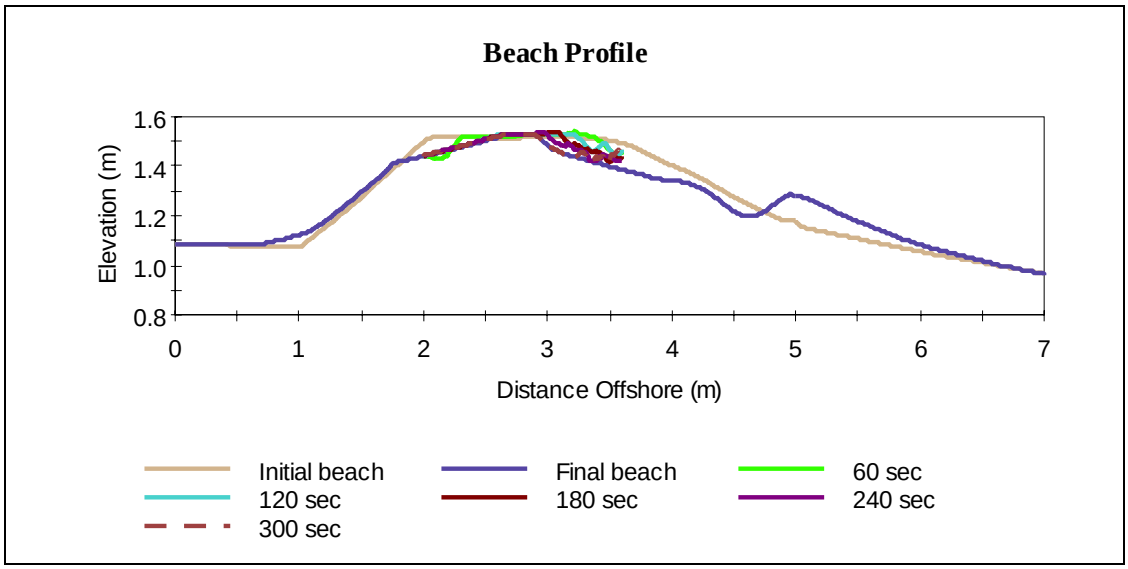


**Fig. A.5. The time series of beach profile changes by regular waves (height = 0.17 m, period = 1.4 sec, slope = 1:4).**

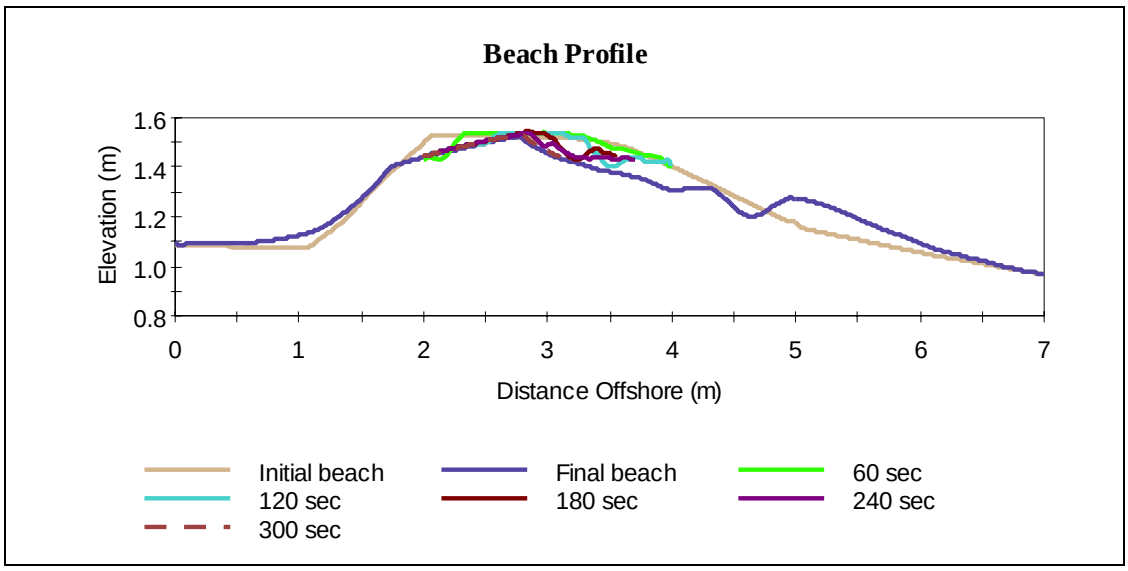


**Fig. A.6. The time series of beach profile changes by regular waves (height = 0.17 m, period = 1.6 sec, slope = 1:4).**

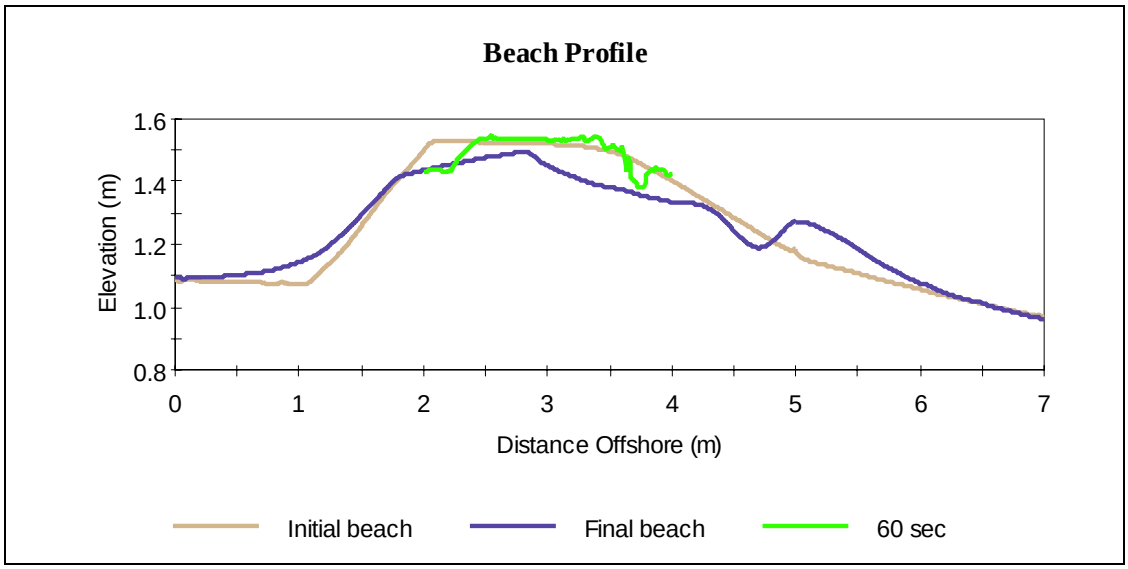


**Fig. A.7. The time series of beach profile changes by regular waves (height = 0.17 m, period = 1.8 sec, slope = 1:4).**

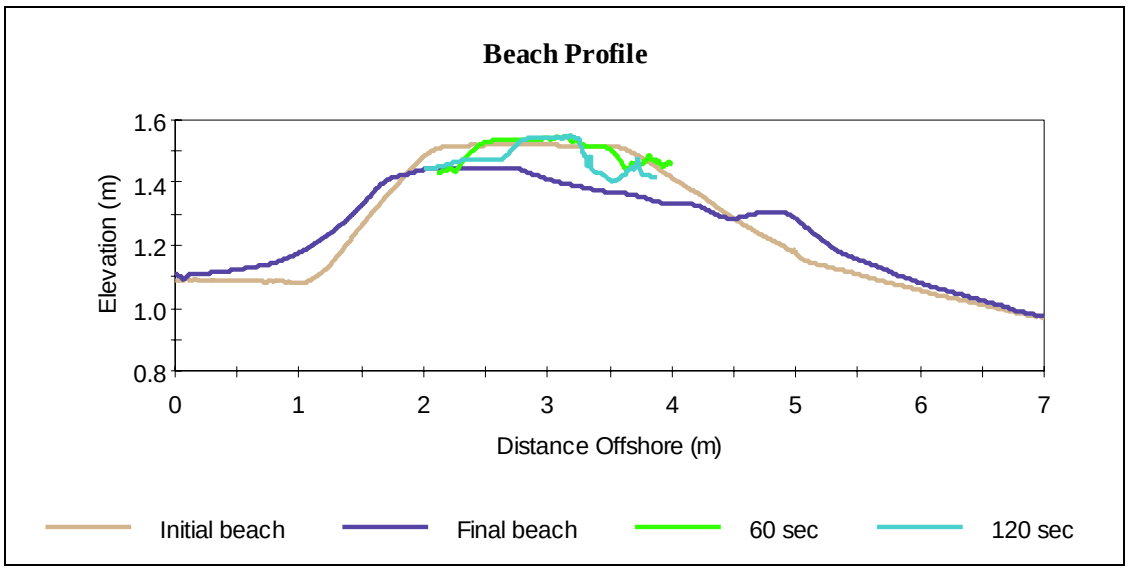


**Fig. A.8. The time series of beach profile changes by regular waves (height = 0.17 m, period = 2.0 sec, slope = 1:4).**

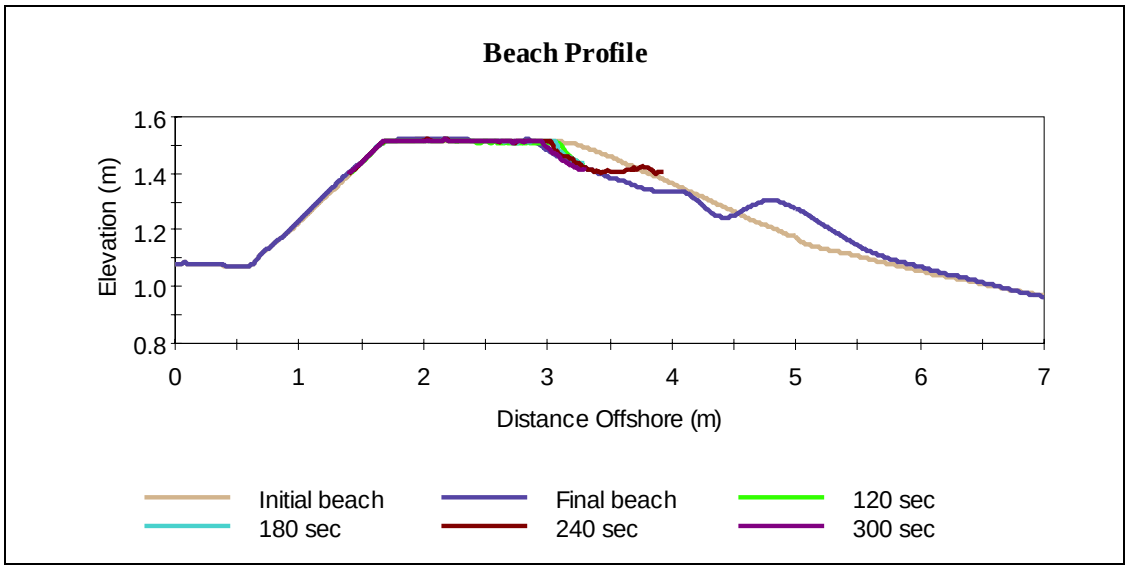


**Fig. A.9. The time series of beach profile changes by regular waves (height = 0.14 m, period = 1.4 sec, slope = 1:5).**

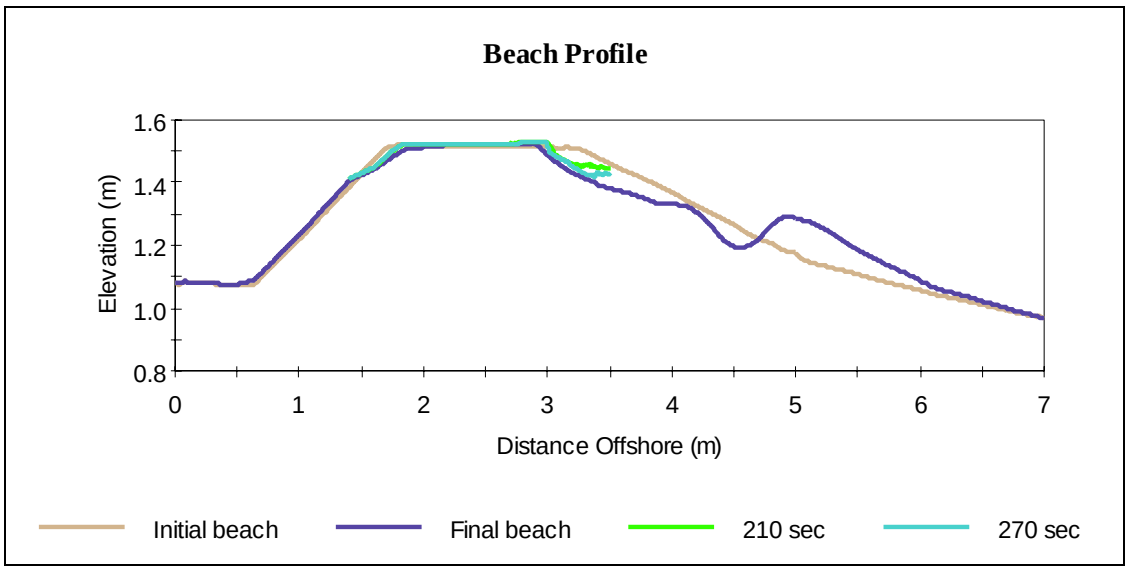


**Fig. A.10. The time series of beach profile changes by regular waves (height = 0.14 m, period = 1.6 sec, slope = 1:5).**

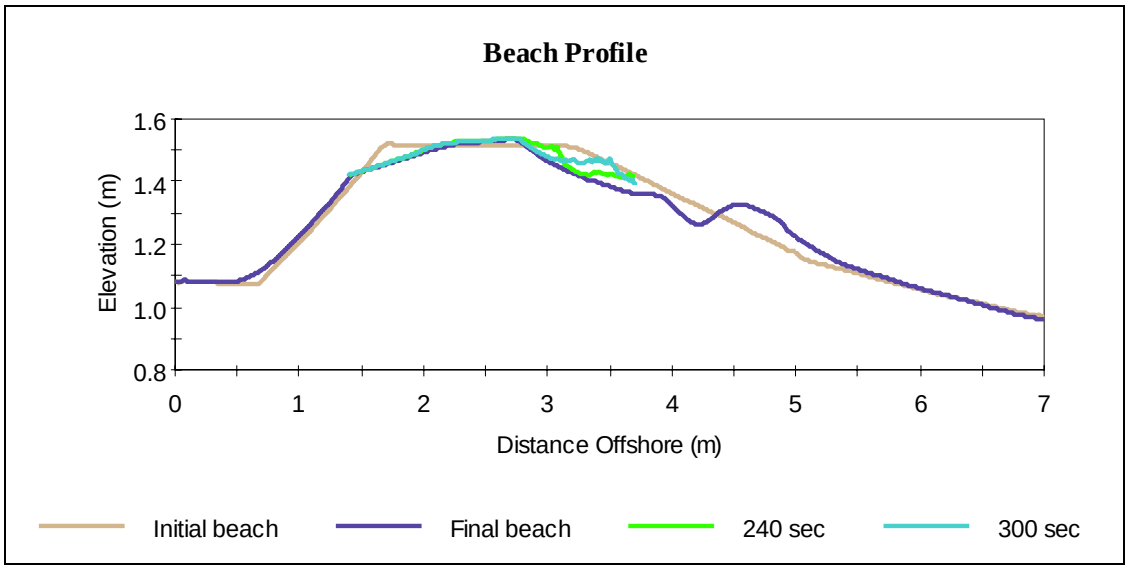


**Fig. A.11. The time series of beach profile changes by regular waves (height = 0.14 m, period = 1.8 sec, slope = 1:5).**

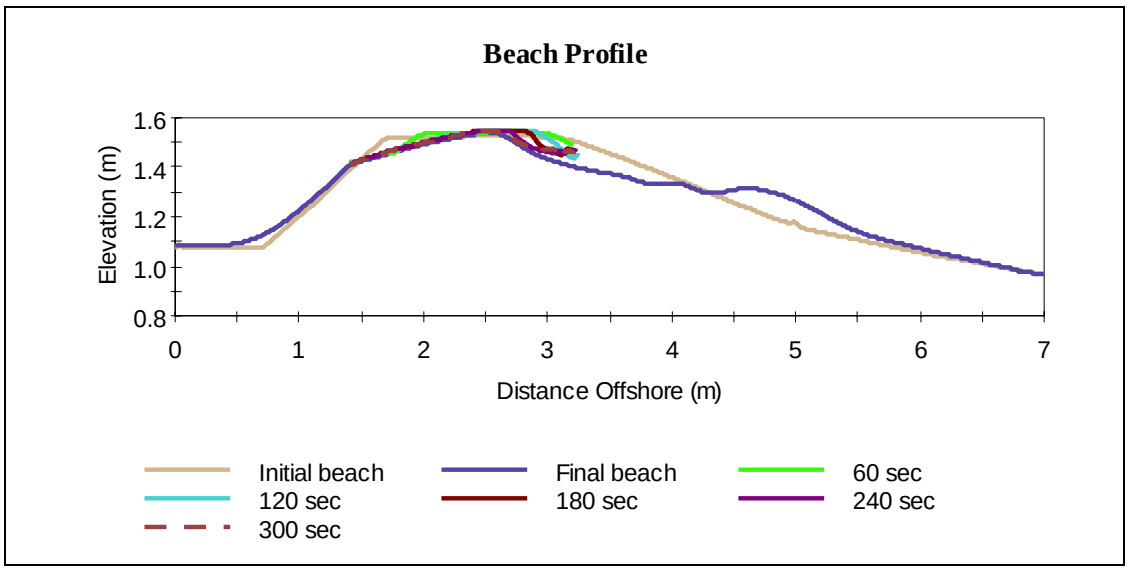


**Fig. A.12. The time series of beach profile changes by regular waves (height = 0.14 m, period = 2.0 sec, slope = 1:5).**

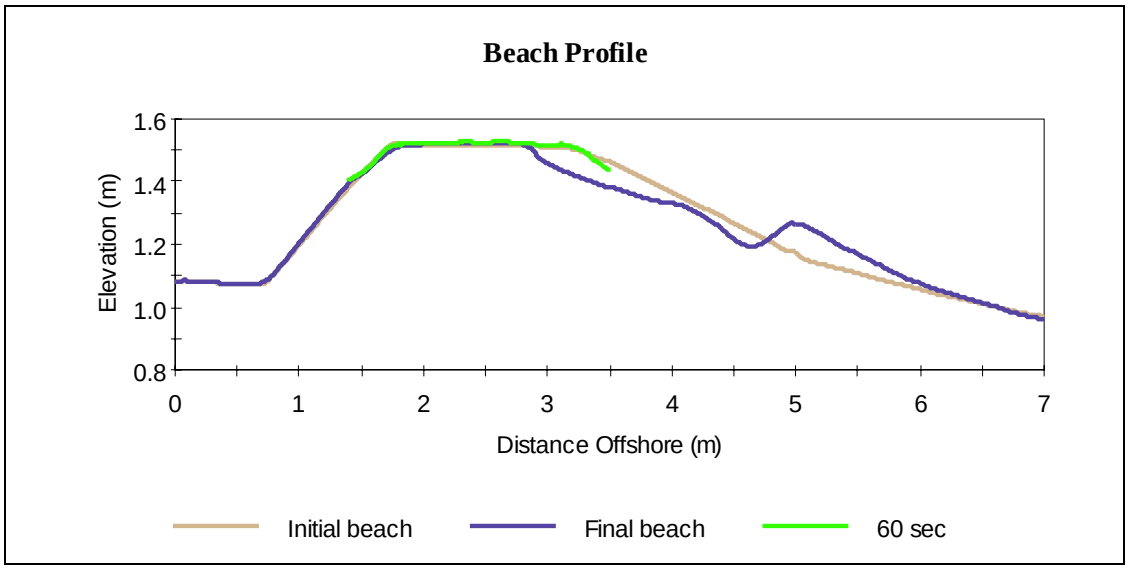


**Fig. A.13. The time series of beach profile changes by regular waves (height = 0.17 m, period = 1.4 sec, slope = 1:5).**

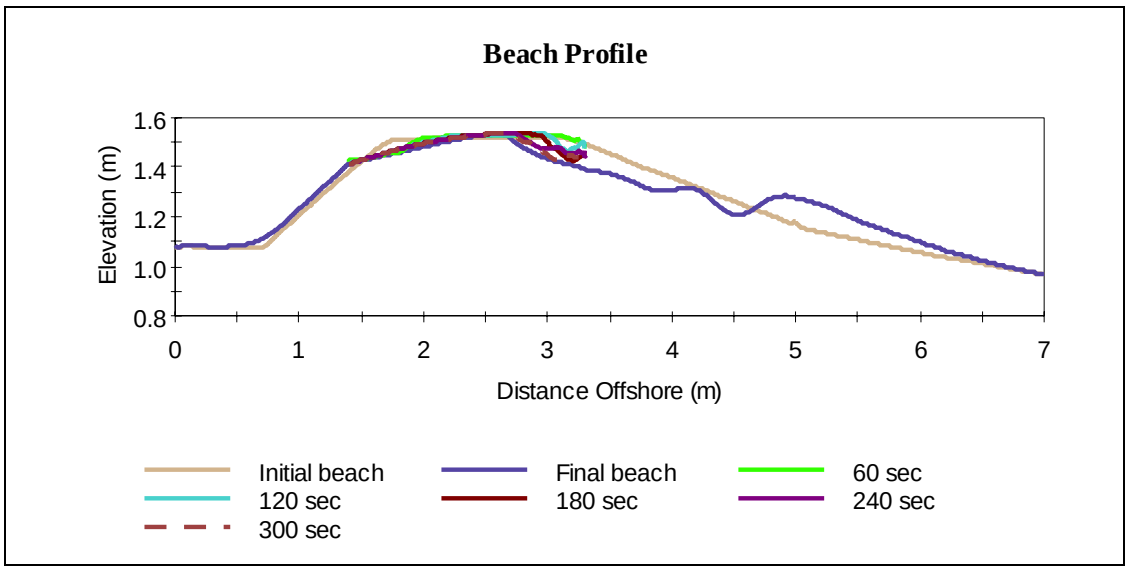


**Fig. A.14. The time series of beach profile changes by regular waves (height = 0.17 m, period = 1.6 sec, slope = 1:5).**

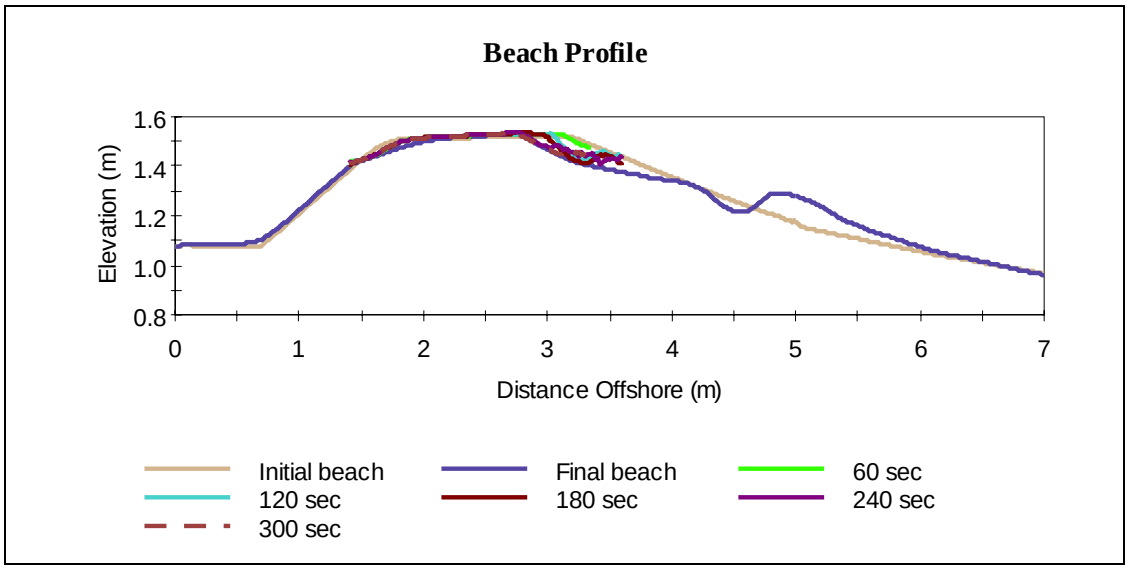


**Fig. A.15. The time series of beach profile changes by regular waves (height = 0.17 m, period = 1.8 sec, slope = 1:5).**

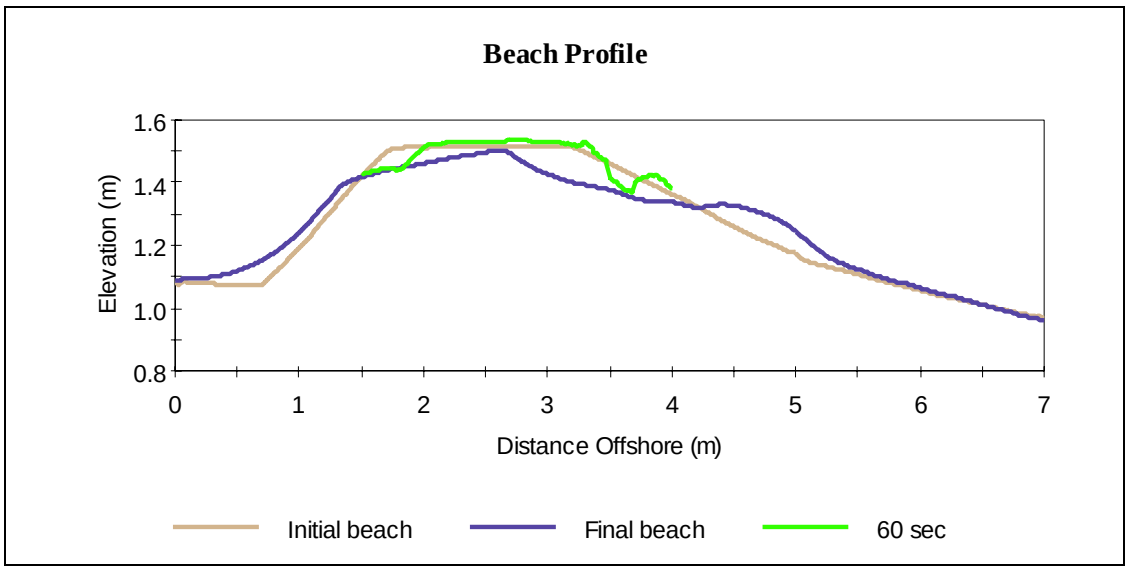


**Fig. A.16. The time series of beach profile changes by regular waves (height = 0.17 m, period = 2.0 sec, slope = 1:5).**

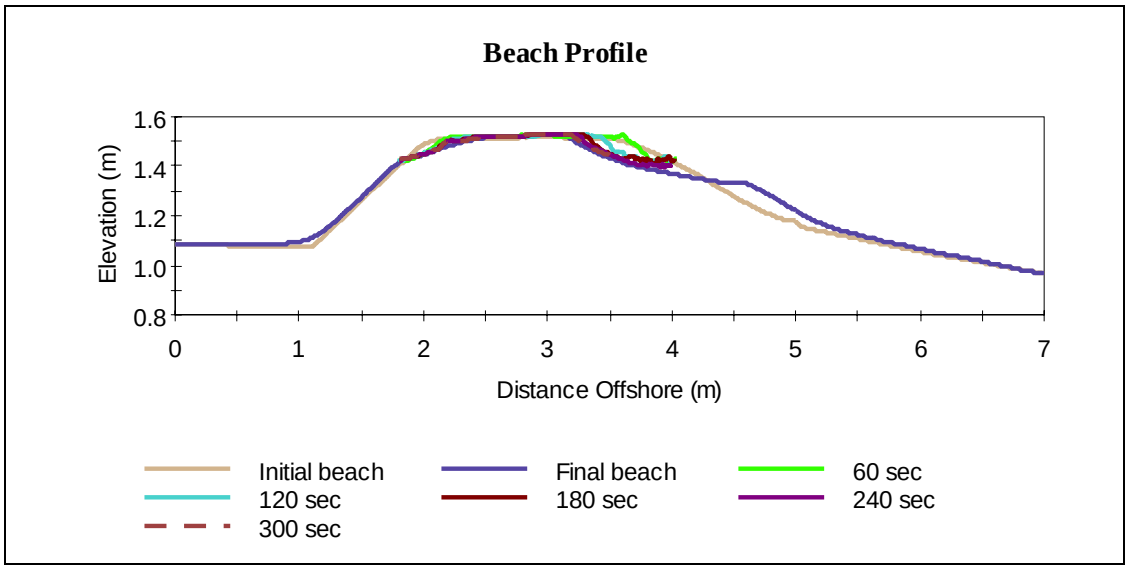


**Fig. A.17. The time series of beach profile changes by irregular waves ($H_{mo}$ = 0.10 m, $T_p$ = 1.4 sec, slope = 1:4).**

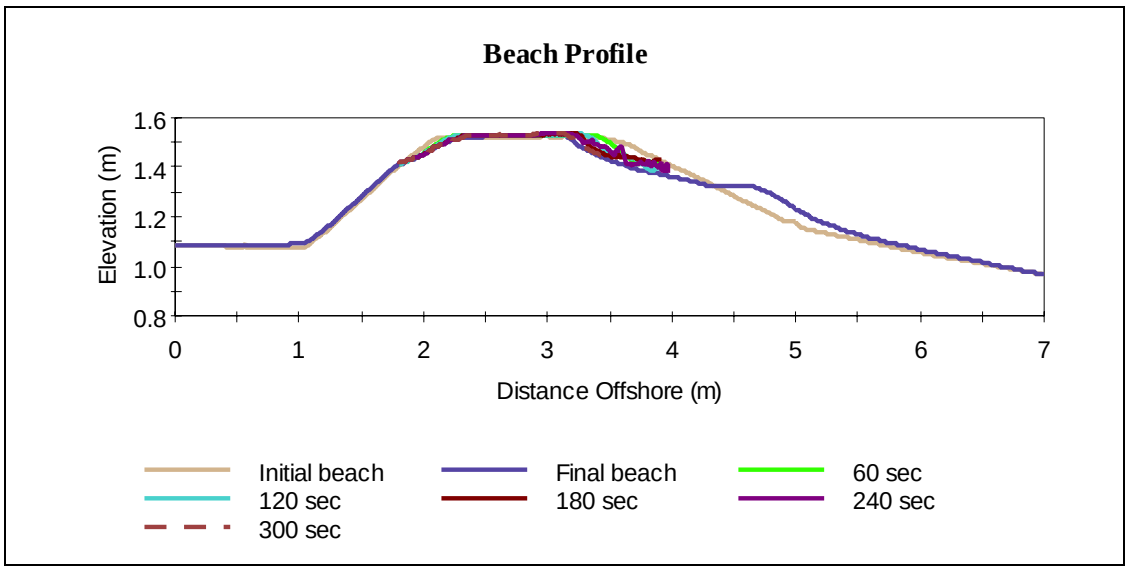


**Fig. A.18. The time series of beach profile changes by irregular waves ($H_{mo}$ = 0.10 m, $T_p$ = 1.6 sec, slope = 1:4).**

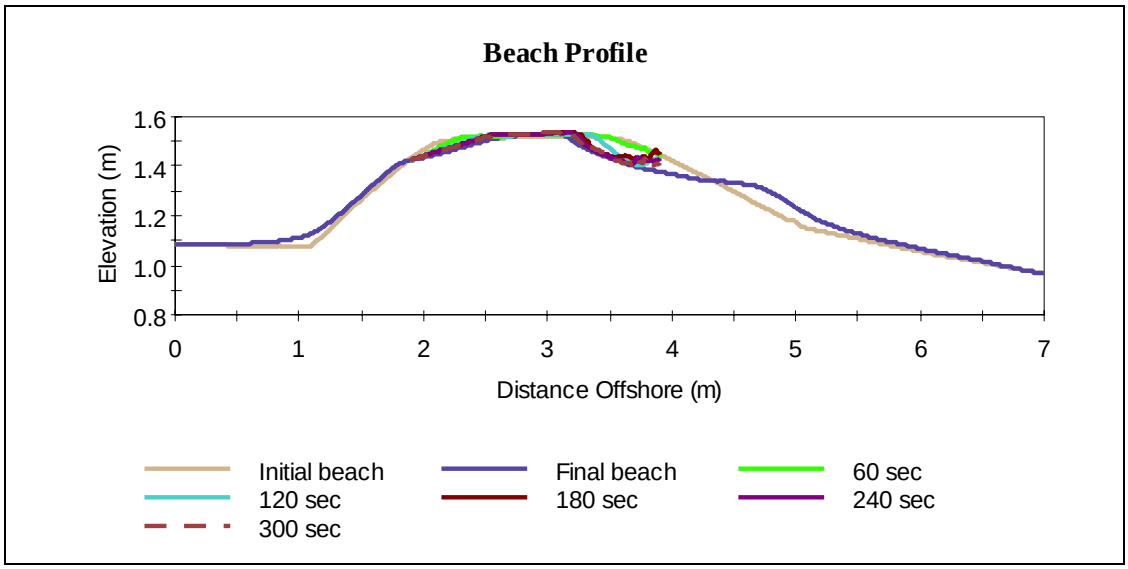


**Fig. A.19. The time series of beach profile changes by irregular waves ($H_{mo}$ = 0.10 m, $T_p$ = 1.8 sec, slope = 1:4).**

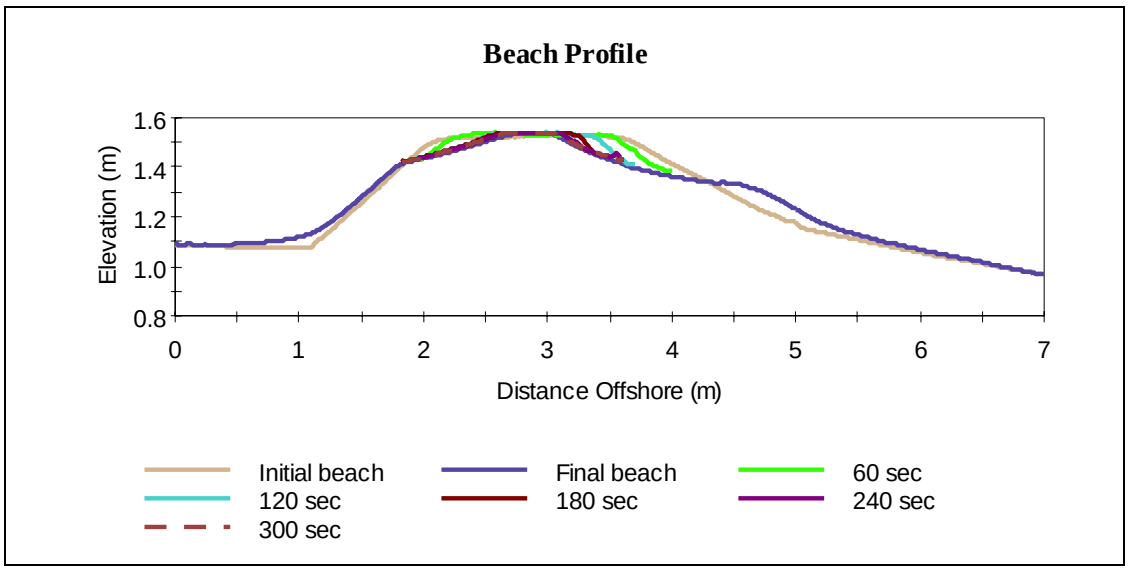


**Fig. A.20. The time series of beach profile changes by irregular waves ($H_{mo}$ = 0.10 m, $T_p$ = 2.0 sec, slope = 1:4).**

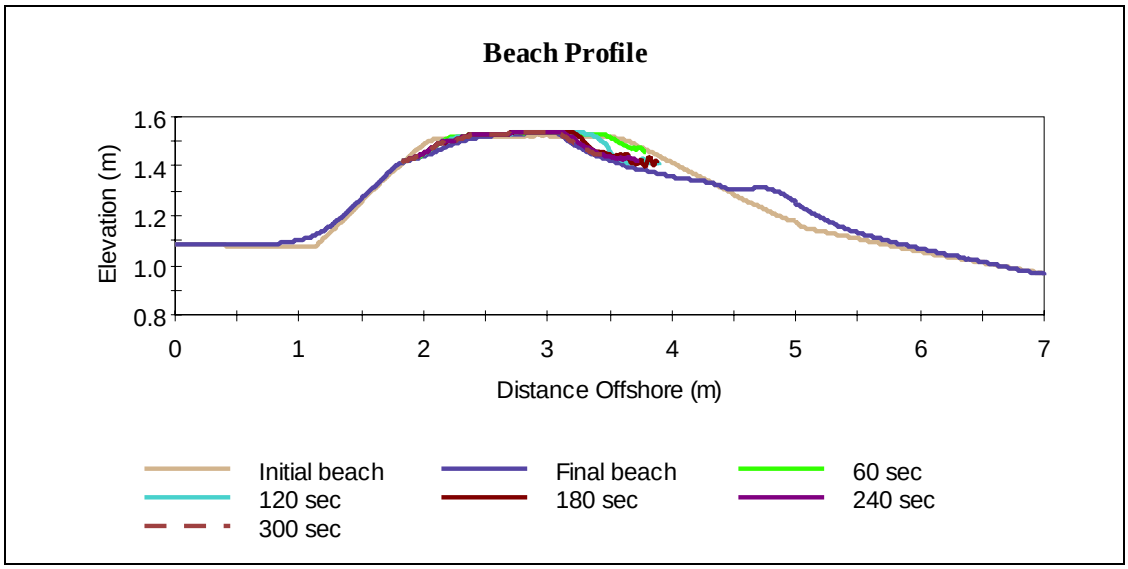


**Fig. A.21. The time series of beach profile changes by irregular waves ($H_{mo}$ = 0.15 m, $T_p$ = 1.4 sec, slope = 1:4).**

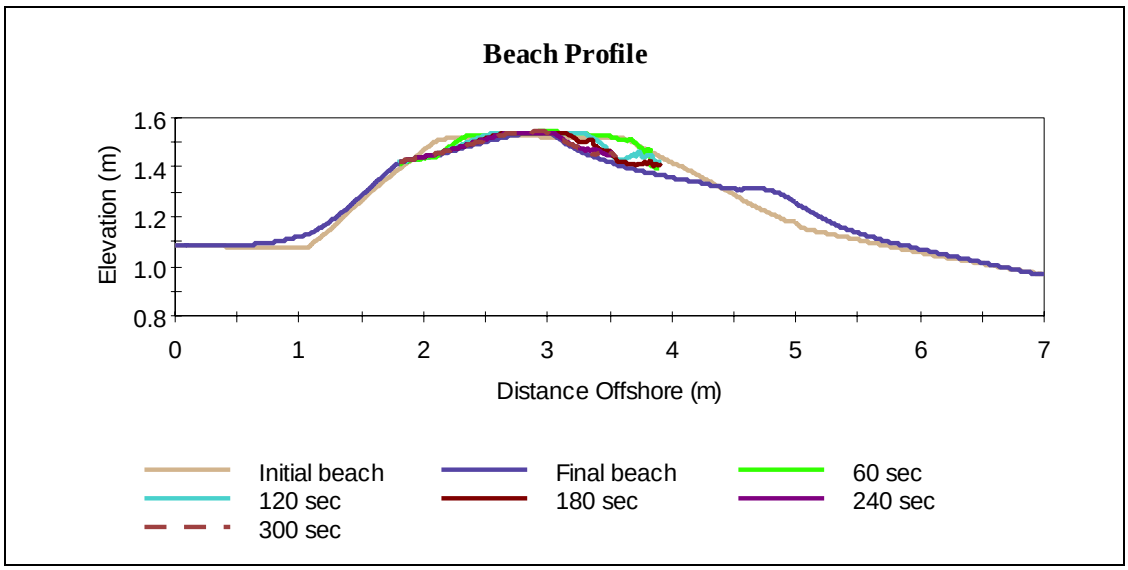


**Fig. A.22. The time series of beach profile changes by irregular waves ($H_{mo}$ = 0.15 m, $T_p$ = 1.6 sec, slope = 1:4).**

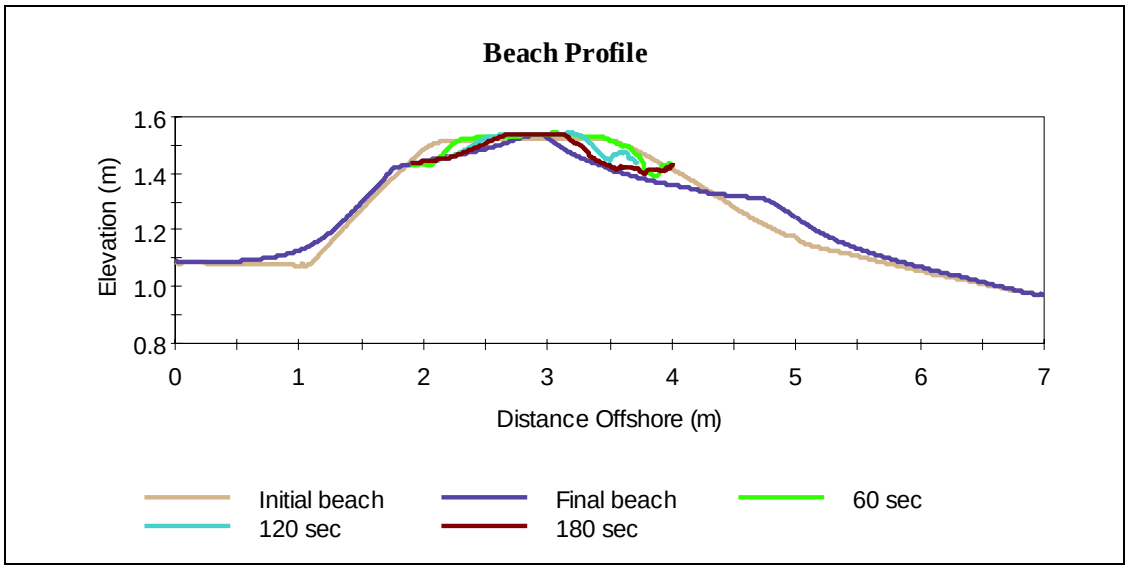


**Fig. A.23. The time series of beach profile changes by irregular waves ($H_{mo}$ = 0.15 m, $T_p$ = 1.8 sec, slope = 1:4).**

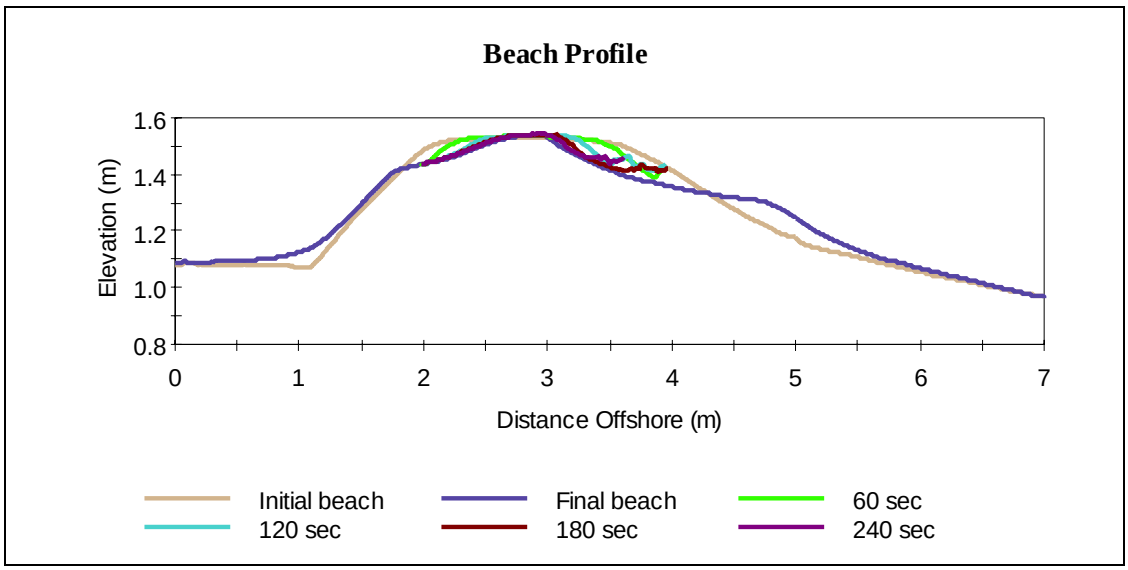


**Fig. A.24. The time series of beach profile changes by irregular waves ($H_{mo}$ = 0.15 m, $T_p$ = 2.0 sec, slope = 1:4).**

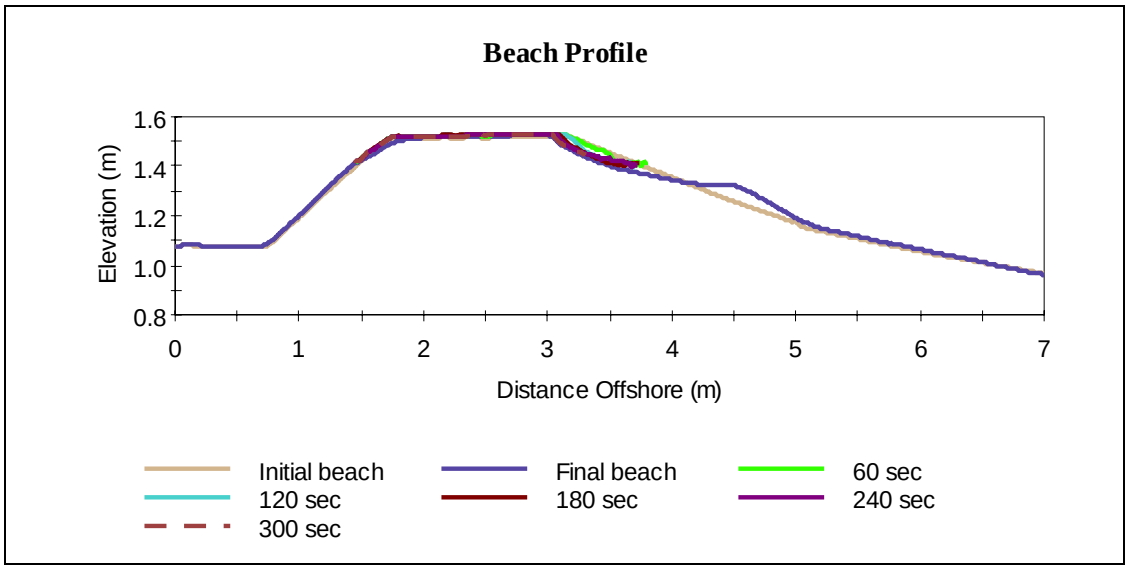


**Fig. A.25. The time series of beach profile changes by irregular waves ($H_{mo}$ = 0.10 m, $T_p$ = 1.4 sec, slope = 1:5).**

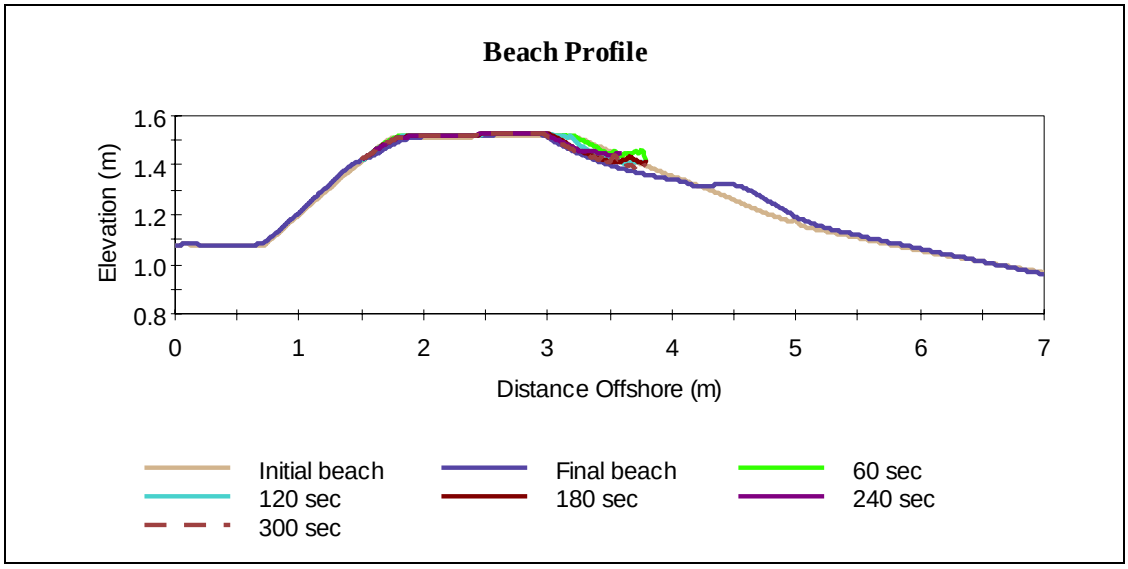


**Fig. A.26. The time series of beach profile changes by irregular waves ($H_{mo}$ = 0.10 m, $T_p$ = 1.6 sec, slope = 1:5).**

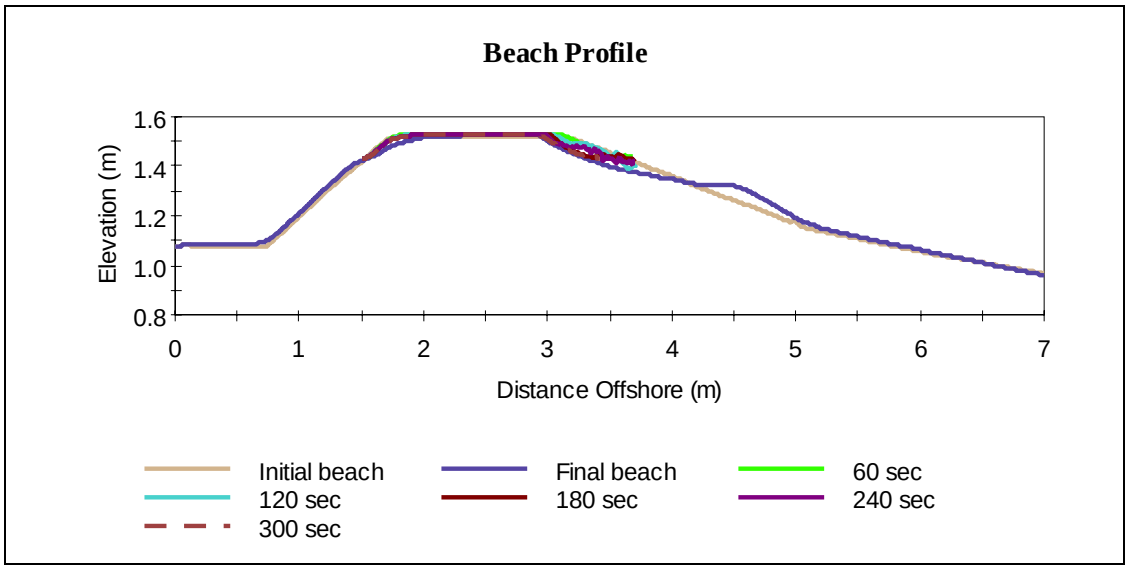


**Fig. A.27. The time series of beach profile changes by irregular waves ($H_{mo}$ = 0.10 m, $T_p$ = 1.8 sec, slope = 1:5).**

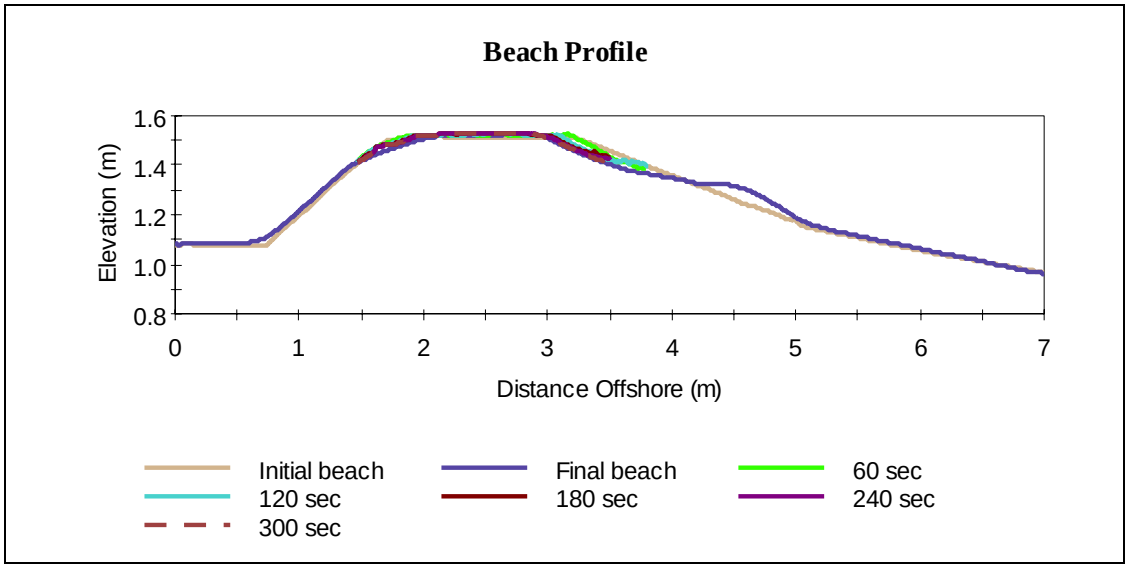


**Fig. A.28. The time series of beach profile changes by irregular waves ($H_{mo}$ = 0.10 m, $T_p$ = 2.0 sec, slope = 1:5).**

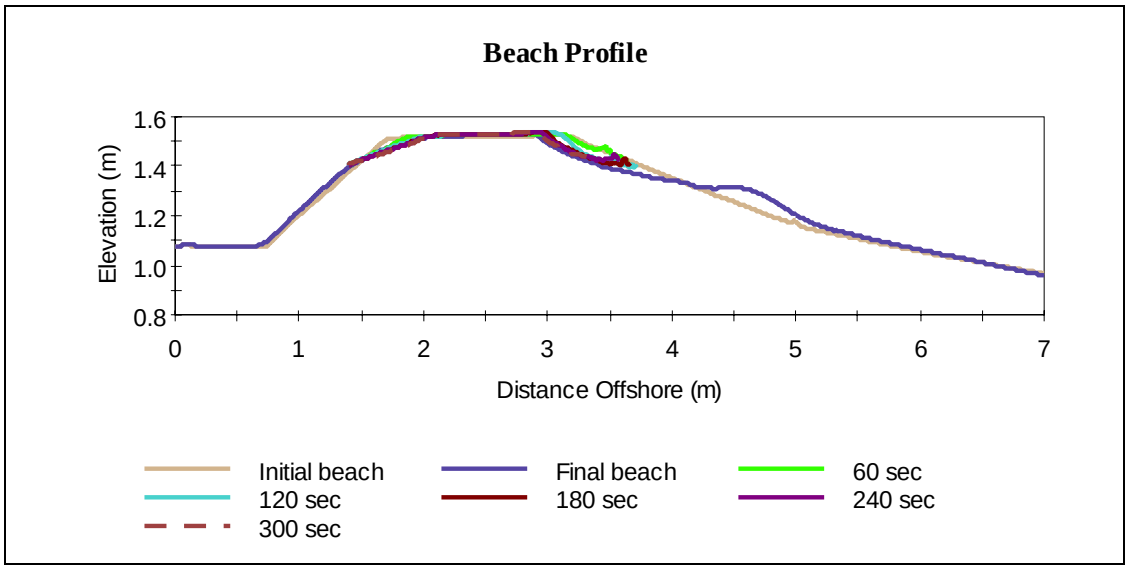


**Fig. A.29. The time series of beach profile changes by irregular waves ($H_{mo}$ = 0.15 m, $T_p$ = 1.4 sec, slope = 1:5).**

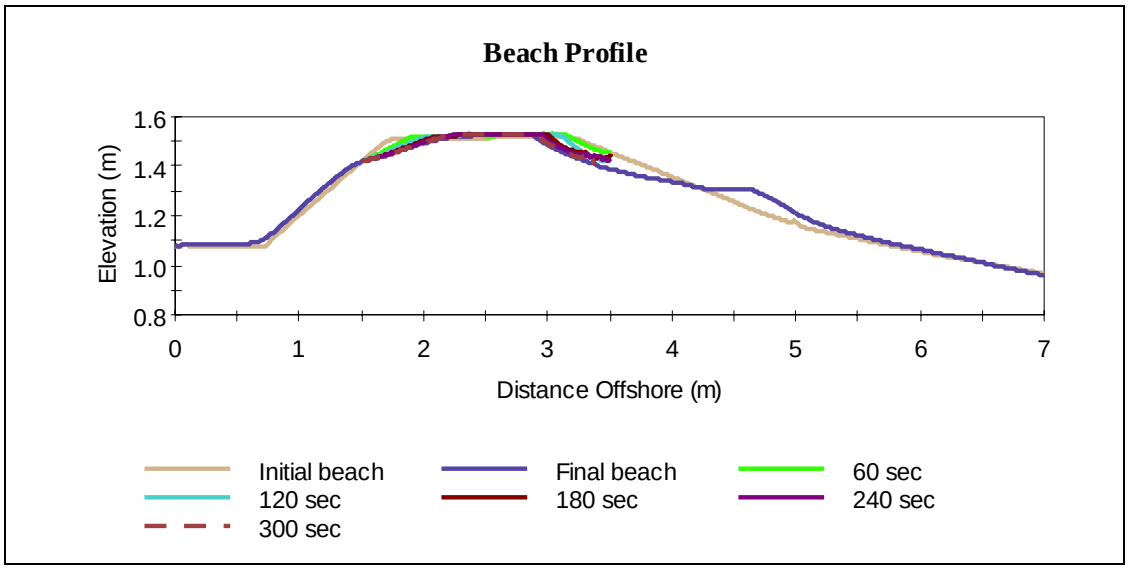


**Fig. A.30. The time series of beach profile changes by irregular waves ($H_{mo}$ = 0.15 m, $T_p$ = 1.6 sec, slope = 1:5).**

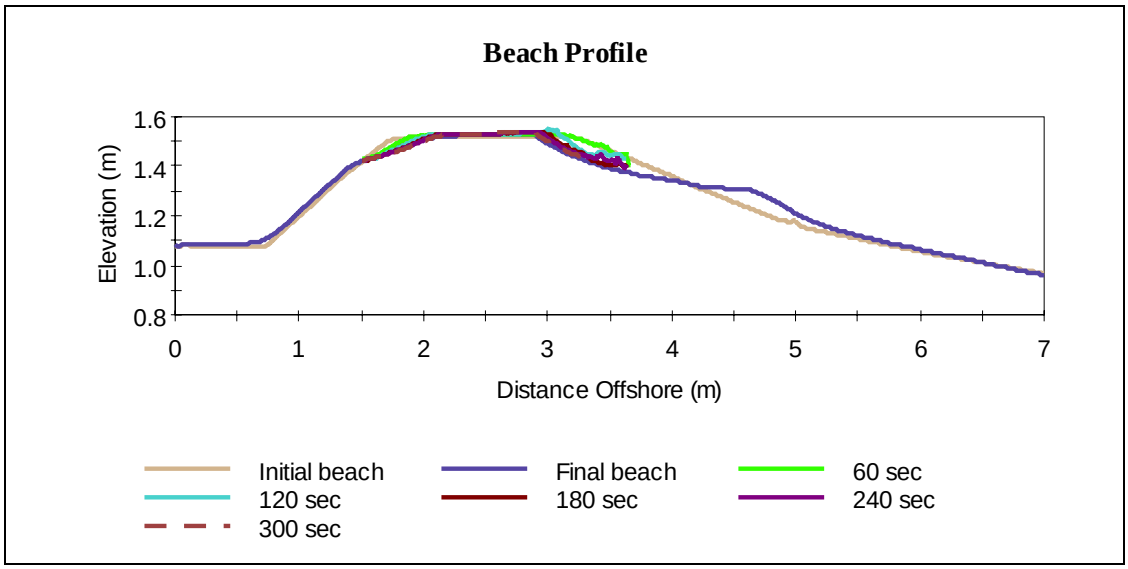


**Fig. A.31. The time series of beach profile changes by irregular waves ($H_{mo}$ = 0.15 m, $T_p$ = 1.8 sec, slope = 1:5).**

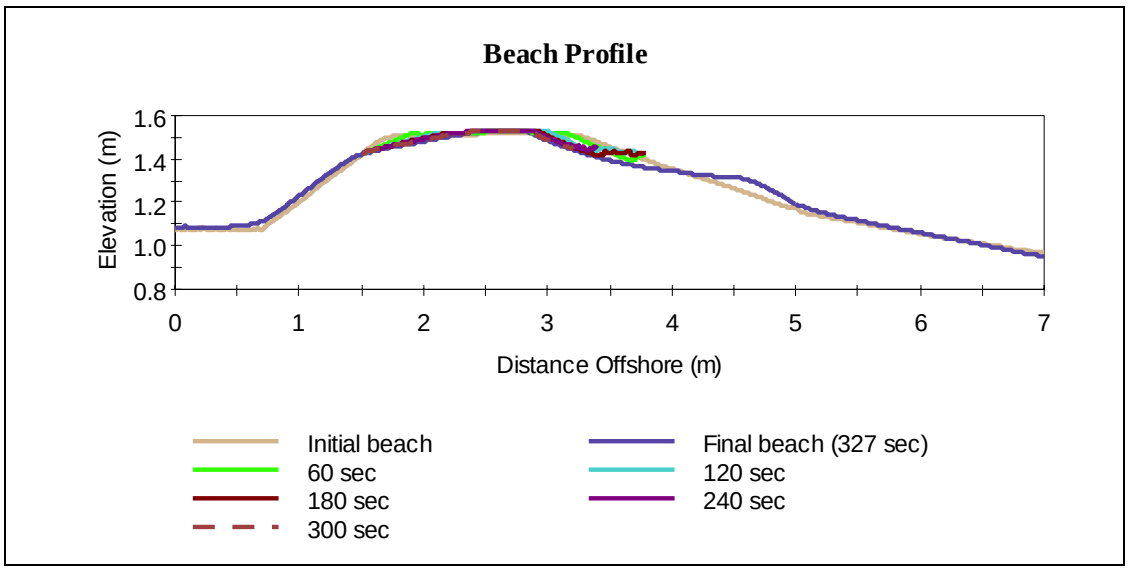


**Fig. A.32. The time series of beach profile changes by irregular waves ($H_{mo}$ = 0.15 m, $T_p$ = 2.0 sec, slope = 1:5).**

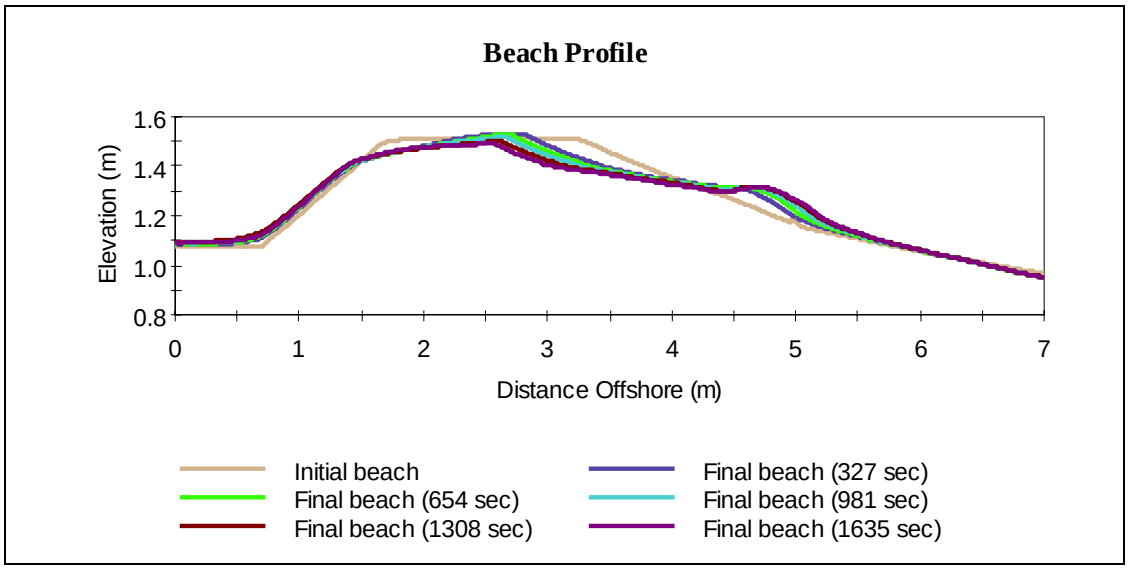


**Fig. A.33. The time series of beach profile changes by irregular waves for 1635 seconds ($H_{mo}$ = 0.15 m, $T_p$ = 2.0 sec, slope = 1:5).**

# VITA

Young Hyun Park was born in Seoul, Korea. He graduated from Dankook University with a bachelor of science in civil engineering in February, 1996. After graduation, he worked for Samsung Engineering and Construction Corporation in Korea from 1996 to 1997 as an engineer. He attended the graduate school at Seoul National University in March, 1998 and received a master of science in civil engineering in February, 2000. After graduation, he entered the graduate program at Texas A&M University in College Station, Texas in January, 2001 to study for a Ph.D. in the Coastal and Ocean Engineering division of Civil Engineering. He may be contacted at the following address:

Unjeongmaeul Ssangyong 2-cha Apt., #103-502

Mabuk-dong, Giheung-gu, Yongin-si,

Gyeonggi-do, Korea (ROK) 446-560

E-mail: tomypark@hotmail.com, tomypark@yahoo.co.kr